PROTECTIVE EFFECT OF RICE BRAN WATER EXTRACT ON PANCREAS OF RATS FED A HIGH-FAT DIET

BY

MR. WASON PARKLAK

A DISSERTATION SUBMITTED IN PARTIAL FULFILLMENT OF THE REQUIREMENTS FOR THE DEGREE OF THE DOCTOR OF PHILOSOPHY IN MEDICAL SCIENCES

FACULTY OF MEDICINE

THAMMASAT UNIVERSITY

ACADEMIC YEAR 2016

PROTECTIVE EFFECT OF RICE BRAN WATER EXTRACT ON PANCREAS OF RATS FED A HIGH-FAT DIET

BY

MR. WASON PARKLAK

A DISSERTATION SUBMITTED IN PARTIAL FULFILLMENT OF THE REQUIREMENTS FOR THE DEGREE OF THE DOCTOR OF PHILOSOPHY IN MEDICAL SCIENCES

FACULTY OF MEDICINE

THAMMASAT UNIVERSITY

ACADEMIC YEAR 2016

THAMMASAT UNIVERSITY
FACULTY OF MEDICINE

DISSERTATION

BY

MR. WASON PARKLAK

ENTITLED

PROTECTIVE EFFECT OF RICE BRAN WATER EXTRACT ON PANCREAS OF RATS FED A HIGH-FAT DIET

was approved as partial fulfillment of the requirements for
the degree of Doctor of Philosophy in Medical Sciences

on July 31, 2017

Chairman _____
(Assistant Professor Naovarat Tarasub, Ph.D.)

Member and Advisor _____
(Associate Professor Nusiri Lerdvuthisopon, Ph.D.)

Member _____
(Associate Professor BhornpromYoysungnoen, Ph.D.)

Member _____
(Assistant Professor Nuntiya Somparn, Ph.D.)

Member _____
(Assistant Professor Jarinyaporn Naowaboot, Ph.D.)

Dean _____
(Associate Professor Preecha Wanichsetakul, M.D.)

Dissertation Title	PROTECTIVE EFFECT OF RICE BRAN WATER EXTRACT ON PANCREAS OF RATS FED A HIGH-FAT DIET
Author	Mr. Wason Parklak
Degree	Doctor of Philosophy
Major Field/Faculty/University	Medical Sciences Faculty of Medicine Thammasat University
Dissertation Advisor	Associate Professor Nusiri Lerdvuthisopon, Ph.D.
Academic Years	2016

ABSTRACT

Obesity is generally associated with the infiltration of fat in multiple organs including the liver, heart, kidneys, as well as pancreas. This ectopic fat deposition in the pancreas may trigger lipotoxicity in the pancreas and leads to the pancreatic abnormalities. Many studies have reported the beneficial effects of rice bran water extract (RBE) against obesity, insulin resistance, hyperglycemia, dyslipidemia and oxidative stress. However, the mechanisms of how RBE can modulate fat accumulation, insulin signaling, glucose sensing, and cellular senescence, particularly in the pancreas, are still unknown. Thus, this study aimed to investigate the effects of RBE on the pancreatic abnormalities in high-fat diet (HFD)-fed rats. The study was performed on male Sprague-Dawley rats. The rats were divided into five groups including the control group (C), HFD alone group (HF), HFD treated with RBE at 2,205 or 4,410 mg/kg/day groups (HFR1 and HFR2, respectively) and HFD treated with metformin at 19.1 mg/kg/day group (HFM). After 4 weeks, body weight, glucose homeostasis parameters, blood lipid profile, lipid peroxidation marker (both in serum and pancreas) and pancreatic fat accumulation were assessed. The mRNA expression levels of sterol regulatory element-binding protein-1c (SREBP-1c), insulin receptor substrate-2 (IRS-2), glucose transporter-2 (GLUT-2), glucokinase (GK), and nuclear factor-kappa B p50 and p65 (NF-κB p50 and p65) genes in pancreas were also analyzed. Moreover, senescence in rat pancreatic islet

cells were analyzed by immunohistochemistry. The results showed the rats in HF group developed metabolic disturbances compared with the control rats; these disturbances were characterized by obesity, hyperglycemia, hyperinsulinemia, impaired glucose tolerance and dyslipidemia. However, two doses of RBE-treated rats significantly reversed the HFD-induced obesity, hyperglycemia, impaired glucose tolerance and hyperlipidemia in rats when compared with HF group. Metformin treatment had no effect on levels of fasting blood glucose (FBG) and serum insulin, but body weight gain, the area under the curve of blood glucose levels (AUC-G), and serum total-cholesterol (total-C) and low-density lipoprotein-cholesterol (LDL-C) levels were significantly decreased in the HFM group. Histological examination of HFD-induced obese rats revealed fat droplets in acinar cells, and irregular and larger shapes of islets, but these alterations were ameliorated in RBE- and metformin-treated rats. Moreover, the pancreatic triglyceride (TG) and SREBP-1c mRNA levels were also significantly decreased in RBE- and metformin-treated rats compared with the rats fed an HFD alone. The HF group also exhibited impaired insulin signaling and glucose-sensing pathways, which RBE could prevent these alterations via the improvement of IRS-2, GLUT-2, and GK expression. Unfortunately, metformin-treated rats had no effect on transcript levels of IRS-2 and GK, however GLUT-2 mRNA levels were significantly increased in the HFM group when compared with HF group. In addition, islet cell senescence was also observed in the HF group accompanied by enhanced malondialdehyde (MDA) level, and NF-κB expression. Interestingly, all RBE treatments resulted in a decrease in these alterations. The oxidative markers in pancreas were not significantly improved in the HFM group. However, metformin treatment effectively reduced serum MDA level and pancreatic islet senescence in rats fed an HFD. In conclusion, RBE consumption may attenuate pancreatic abnormalities by inhibiting fat accumulation, senescence, and oxidative damage, as well as enhancing insulin sensitivity and glucose sensing in the pancreas of HFD-induced obese rats. These data are likely to be associated with the improvement of impaired glucose homeostasis.

Keywords: Rice bran, Obesity, Pancreatic steatosis, Insulin signaling, Glucose sensing, Pancreatic senescence, Oxidative stress

ACKNOWLEDGEMENTS

The achievement of this doctoral dissertation was accomplished by the support of several people. First of all, I am extremely grateful to my advisor, Associate Professor Dr. Nusiri Lerdvuthisopon, for her scientific advices, knowledge, excellent suggestions, many insightful discussions, encouragement and support for my work.

My special thanks also goes to committee members, Associate Professor Dr. Bhornprom Yoysungnoen, Assistant Professor Dr. Nuntiya Somparn, and Assistant Professor Dr. Jarinyaporn Naowaboot, Faculty of Medicine, Thammasat University and Assistant Professor Dr. Naovarat Tarasub, Faculty of Science, Rangsit University, for their comments and assistance during the development of this dissertation.

Thanks must also go to all of the staff at the Faculty of Medicine, Thammasat University, for their help, support and valuable advice. This study was supported by grants from the Research Unit, Faculty of Medicine, Thammasat University, the National Research Council of Thailand and the Higher Education Research Promotion and National Research University Project of Thailand (Grant numbers 2-17/2013, 2011-67 and 14/2015, respectively).

I would also like to give a heartfelt thanks to Assistant Professor Dr. Nuntiya Somparn and Assistant Professor Dr. Jarinyaporn Naowaboot for providing me with the MDA reagents and FFA assay kits, respectively.

Every result described in this dissertation was accomplished by the help and support of fellow collaborators, Dr. Narongsuk Munkong, Miss Noppamat Kaendee, Miss Surasawadee Somnuk and Dr. Kevalin Vongthoung. I would like to thank all of them for their help and suggestions for the laboratory techniques.

Finally, I would like to thanks my family. They were always supporting me and encouraging me with their best wishes.

Mr. Wason Parklak

TABLE OF CONTENTS

LIST OF TABLES

LIST OF FIGURES

LIST OF ABBREVIATIONS

Symbols/Abbreviations	Terms
°C	Degrees Celsius
α	Alpha
β	Beta
γ	Gamma
δ	Delta
κ	Kappa
μ	Mu
μg	Microgram
μL	Microliter
μm^2	Square micrometers
ACC	Acetyl CoA carboxylase
ACOD	Acyl-CoA oxidase
ACS	Acyl-CoA synthetase
Akt	Protein kinase B
AMP	Adenosine monophosphate
AMPK	AMP-activated protein kinase
ANOVA	One-way analysis of variance
ATP	Adenosine triphosphate
AUC-G	Area under the curve of blood glucose levels
bHLH	Basic helix-loop-helix
BMI	Body mass index
BSA	Bovine serum albumin
BW	Body weight
C	Control
Ca^{2+}	Calcium cation

Cdk4	Cyclin-dependent kinase 4
cDNA	Complementary deoxyribonucleic acid
CETP	Cholesteryl ester transfer protein
ChREBP	Carbohydrate response element binding protein
C_T	Threshold cycle
DAB	3', 3'-diaminobenzidine
DAG	Diacylglycerol
DAP	Dihydroxyacetone phosphate
DEPC-treated water	Diethylpyrocarbonate-treated water
DGAT	Diacylglycerol acyltransferase
dL	Deciliter
DNA-SCARS	DNA segments with chromatin alterations reinforcing senescence
dNTPs	Deoxyribonucleotide triphosphates
DW	Distilled water
dUTPs	Deoxyuridine triphosphate
FFA	Free fatty acid
G-1-P	Glycerol-1-phosphate
G-3-P	Glycerol-3-phosphate
G-6-P	Glycerol-6-phosphate
GAPDH	Glyceraldehyde 3-phosphate dehydrogenase
GIP	Glucose-dependent insulinotropic polypeptide
GK	Glucokinase
GLP-1	Glucagon-like peptide-1
GLUT-2	Glucose transporter-2
GPAT	Glycerol-3-phosphate acyltransferase
Grb2	Growth receptor bound factor 2
GSIS	Glucose-stimulated insulin secretion

GSK3	Glycogen synthase kinase-3
h	hour
H and E	Hematoxylin and eosin
HDL-C	High-density lipoprotein-cholesterol
HFD	High-fat diet
IκB	Inhibitor of kappa B
IGT	Impaired glucose tolerance
IKK	Inhibitor of nuclear factor kappa-B kinase
IL	Interleukin
iNOS	Inducible nitric oxide synthase
IR	Insulin receptor
IRS-1	Insulin receptor substrate-1
IRS-2	Insulin receptor substrate-2
JNK	c-Jun N-terminal kinase
K^+	Potassium ion
kcal	Kilocalories
KDML 105	Khao Dawk Mali 105
kg	Kilogram
L	Liter
LDL-C	Low-density lipoprotein-cholesterol
LKB1	Liver kinase B1
MAPK	Mitogen-activated protein kinase
MCP-1	Monocyte chemoattractant protein-1
M-CSF-1	Macrophage-colony stimulating factor-1
MDA	Malondialdehyde
MEHA	3-methyl-N-ethyl-N-(*β*-hydroxyethyl)-aniline
mg	Milligram
MIF	Macrophage migration inhibitory factor
min	Minutes
mL	Milliliter

mm^2	Square millimeters
mmol	Millimole
mRNA	Messenger ribonucleic acid
mU	Milliunit
MW	Molecular weight
NADPH	Nicotinamide adenine dinucleotide phosphate
NCDs	Non-communicable diseases
NCEP ATPIII	National Cholesterol Education Programme Adult Treatment Panel III
NF-κB p50	Nuclear factor NF-kappa B p50 subunit
NF-κB p65	Nuclear factor NF-kappa B p65 subunit
ng	Nanogram
NIDDM	Non-insulin-dependent diabetes mellitus
nm	Nanometer
OCT1	Organic cation transporter 1
PACAP	Pituitary adenylate cyclase-activating polypeptide
PBS	Phosphate-buffered saline
PBST	PBS supplemented with 0.1% Tween-20
PCR	Polymerase chain reaction
PDK1	Phosphoinositol-dependent kinase 1
PDK2	Phosphoinositol-dependent kinase 2
PDX-1	Pancreas duodenum homeobox 1
PI3K	Phosphatidylinositol 3-kinase
PIP_2	Phosphatidylinositol 3,4 bisphosphate
PIP_3	Phosphatidylinositol 3,4,5 trisphosphate
PKB	Protein kinase B
POD	Peroxidase
PPARγ	Peroxisome proliferator-activated receptor gamma

RBE	Rice bran water extract
RBE1	Rice bran water extract dose 2,205 mg/kg BW
RBE2	Rice bran water extract dose 4,410 mg/kg BW
RNase	Ribonuclease
ROS	Reactive oxygen species
rpm	Revolutions per minute
RQ	Relative quantitation
RT	Reverse transcription
s	Second
SABG	Senescence-associated β-galactosidase
SASP	Senescence-associated secretory phenotype
S.E.M	Standard error of the means
SHC	Src-homology-2-containing protein
SPSS	Statistics Package for the Social Sciences
SREBP-1c	Sterol regulatory element-binding protein-1c
T2D	Type 2 diabetes
TCA	Tricarboxylic acid
TG	Triglyceride
TNF-α	Tumor necrosis factor-α
Total-C	Total cholesterol
U	Unit
UDG	Uracil-DNA glycosylase
VIP	Vasoactive intestinal peptide
VLDL	Very low-density lipoprotein-cholesterol
WHO	World Health Organization

CHAPTER 1
INTRODUCTION

1.1 Research problem

Obesity is one of the greatest public health problems, and its prevalence has increased dramatically over several decades. It is a complex metabolic disorder that is caused by a positive energy balance, where energy intake exceeds energy expenditure [1]. Obesity, especially abdominal obesity, appears to play an important role in the impairment of glucose and lipid metabolism, such as hyperglycemia, insulin resistance, ectopic fat deposition, and dyslipidemia. The consumption of high-energy diets with increased saturated and/or trans fats, an important environmental cause of obesity, is also associated with the initiation of these metabolic disturbances [2]. Under physiological conditions, the pancreas is an important organ for the regulation of cellular and whole-body energy homeostasis. It normally regulates energy homeostasis though the production of the main metabolic hormones, such as insulin and glucagon [3]. An important mechanism in the development of metabolic dysfunctions in animals is pancreatic abnormalities, which may lead to the abnormalities in both glucose and lipid metabolism [4]. Ectopic fat deposition in the pancreas (pancreatic steatosis) has recently gained much attention. Pancreatic steatosis could occur in the presence of obesity [5]. In rats, a high-fat diet (HFD) consumption could also cause fat accumulation in the pancreas accompanied by inflammation and fibrosis [6]. Sterol regulatory element-binding protein-1c (SREBP-1c) is now well established as a key transcription factor in the regulation of lipogenesis in the pancreas [7]. Previous report has indicated that the activation of SREBP-1c is essential for impaired insulin secretion and islet mass associated with the accumulation of triglyceride (TG) [8].

Insulin signals are mediated by tyrosine phosphorylation of the insulin receptor and its downstream targets, such as insulin receptor substrate-2 (IRS-2). IRS-2 acts as important coordinator of insulin signaling. It plays a major role in maintaining pancreatic structure and function by regulating the insulin secretion and pancreatic cell mass [9]. The down-regulation of IRS-2 gene in the β-cells led to impaired glucose-stimulated insulin secretion (GSIS) [9-10]. In addition, the impaired glucose sensing of the pancreatic β-cell resulted in the decrease of insulin secretion, thus, promoting of glucose intolerance in human study [11]. This impairment is believed to be initiated after the down-regulation of glucose transporter-2 (GLUT-2) and glucokinase (GK) gene, which are important glucose-sensing genes [12].

Progressive pancreatic β-cell senescence and its failure have been highlighted as early features of type 2 diabetes (T2D) [13]. Senescence-associated β-galactosidase (SABG) is known as senescent marker protein present within senescent cells [14]. In diabetic rats, HFD consumption led to progressive loss of β-cell mass associated with a prolonged increase activity of SABG [15]. It is widely accepted that the generation of reactive oxygen species (ROS) caused by increased β-cell proliferation plays a major role in the development of islet cell senescence [15]. Additionally, ROS generated during oxidative stress can damage biochemical molecules, thereby, producing oxidative stress by-products, such as malondialdehyde (MDA) [16]. Oxidative stress in the pancreas can be triggered by numerous pro-oxidant stimuli, such as hyperglycemia and high free fatty acid (FFA) levels [17-18]. Recently, Rovillain et al. [19] reported that the suppression of nuclear factor-kappa B (NF-κB) signaling by silencing of NF-κB subunits led to the evasion of senescence. Tilstra et al. [20] also reported that the inhibition of NF-κB could reduce cellular senescence, oxidative stress and oxidative damage *in vitro* and *in vivo*. These results support a pathogenic role for the activation of NF-κB signaling in cellular senescence and oxidative stress.

There are many reports on anti-obesity, anti-dyslipidemic, and antioxidant effects of rice bran and rice bran enzymatic extract [21-22]. According to previous research, the consumption of rice bran water extract (RBE) could reduce hyperglycemia and hyperlipidemia in humans with diabetes mellitus [23]. Consistently, in previous study [24-25], the consumption of RBE (at least 2,205 mg /kg) exhibited reduced abdominal fat weight, insulin resistance, and hyperlipidemia in HFD-fed rats. These results indicate a role of RBE in the regulation of glucose, lipid, and redox homeostasis, but the mechanisms that regulate fat accumulation, insulin signaling, glucose sensing, cellular senescence, and oxidative stress in the pancreas remains unknown. Therefore, the present study was aimed to investigate the protective effect of RBE on pancreatic abnormalities in rats fed an HFD as a model of obesity induced by diet.

1.2 Objectives

The aim of the study is to verify the effect of the RBE from Khao-Dawk Mali (KDML) 105 rice bran on the prevention of abnormality of pancreas in a model of obesity induced by an HFD. The specific objectives of the study are as following:

1.2.1 To investigate the effect of RBE on abdominal fat accumulation and adipocyte size.

1.2.2 To investigate the effect of RBE on blood lipid profile.

1.2.3 To investigate the effect of RBE on glucose homeostasis.

1.2.4 To determine the effect of RBE on pancreatic IRS-2, GLUT-2, and GK gene expression.

1.2.5 To study the role of RBE on SREPB-1c gene expression relating to lipogenesis mechanisms and fat accumulation in pancreas.

1.2.6 To investigate the effect of RBE on mass and histology of the pancreas.

1.2.7 To investigate the effect of RBE on the cellular senescence of pancreatic islets.

1.2.8 To study the role of RBE on pancreatic NF-κB gene expression and lipid peroxidation marker levels in serum and pancreatic tissue.

CHAPTER 2
REVIEW OF LITERATURE

2.1 Obesity-related health problems

Globally, overweight and obesity are considered a problem public health issue because of their contribution to the development of chronic non-communicable diseases (NCDs). Overweight and obesity are defined as abnormal or excessive fat accumulation that may cause many diseases [26]. Apart from fat accumulation, adipocyte dysfunction may occur, leading to metabolic changes enhancing the risk of chronic diseases. One of the most commonly used indices of relative weight is the body mass index (BMI). Classification of overweight and obesity by BMI, waist circumference, and associated disease risk are shown in Table 2.1. BMI is defined as body weight in kilogram divided by height, in meters squared. A BMI of over 25 kg/m^2 is defined as overweight, and a BMI of over 30 kg/m^2 as obese. Adult mean BMI levels of 22-23 kg/m^2 are found in Africa and Asia people, while levels of 25-27 kg/m^2 are prevalent across North America, Europe, and in some Latin American, North African and Pacific Island countries. BMI increases amongst middle-aged elderly people, who are at the greatest risk of health complications. In countries undergoing nutrition transition, overnutrition often co-exists with undernutrition. People with a BMI below 18.5 kg/m^2 tend to be underweight [26].

Table 2.1 Classification of overweight and obesity by BMI, waist circumference, and associated disease risk

Classification	BMI (kg/m^2)	Obesity class	Disease risk[a] relative to normal weight and waist circumference	
			Men ≤ 102 cm Women ≤ 88 cm	> 102 cm > 88 cm
Underweight	< 18.5		-	-
Normal[b]	18.5 - 24.9		-	-
Overweight	25.0 - 29.9		Increased	High
Obesity	30.0 - 34.9	I	High	Very high
	35.0 - 39.9	II	Very high	Very high
Extreme obesity	≥ 40	III	Extremely high	Extremely high

Source: Adapted from WHO [26].

[a] Disease risk for T2D, hypertension, and cardiovascular disease.

[b] Increased waist circumference can also be a marker for increased risk even in persons of normal weight.

Obesity rates are increasing, not only in the general population, but also in patients with chronic disease. Chronic diseases are a group of diseases that slowly develop and need continuously medical care because of short periods of exacerbation of the symptoms of the disease, such as chronic heart failure, chronic renal failure, T2D and the metabolic syndrome. Obesity is clearly related to the development of diabetes and the metabolic syndrome, other pathogenetic associations are emerging suggesting that obesity may enhance the risk to develop further organ failures and related chronic diseases.

Pathogenesis of an HFD-initiated obesity can be explained as a sustained disequilibrium between energy intake and energy expenditure in the body, may result from either on nutrient overload relative to utilizable capacity, a decreased in energy efflux ability to limit increased energy influx, or combination of both situations. Disruption of this balance potentially can affect increase the positive energy balance

and fat deposits in adipose tissue, especially abdominal fat accumulation and ectopic fat accumulation.

Adipose tissue plays a key role in the development of obesity and metabolic complications, functioning both as an energy store and as a major endocrine organ. The adipocyte is the main cell type in adipose tissue, but the tissue is also comprised of adipocyte precursor cells, stromal-vascular cells, immune cells, and nerve cells. In mammals, two types of adipose tissues are present: white adipose tissue which mainly serves as an energy storing tissue, and brown adipose tissue which is mainly a thermogenic tissue. White adipocytes are characterized by a large lipid droplet that occupies the major part of the cytoplasmic space, while brown adipocytes contain multiple and relatively smaller lipid droplets and a large number of mitochondria [27-28].

The main function of the white adipocyte is to store excess energy and to provide other tissues with energy during periods of negative energy balance, by releasing fatty acids and glycerol from lipolysis of triglycerides stored in the adipocyte lipid droplet. But, under situations of chronic overnutrition that results from a combination of increased caloric intake and decreased energy expenditure conduces to expanding adipose tissue mass (adipocyte hypertrophy and hyperplasia), initiating a conditions of cellular stress and stimulation of pro-inflammatory pathways, especially NF-κB signaling, c-Jun N-terminal kinase (JNK) and endoplasmic reticulum stress (ER stress) [29-30]. This results in upregulated adipocyte production of pro-inflammatory adipokines such as monocyte chemoattractant protein-1 (MCP-1), m-colony stimulating factor-1 (M-CSF-1) and macrophage migration inhibitory factor (MIF) that recruits monocytes-macrophages and other immune cells infiltration into the adipose tissue and aggravates the inflammatory response [29-33]. These macrophages are activated to release inflammatory cytokines such as tumor necrosis factor-α (TNF-α), interleukin-6 (IL-6) and IL-1β, and induced inducible nitric oxide synthase (iNOS) which interfere the antilipolytic and liposynthetic effect of insulin. Insulin-resistant adipocytes lead to an elevated efflux of FFA from adipocytes to circulation and extra-adipose tissues such as liver, muscle, pancreatic β-cell, hypothalamus, kidney, macrophage, heart and blood vessel as well as reflect to adipose tissue. This active adipocytes-macrophages crosstalk leading to dysregulated

secretion of a variety of adipokines such as low adiponectin levels and massive amounts of intracellular lipid and its toxic metabolites accumulation (lipotoxicity) result in metabolic derangement, insulin resistance, inflammation, oxidative stress and multiple organ dysfunction on numerous ectopic tissues. These systemic dysfunction increases the risk for development of the metabolic syndrome (dyslipidemia and abnormal glucose homeostasis), and T2D [29-33]. The pathogenesis of obesity is shown in Figure 2.1.

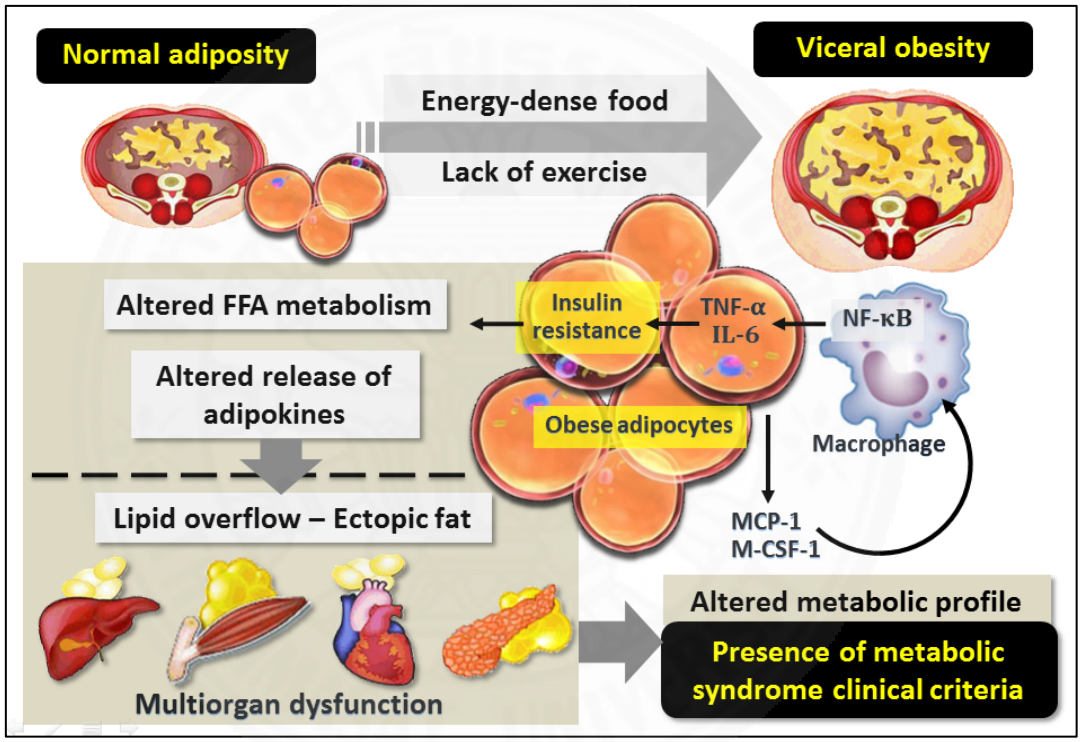

Figure 2.1 The pathogenesis of obesity

Increased FFA delivery to nonadipose tissues such as the liver may contribute to hepatosteatosis (fatty liver), which may also be considered an indicator of impaired energy storage in subcutaneous adipose tissue. Accordingly, fatty liver is a common clinical finding among overweight patients, especially those with other adiposopathic-related metabolic abnormalities such as T2D, high blood pressure, and dyslipidemia. From a lipid standpoint, increased free fatty acid delivery to the liver often increases hepatic secretion and TG enrichment of very-low-density lipoprotein

(VLDL), which is clinically manifested by elevated fasting TG levels [34]. Once in the circulation, hepatically derived VLDL particles undergo enzymatic exchanges with other lipoprotein particles such as high-density lipoproteins (HDL) and low-density lipoproteins (LDL), via cholesteryl ester transfer protein (CETP). Once these TG-rich lipoprotein particles are subjected to various lipases, then the HDL particles may become smaller and excretion by the kidney, resulting in low HDL-cholesterol (HDL-C) levels. Similarly, when TG-rich LDL particles interact with lipases, they may also become smaller and denser. The VLDL particles may undergo further lipolysis, resulting in VLDL remnants, which are also atherogenic. This adiposopathic dyslipidemic pattern is distinctly characteristic of the abnormal lipid levels found with pathogenic adipocyte and adipose tissue dysfunction [34-36].

Dyslipidemia was observed in patients with obesity, which include elevated triglyceride, VLDL, apolipoprotein B, and non-HDL-C levels. HDL-C levels are typically low. LDL levels are frequently in the normal range, but an increase in small dense LDL is frequently seen. These small dense LDL particles are considered to be more pro-atherogenic than large LDL particles for a number of reasons. Small dense LDL particles have a decreased affinity for the LDL receptor resulting in a prolonged period of time in the circulation. Additionally, these small particles enter the arterial wall more easily than large particles and then they bind more avidly to intra-arterial proteoglycans, which traps them in the arterial wall. Finally, small dense LDL particles are more susceptible to oxidation, which could result in an enhanced uptake by macrophages. Postprandial triglyceride levels are also increased in obese subjects and these chylomicron remnants are also pro-atherogenic. The increase in BMI associated with increasing the abnormalities in lipid levels. Approximately 60-70% of obese patients are dyslipidemia while 50-60% of overweight patients are dyslipidemia. The increased risk for cardiovascular disease in patients with obesity is partially accounted for by this dyslipidemia [34-36].

An increase in the intra-abdominal fat depot will decrease adiponectin and increase FFA levels, which will antagonize insulin effects in liver and muscle, leading to increased gluconeogenesis and less efficient glucose uptake, respectively. In the human studies, Fery and Radziuk et al. [37-38] reported that the hepatic insulin resistance associated with obesity and T2D results in impaired insulin-induced

suppression of glycogenolysis and gluconeogenesis. These defects persist when glucagon secretion is inhibited, indicating that factors other than hyperglucagonemia cause these abnormalities. The correlation between plasma FFA and rates of glycogenolysis and gluconeogenesis suggest that FFA may be one such factor. The observation that glycogenolysis contributes to excessive glucose production in T2D patients provides insight as to why prolonged fasting and its associated decrease in hepatic glycogen content results in a marked decrease in glucose concentration and restoration of glucose production to rates observed in nondiabetic subjects. Furthermore, these data add to the growing body of evidence indicating that both obesity and diabetes cause hepatic insulin resistance. They also suggest that complete normalization of hepatic glucose metabolism will require correction of the pathogenic processes that alter regulation of glycogenolysis as well as gluconeogenesis in people with T2D.

2.2 Pancreas

The pancreas is a particularly important organ from the point of view of human medicine because it suffers from two important diseases: diabetes mellitus and pancreatic cancer. Diabetes affects at least 30 million people worldwide and despite the availability of insulin remains a major problem. In humans, it is an organ weight 70-150 grams, measuring 15-25 cm in length. It is connected to the duodenum by the ampulla of Vater, where the main pancreatic duct joins with the common bile duct (Figure 2.2a). In the human, the terms head, neck, body and tail are used to designate regions of the pancreas from proximal to distal, while in rodents the shape of the pancreas is rather less well defined.

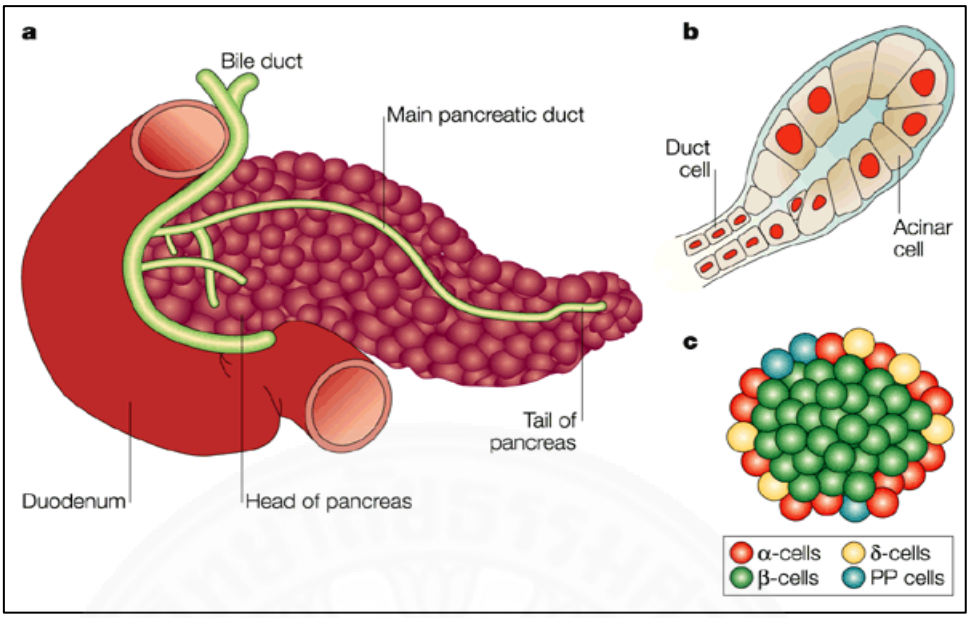

Figure 2.2 a) The mature pancreas is adjacent to the duodenum b) The exocrine pancreas c) The endocrine pancreas [39]

The pancreatic tissue consists of endocrine and exocrine portions. The exocrine portion accounts for over 80% of the pancreatic mass, and is composed of acinar cells that secrete digestive enzymes, and centroacinar and ductal cells that secrete fluid and electrolytes, particularly bicarbonate (Figure 2.2b). The endocrine portion, islets of Langerhans, is an important portion for the regulation of cellular and whole-body energy homeostasis. The islets of Langerhans are islands of cells scattered throughout the pancreas. The majority of the islet cells are β-cells (green), which secrete insulin and make up 60-80% of the endocrine pancreas. α-cells (red) secrete glucagon and make up 15-20% of the endocrine pancreas. δ-cells (yellow) secrete somatostatin and make up 5-10% of the endocrine pancreas, whereas PP cells (blue) secrete pancreatic polypeptide and make up less than 2% of the endocrine pancreas (Figure 2.2c).

2.2.1 Pancreatic β-cell function

2.2.1.1 Insulin secretion and glucose sensor

Blood glucose levels are tightly controlled by regulation of insulin release from pancreatic β-cells. GSIS in pancreatic β-cells depends on coordinated glucose uptake, oxidative metabolism and the subsequent signaling pathways that influence the rate of exocytosis. Impaired GSIS is a hallmark of T2D.

Insulin secretion is influenced by alterations in synthesis at the level of gene transcription, translation, and post-translational modification in the Golgi as well as by factors influencing insulin release from secretory granules. Long-term modification may occur via influences on β-cell mass and differentiation [40]. Pivotal role of insulin in glucose utilization and metabolism, it is not surprising that glucose has multiple influences on insulin biosynthesis and secretion. However, other factors such as amino acids, fatty acids, acetylcholine, pituitary adenylate cyclase-activating polypeptide (PACAP), glucose-dependent insulinotropic polypeptide (GIP), glucagon-like peptide-1 (GLP-1), and several other agonists, together in combination, also influence these processes [41].

Increased levels of glucose induce the GSIS by release of insulin from secretory granules in the β cell. In pancreatic β-cells, the low-affinity GLUT-2 mediates uptake of glucose, which is then phosphorylated by the glycolytic enzyme GK, which phosphorylates glucose to glucose-6-phosphate (G-6-P), generating adenosine triphosphate (ATP) [42]. Closure of K^+-ATP-dependent channels results in membrane depolarization and activation of voltage dependent calcium channels leading to an increase in intracellular calcium concentration; this triggers pulsatile insulin secretion [43]. Augmentation of this response occurs by both a K^+-ATP channel-independent Ca^{2+}-dependent pathway and K^+-ATP channel-independent Ca^{2+}-independent pathways of glucose action [41]. The other mediators of insulin release include activation of phospholipases and protein kinase C (e.g. by acetyl choline) and by stimulation of adenyl cyclase activity and activation of β-cell protein kinase A, which potentiates insulin secretion. This latter mechanism may be activated by hormones, such as vasoactive intestinal peptide (VIP), PACAP, GLP-1, and GIP. These factors appear to play a significant role in the second phase of glucose mediated

insulin secretion, after refilling of secretory granules translocated from reserve pools [41, 44]. Metabolic of GSIS from pancreatic β-cells is shown in Figure 2.3.

Synthesis and secretion of insulin is regulated by both nutrient and non-nutrient secretagogues, in the context of environmental stimuli and the interplay of other hormones [45]. Nutrient secretagogues such as glucose appear to trigger insulin secretion from the β-cell by increasing intracellular ATP and closing of K^+-ATP channels as outlined above. Generation of cyclic adenosine monophosphate (AMP) and other cellular energy intermediates are also augmented, further enhancing insulin release. Non-nutrient secretagogues may act via neural stimuli such as cholinergic and adrenergic pathways, or through peptide hormones and cationic amino acids [45].

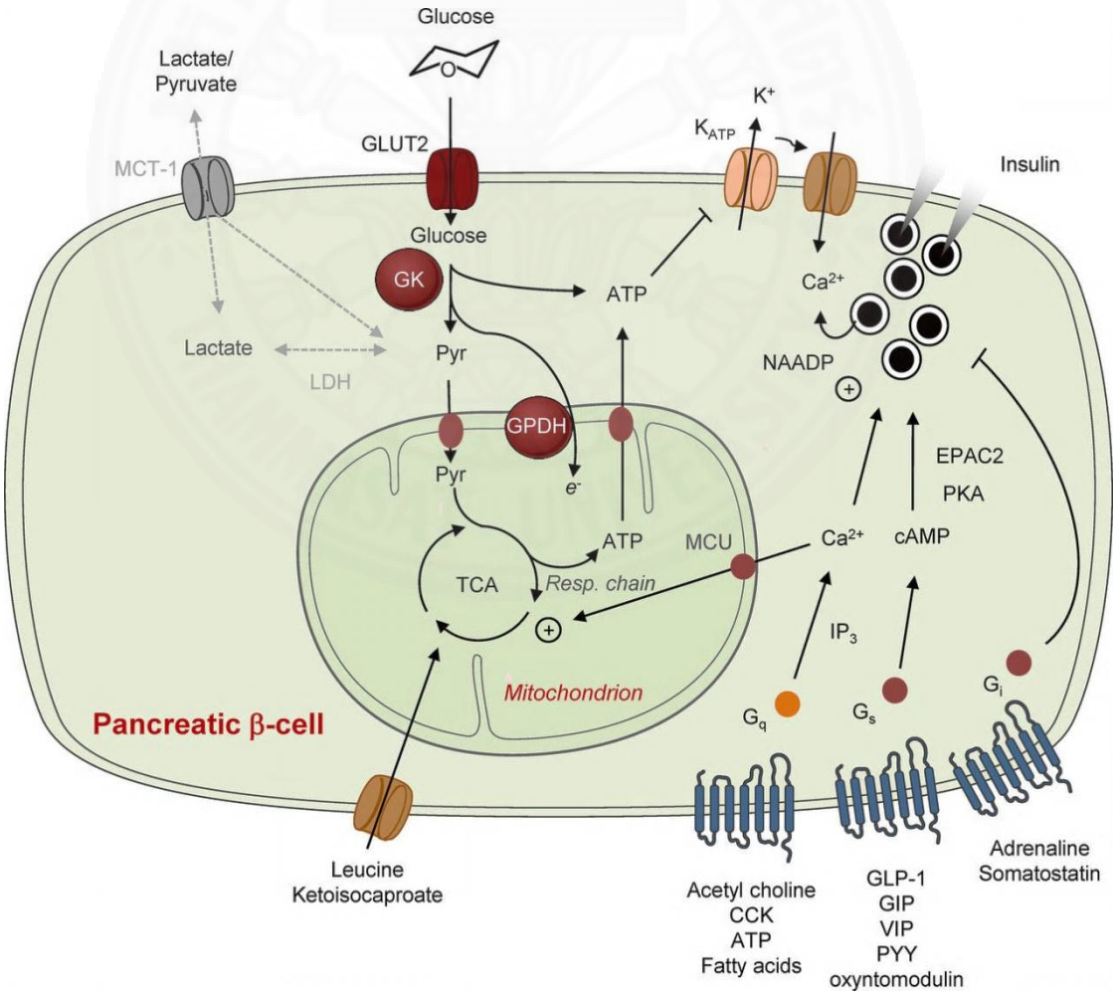

Figure 2.3 Metabolic of GSIS from pancreatic β-cells [44]

Impaired glucose tolerance (IGT) and non-insulin-dependent diabetes mellitus (NIDDM) are both wide spread among humans. In animal models illustrate the metabolic disturbances associated with T2D [46]. Glucose is required as an energy substrate, but also functions as a signalling molecule in primary processes. Indeed, alterations of normoglycemic levels have deleterious consequences that increase morbidity and mortality rates. Glucose sensors, molecular systems that accurately detect glucose concentrations in the extracellular space, contribute to maintaining glucose homeostasis by controlling several key processes. The glucose sensor was described in the pancreatic β-cell and is constituted by GLUT-2 and GK. Through elucidation of the mechanisms of β-cell glucose uptake by GLUT-2 and phosphorylation by GK, glucose sensing has come into focus as a vital β-cell function. In NIDDM, the loss of β-cells, the progressive decline in the expression of genes involved in glucose sensing [47], the phenomenon of glucose cycling [48], and the meaning of glucose sensing, especially for the first-phase response of GSIS, have become evident.

An HFD has been reported to correlate with the suppression of GLUT-2 and GK expression that linked to the development of obesity, insulin resistance and T2D. A reduction of GLUT-2 protein expression in β-cell is reflective of a loss of β-cell function in diabetic models, resulting in lower glucose uptake into β-cells and significantly less insulin being secreted [49]. Kim et al. [50] revealed that an HFD feeding of 4-week-old rats, for a period of 10 weeks, has previously been shown to induce hyperglycemia, and decrease GSIS via the reduction in GLUT-2 and GK mRNA expression. An HFD and specific FFA both have deleterious effects on glycemia, glucose sensing and insulinemia. Circulating glucose concentrations increase after high fat feeding. The initial events in GSIS, which involve glucose uptake into the β-cell by GLUT-2 and its subsequent phosphorylation by GK to initiate glycolysis, are impaired by an HFD evident by the reduced expression of these key genes. In addition, circulating insulin concentrations are reduced by an HFD. High fat feeding increases oxidative stress which may induce β-cell apoptosis. Thus, these data suggest that an HFD-induced reduction of glucose sensing and insulin secretion which linked to the development of T2D [12, 51].

In terms of therapeutic modulation, the pivotal role of glucose sensor in controlling blood glucose has made it attractive as a potential drug target for the treatment of T2D. Peroxisomal proliferator-activated receptor-γ (PPAR-γ) regulates gene expression of the glucose sensing apparatus to improve the glucose sensing ability of β-cells, and contributes to the restoration of β-cell function [52]. Thiazolidinediones, synthetic ligands of PPAR-γ, improve peripheral insulin sensitivity and GSIS in pancreatic β-cells. This is achieved by increasing the expression of the GLUT-2 gene and endogenous GK, as well as the GK enzymatic activity in β-cell lines. GK activators have been shown to enhance glucose metabolism and increase glucose uptake. Furthermore, in several rodent models of T2D, GK activators had the ability to reduce blood glucose concentrations, improve glucose tolerance and increase GSIS [53-58].

2.2.1.2 Insulin signaling and action in β-cells

The effects of insulin signaling in β-cells are shown in Figure 2.4. Binding of insulin to the insulin receptor (IR) induces autophosphorylation of the IR, leading to the binding of various scaffold proteins, including the insulin receptor substrate (IRS) proteins, but also Src-homology-2-containing protein (SHC), and among others. Phosphorylation of these scaffold proteins by the IR, in turn, engages various signaling pathways. IRS family members seem to have particularly important roles in the control of metabolic fuel homeostasis. Phosphorylation of IRS1 and IRS2 leads to their association with the p85 regulatory subunit of phosphatidylinositol 3-kinase (PI3K). This interaction recruits the p110 catalytic subunit of PI3K to the plasma membrane, resulting in conversion of phosphatidylinositol (4,5) bisphosphate (PIP_2) to phosphatidylinositol (3,4,5) trisphosphate (PIP_3). PIP_3 facilitates additional signaling events by binding to phosphoinositide-dependent protein kinase-1 (PDK1), PDK2 and Akt (also known as protein kinase B (PKB)). Colocalization of PDKs and Akt facilitates activation of Akt by phosphorylation at Thr308 (PDK1) and Ser473 (PDK2), leading to phosphorylation of downstream targets such as glycogen synthase kinase-3 (GSK3) and the AS160 Rab GTPase-activating protein, which in turn interacts with the small GTPase Rab10 to facilitate translocation of GLUT vesicles to the cell surface. These actions of insulin promote glucose uptake and storage under

anabolic conditions. Moreover, insulin signaling in β-cells leads to increased levels of PIP_3, activating Akt through PDK1/2. Akt in turn positively regulates β-cell mass by activating the cell cycle regulators Cyclin D1 (CcnD1), CcnD2, and Cyclin-dependent kinase 4 (Cdk4) [59] as well as regulating several anti-apoptotic genes [60]. Insulin signaling also stimulates β-cell replication and inhibits apoptosis via IRS-mediated activation of the mitogen-activated protein kinase (MAPK) pathway through growth receptor bound factor 2 (Grb2) [61-62].

Impaired insulin signaling in β-cells leads to increased apoptosis and decreased proliferation. Although β-cell mass expansion and increased insulin secretion can compensate for elevated insulin demand during the initial stages of insulin-resistance induced glucose intolerance, studies in diabetic patients and in rodents suggest that diabetes results when β-cells can no longer proliferate or secrete enough insulin to compensate for insulin resistance [63-64].

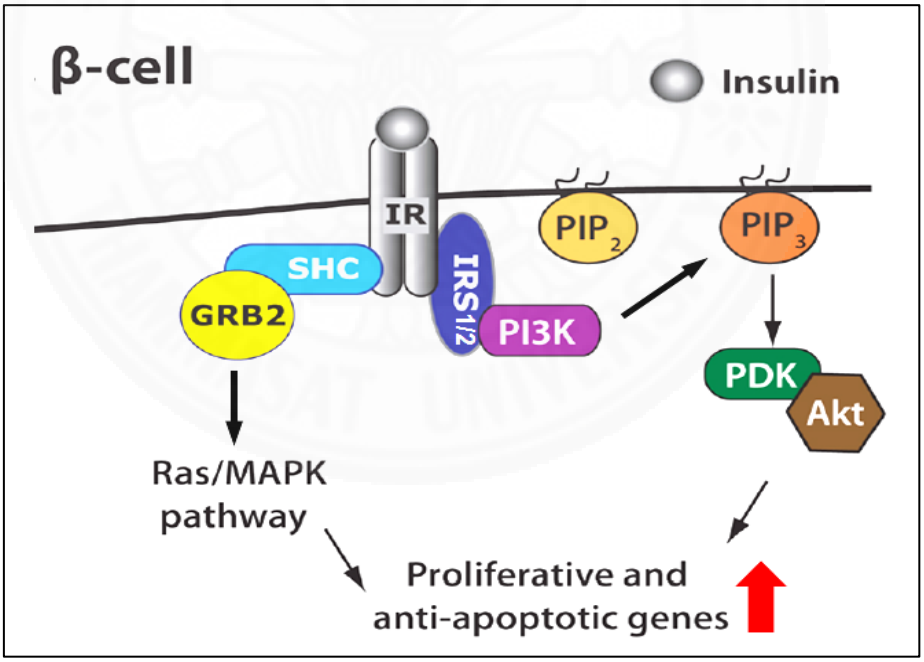

Figure 2.4 The effects of insulin signaling in β-cells (adapted from Golson et al.) [64]

The onset of T2D is marked by failure of the functional pancreatic β-cell mass to compensate for inherent insulin resistance. As such, T2D is a disease of insulin insufficiency, and a means to preserve sufficient functional β-cell

mass is a reasonable therapeutic approach to treat the condition. One conception is IRS-2, which is essential for β-cell survival [65-66]. When IRS-2 expression is specifically increased in β-cells, it is protective, maintains adequate functional β-cell mass, and avoids the onset of diabetes [67]. Therefore, upregulation of IRS-2 in pancreatic β-cells, and downstream signaling pathways are key to controlling normal β-cell growth and survival.

2.2.2 Pancreatic steatosis

The TG storage in adipose tissue is a well-established feature of energy homeostasis. In recent years, it has become apparent that the ectopic accumulation of lipid stores in pancreatic tissue is associated with a number of diseases such as insulin resistance, metabolic syndrome and T2D. Fatty infiltration in the pancreas has been termed fatty pancreas (pancreatic steatosis), which may lead to pancreatitis as well as pancreatic cancer [5]. Excess intracellular fatty acids, associated with accumulation of TG in β-cells, can induce a variety of cellular stresses, leading to β-cell dysfunction such as impaired insulin secretion.

Studies in the Zucker diabetic fatty rat, a rodent model for obesity-related diabetes, suggested that high circulating FFA induce massive triacylglycerol accumulation in pancreatic islets [68]. In the pancreas of patients with obesity, adipocytes were observed to accumulate in the area between pancreatic lobules (interlobular fat), especially around great vessels, or to be scattered in the lobules (intralobular fat), as shown in Figure 2.5. Hori et al. [69] reported that pancreas tissue with moderate to severe fatty infiltration is shown in Figure 2.5a and b. Most of the pancreas parenchyma has been replaced by adipocytes, and the remaining pancreas lobules resemble islets surrounded by a fatty lake. Most adipocytes have accumulated interlobularly (arrow in Figure 2.5b), but some are scattered within the lobules (arrowhead in Figure 2.5b). Pancreas tissue with mild fatty infiltration is shown in Figure 2.5c. Adipocytes have accumulated around arterioles (arrow), and several adipocytes are scattered within the lobules (arrowhead). Pancreas tissue with fatty infiltration is shown in Figure 2.5d.

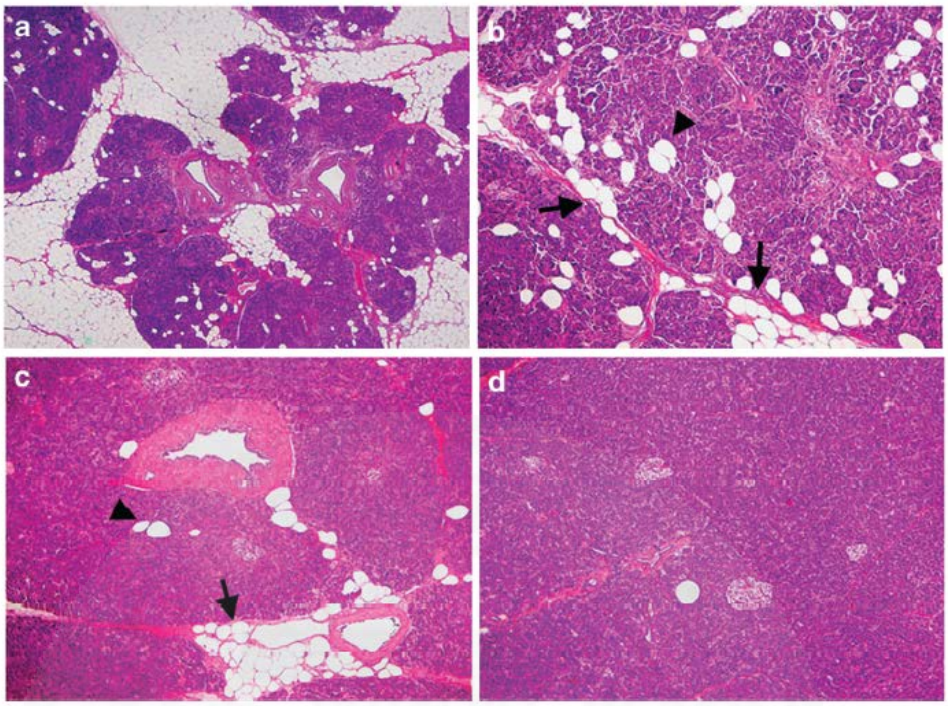

Figure 2.5 Histology of the human pancreas with fatty infiltration. Super low magnification in a, and low magnification in b-d [69]

SREBP-1c is a membrane-bound transcription factor of the basic helix-loop-helix (bHLH) leucine zipper family and has been established as a regulator of lipogenic enzymes and addressing its potential importance in metabolic diseases. Expression of SREBP-1c is highly upregulated by dietary intake of carbohydrates, sugars, and saturated fatty acids [7, 70-71]. Epidemiological evidence that changes in nutritional states could be triggers of metabolic disturbances in β-cells and experimental observations that SREBP-1c is highly regulated by nutrition, it is conceivable that endogenous fatty acid synthesis controlled by SREBP-1c in β-cells could be also deeply involved in β-cell lipotoxicity [7].

Several studies demonstrated that over-expression of SREBP-1c in pancreatic β-cell lines or islets lead to a marked reduction in GSIS and this was attributed to the concomitant TG accumulation and the subsequent lipotoxicity [72-73]. In Zucker diabetic *fa/fa* rats, an inappropriately high expression of SREBP-1c

and its target lipogenic genes was found in islets inducing increased TG storage that can lead to lipotoxicity and end up in diabetes [74].

Subsequent studies revealed that the SREBP-1c can involve multiple functional mechanisms of insulin secretion in β-cells. Figure 2.6 depicts these mechanisms in the sequences of intracellular events in the pathway of GSIS. Theoretically, any step of this pathway could be a target of lipotoxicity. Impaired ATP production in response to elevation of plasma glucose is the primary event of T2D pathophysiology. The data suggest that overexpression of SREBP-1c by gene transfer or exogenous palmitic acid treatment impaired GSIS [75], indicating that there should be other disturbances in post-ATP production steps of insulin secretion pathway. Therefore, investigation of the molecular mechanism of SREBP-1c or fatty acid-mediated insulin secretion defects should involve an entire pathway as potential target sites of lipotoxicity. Moreover, the SREBP-1c could modulate granuphilin [75-76] and other channel or vesicle molecules involved in insulin secretion. It should also be noted that SREBP-1c does not only lead to functional disturbances in mature β-cells but also causes disturbances in β-cell differentiation and replication, resulting in loss of β-cell mass. The β-cell loss by SREBP-1c in SREBP-1c transgenic mice is mediated through suppression of IRS-2 and pancreas duodenum homeobox 1 (PDX-1) and is more prominent on an HFD than on a standard chow [75-76].

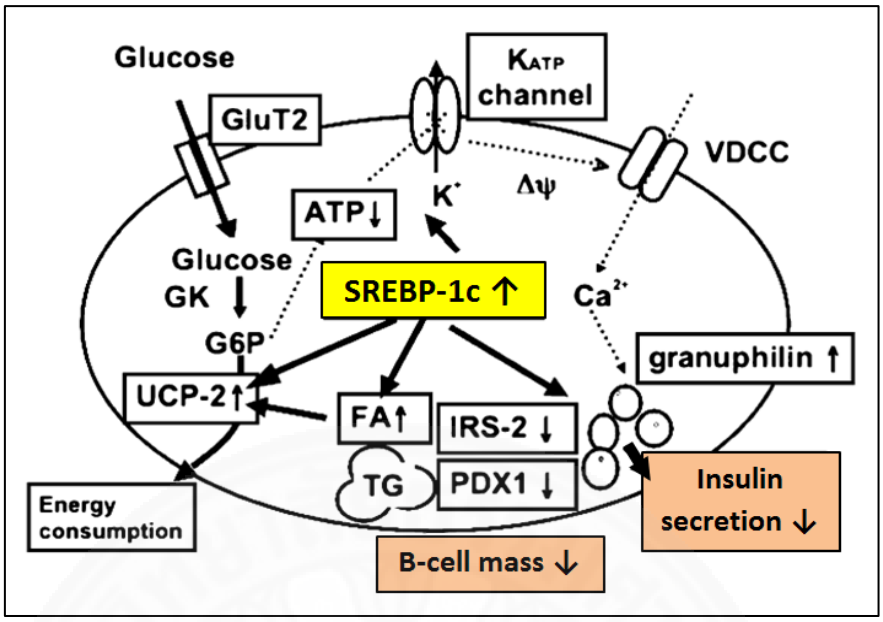

Figure 2.6 Schematic representation of GSIS in β-cells and the molecular effects of SREBP-1c activation [76]

2.2.3 Pancreatic β-cell senescence and oxidative stress

Obesity leads to fat infiltration of multiple organs including the heart, kidneys, liver, and pancreas. Under conditions of oxidative stress, fat-derived cytokines are released locally and result in an inflammatory process and organ dysfunction [30, 33]. Figure 2.7 show model of the increased ROS production in accumulated fat contributes to metabolic syndrome. The increased oxidative stress in accumulated fat, via increased nicotinamide adenine dinucleotide phosphate (NADPH) oxidase and decreased antioxidant enzymes, causes dysregulated production of adipocytokines, locally. Increased ROS production from accumulated fat also leads to increased oxidative stress in blood, hazardously affecting other organs including the liver, skeletal muscle, pancreas, and aorta. The increased oxidative stress in accumulated fat is an early instigator and one of the important underlying causes of obesity-associated metabolic syndrome [29-33, 77]. Fullenkamp et al. [78] reported that the atherogenic diet group exhibited increased obesity, metabolic disorders, islet enlargement, and pancreatic steatosis in Ossabaw miniature swine. Moreover, the modified atherogenic diet group showed significantly increased

oxidative stress levels as evidenced by elevated serum MDA and pancreatic MDA when compared the normal control group.

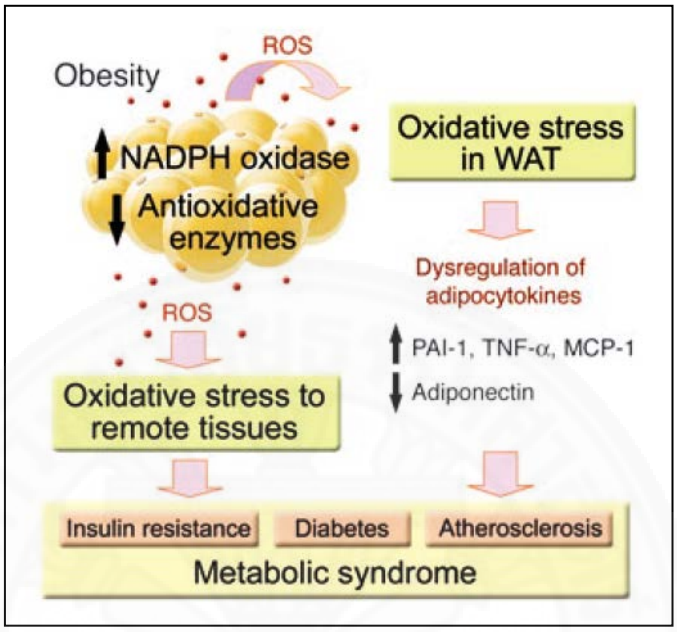

Figure 2.7 The increased ROS production in accumulated fat contributes to metabolic syndrome [77]

MDA is a major and stable end product formed during the peroxidation of lipids and is regarded as marker of lipid peroxidation in tissues [79]. Lipid peroxidation is the other important mediator of the second hit, with FFA being the major source. The primary site of lipid peroxidation is the mitochondria. In the pancreas of patients with T2D mitochondrial dysfunction, which leads to increased oxidation and generation of ROS, has been documented [80]. Lending more credence to our theory are the recent data from Yan et al. [81], who have shown that an HFD-induced obese rats increases lipid peroxidation and ROS, and decreases pancreatic microcirculation. These changes would result in an inflammatory state which was induced cellular senescence. Thus, the measuring tissues MDA was required to determine whether obese rats have increased oxidative stress and are more prone to cellular senescence.

Cellular senescence is unlikely to contribute solely to the development and/or progression of age-related diseases, but also other diseases or tissue dysfunction unrelated to age. Some age-related diseases may progress as a result of gradual accumulation of senescent cells, while other diseases, unrelated to age, may progress at a faster rate due to factors which accelerate the formation of cellular senescence. The underlying mechanism of both is the same, but the rate at which they progress differ.

At the cellular level, senescence is a state of permanent growth arrest in which cells are alive and metabolically active for months, but are unresponsive to mitogenic stimuli [82]. Free radical-dependent cellular damage theory was developed since 1956 and remains the theory basis of aging. Accumulating evidence supports the link between oxidative stress and aging by showing that oxidative stress induces cellular senescence [83].

Senescent cells have characteristic features (Figure 2.8), displaying a large and flat morphology, an increase in SABG (also called SA-Bgal) activity [84], and in most senescent cells express p16INK4a, which is not commonly expressed by quiescent or terminally differentiated cells. In some cells, p16INK4a, by activating the Rb protein (pRB) tumor suppressor, causes formation of senescence-associated heterochromatin foci (SAHF), which silence critical pro-proliferative genes. p16INK4a, a tumor suppressor, is induced by culture stress and as a late response to telomeric or intrachromosomal DNA damage. Moreover, p16INK4a expression increases with age in mice and humans [85-86]. Senescent cells have a persistent DNA damage response signaling harbor persistent nuclear foci, termed DNA segments with chromatin alterations reinforcing senescence (DNA-SCARS). DNA-SCARS include dysfunctional telomeres or telomere dysfunction-induced foci [87]. In addition to executing a cell-cycle arrest program, senescent cells undergo massive changes in the expression of genes thought to influence the tissue microenvironment in vivo. Thus, in addition to repressing genes related to proliferation, senescent cells often secrete inflammatory cytokines and immune modulators, downregulate extracellular matrix proteins and upregulate enzymes that degrade extracellular matrix, resulting in the senescence-associated secretory phenotype (SASP) (also called the senescence-messaging secretome) [88]. The senescence secretome has

tumor suppressive effects, inducing growth arrest and stimulating the immune system to clear senescent cells. However, components of the secretome can induce pro-tumorigenic effects on premalignant cells in the microenvironment [89]. These non-cell-autonomous activities of SASP show the functional relevance of senescence in pathophysiology, in particular in the tumor microenvironment, enhancing tumorigenesis of neighboring cells and playing a role in the decline of organ function with aging [89-91].

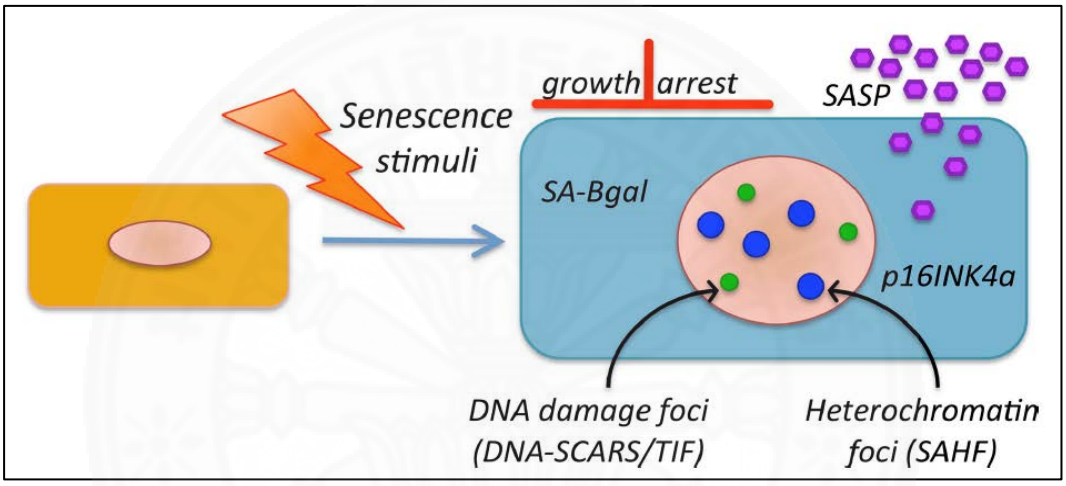

Figure 2.8 Hallmarks of senescent cells [89]. The pink circles in the non-senescent cell (left) and senescent cell (right) represent the nucleus.

Senescence is associated with activation of the NF-κB pathway. Recently, Rovillain et al. [19] used a novel system of conditionally immortal human fibroblasts, which can be induced to undergo senescence to show that senescence was associated with activation of NF-κB signalling and its perturbation by silencing of NF-κB subunits, or by the presence of the super repressor of NF-κB (IκB-SR), led to the evasion of senescence. They further showed that senescent cells were enriched for the transcriptionally active form of RelA (NF-κB subunit p65), with phosphorylation at serine 536 [19]. At the same time, Freund and colleagues [92] showed that increased NF-κB transcriptional activity due to p38MAPK activation was sufficient to induce the SASP of senescent fibroblasts.

NF-κB complexes involve dimerization of five members are p65 (RelA), RelB, c-Rel, p50/p105 (NF-κB1), and p52/p100 (NF-κB2) which the most common form being a dimer composed of p50 and p65 subunits [93]. NF-κB is kept inactive through its sequestration in the cytoplasm by the inhibitor of κB (IκB) family of proteins. Upon signals elicited by bacterial products, cytokines, viral expression, growth factors, and stress stimuli, kinases catalyze the phosphorylation of IκB and the p65 subunit, triggering p65 release and the translocation of p50/p65 transcription factors into the nucleus, where they activate a range of genes involved in immune and inflammatory responses [94].

Although senescent cells undergo phenotypic changes in morphology, including hypertrophy and flattening/enlargement of cells, the most common and reliable method for detection and differentiation from a quiescence state (a temporary arrest of the cell cycle) is the expression of SABG.

Arrest of the pancreatic β-cell cycle, which abolishes this replication capability, results in an inability to meet the metabolic demand for insulin, disrupting glucose homeostasis collectively driving T2D which the most common metabolic disease worldwide. During the pathogenesis of T2D, insulin resistance causes compensatory proliferation of pancreatic β-cells. This compensatory proliferation might accelerate cellular senescence, contributing further to the progression of diabetes. To investigate this, Sone and Kagawa [15] used HFD-induced diabetic mice to analyze β-cells for SABG and the proliferation marker Ki67. At 4 months, the proliferation of β-cells was 2.2-fold higher than in the control group. At 12 months, the frequency of Ki67 decreased to one-third that of the control and SABG-positive cells increased to 4.7-fold that of the control group. This increase in the senescent β-cell fraction correlated with insufficient insulin release, suggesting cellular senescence may contribute to HFD-induced diabetes. In this instance, it is difficult to determine whether cellular senescence is the cause or the consequence of insulin resistance.

2.3 Metformin

Many treatment options are available for overweight and obese adults: behavioral strategies, medications approved by the US Food and Drug Administration (FDA), and bariatric surgery for those at greatest risk. Several FDA-approved drugs for conditions other than obesity have been investigated as treatment of excess body weight [95-96]. Metformin is one such drug.

Metformin (dimethylbiguanide) is an insulin-sensitizing and antihyperglycemic agent used in the treatment of NIDDM [97]. The therapeutic action of the drug is attributed mainly to its effects at the hepatocyte level, with decreased glucose production, and the muscle cell level, with enhanced glucose uptake. In the liver, metformin through its partial mitochondrial uncoupling effect, activates a kinase called AMP-activated protein kinase (AMPK) which is stimulated by a decreased ATP/AMP ratio. When activated, this kinase strongly inhibits the expression of lipogenic enzymes through an inhibition of SREBP-1 and carbohydrate response element binding protein (ChREBP) transcriptional activity and inactivation of acetyl CoA carboxylase (ACC) which plays an essential role in regulating fatty acid synthesis and degradation [98-99]. Activated AMPK switches cells from an anabolic to a catabolic state, resulting in inhibition of glucose, lipid, and protein synthesis while promoting the oxidation of fatty acids and glucose uptake associated with weight loss and lower triglyceride levels. This pathway has been confirmed in several cell types involved directly in metabolism and energy expenditure such as hepatocytes [100], skeletal muscle cells [101], and pancreatic cells [102]. Metformin could thus theoretically contribute to decrease hepatic steatosis and glucose production [103].

Molecular mechanisms of the action of metformin on hepatocyte are shown in Figure 2.9. The preferential action of metformin in hepatocytes is due to the predominant expression of organic cation transporter 1 (OCT1), which has been shown to facilitate cellular uptake of metformin. After hepatic uptake through OCT1, the mitochondria is the primary target of metformin, exerting specific and AMPK-independent inhibition of respiratory chain complex I. The resultant mild decrease in energy status leads to an acute and transient inhibition of the energy-consuming gluconeogenic pathway. In addition, through AMPK-dependent and -independent

regulatory points, metformin can lead to the inhibition of glucose production by disrupting gluconeogenesis gene expression. In parallel, the liver kinase B1 (LKB1)-dependent activation of AMPK triggered by ATP depletion could reduce hepatic lipogenesis and exert an indirect effect on hepatic insulin sensitivity to control hepatic glucose output [99, 104].

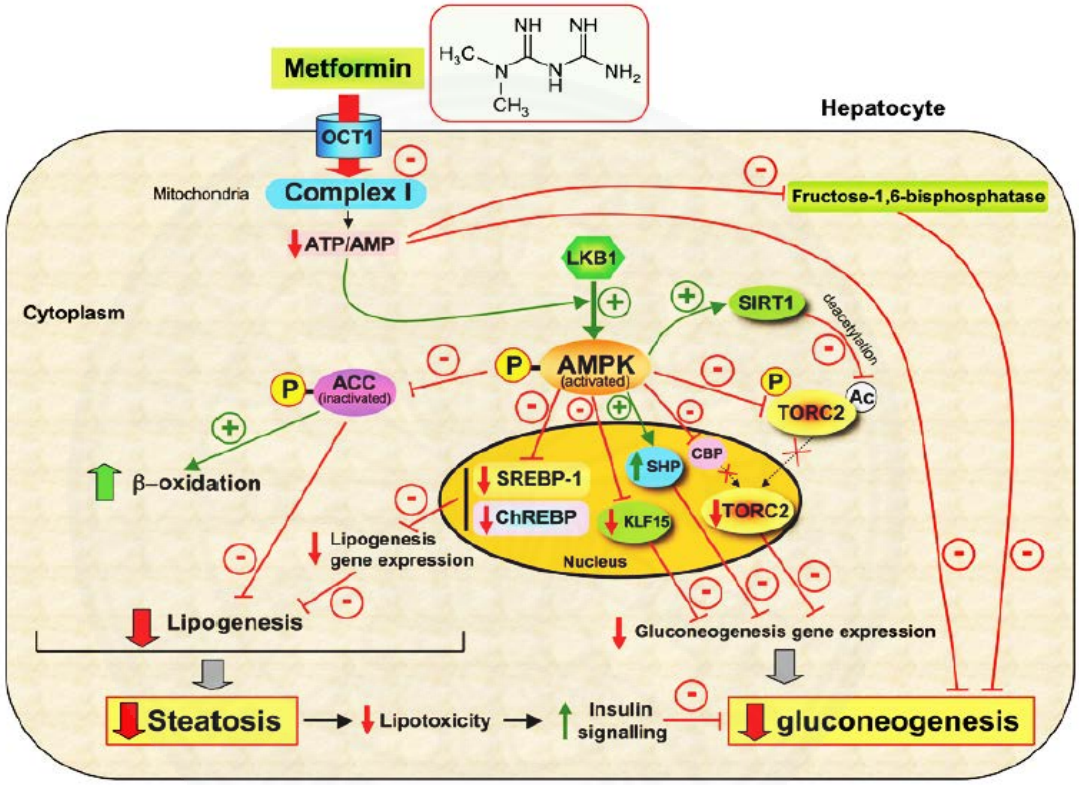

Figure 2.9 Potential molecular mechanisms of the action of metformin on hepatocyte [99]. (SIRT1, sirtuin 1; TORC2, transducer of regulated CREB-binding protein 2; Ac, acetylated; CBP, CREB binding protein; SHP, small heterodimer partner; KLF15, Kr¨ uppel-like factor 15)

In the pancreas, metformin is known about the AMPK-activated regulator in pancreatic islets [105] and AMPK has been suggested to play a role in insulin secretion [106]. Notwithstanding that AMPK activity is regulated by metformin, but elevated AMPK activity has been associated with increased [107], inhibited [108] and neutral [109] effects on the GSIS. In this regards, metformin does not alter membrane

potential or intracellular Ca^{2+} levels, but does stimulate insulin secretion at elevated (100-1,000 μM) concentrations, in BRIN-BD11 insulin-secreting cells at non-stimulatory glucose concentrations [110]. Thus, although there are reports that metformin has no effect or suppress insulin secretion, these accounts relate to much higher metformin and/or glucose concentrations [105].

Moreover, metformin has been shown to restore insulin release under the conditions of chronic FFAs exposure [111-112]. This drug prevents glucose- and fructose-induced permeability transition pore (a mitochondrial channel) opening and hampers glucose-induced cell death [113]. Kefas and co-workers [114] demonstrated that metformin dose-dependently also activates AMPK in insulin-producing MIN6 cells and in primary rat β-cells, leading to increased phosphorylation of ACC [115]. However, this chronic stimulation of metformin in MIN6 cells or primary rat β-cells led to increased AMPK activity, reduced protein synthesis, reduced the secretory and synthetic responsiveness of rat β-cells to glucose and resulted in a progressive increase of apoptosis due to metformin-activated JNK and caspase-3 [114, 116]. Metformin has also been shown to inhibit mitochondrial complex I activity, and led to pancreatic β-cell toxicity [117]. These controversial effects on insulin secretion and susceptibility to apoptosis might be related to the high drug concentrations that are not achieved *in vivo* [118-119].

The most frequent adverse effects of metformin are metallic taste, epigastric discomfort, weight loss, nausea, vomiting, and diarrhea. Administration with food can minimize epigastric discomfort. Other reported adverse effects include abdominal bloating, abdominal fullness, anorexia, and megaloblastic anemia secondary to impairment of folic acid and vitamin B_{12} absorption [120-121]. As many as 30% of patients started on metformin complained of abdominal bloating, nausea, cramping, a feeling of fullness, and diarrhea. Fortunately, these side effects are transitory and self-limiting and can be reduced by starting with a low dose, titrating up slowly, and taking the medication with food [120-121].

2.4 Rice bran

Rice (*Oryza sativa* Linn.) is a major source of nourishment for the world's population, especially in Asia. By-products of rice processing are rice bran and rice hulls, which protect rice seeds during growth. Each year, 63-76 million tons of rice bran is produced in the world and more than 90% of rice bran is sold cheaply as animal feed. Rice bran constitutes about 10% of rough rice grain and contains 18-22% oil [122].

The nutrient composition of rice bran is given in Table 2.2. Rice bran is a rich source of carbohydrate, proteins, fats, minerals, and micronutrients, such as B vitamins and trace elements. Full fat rice bran is a rich source of bioactive phytochemicals. They include phytosterols, gamma oryzanol, tocopherol and tocotrienols, ferulic acid and other phenolic compounds. These compounds have antioxidant properties and can protect against degenerative diseases in which ROS are involved [123]. Rice bran has many beneficial components that prevent obesity, hyperlipidemia, hyperglycemia, and oxidative stress.

Table 2.2 Nutrient composition of stabilized rice bran [123-125]

Nutrients	Content per 100 g	Nutrients	Content per 100 g
Proximate principles		**Micronutrients**	
Protein (*N* ×6.25)	16.5 g	*Vitamins*	
Fat	21.3 g	Thiamine	3.0 mg
Minerals (ash)	8.3 g	Riboflavin	0.4 mg
Crude fiber	11.4 g	Niacin	43 mg
Total complex carbohydrate	49.4 g	Panthothenic acid	7.0 mg
Dietary fiber	25.3 g	Biotin	5.5 mg
Soluble fiber	2.1 g	Folic acid	83 µg
Starch	24.1 g	*Minerals*	
Free sugar	5.0 g	Phosphorous	2.1 g
Energy	359 kcal	Potassium	1.9 g
Bulk density	0.39 (g/mL)	Magnesium	0.9 g
		Sodium	20.3 mg
		Calcium	80 mg
		Manganese	28.6 mg
		Copper	0.6 mg
		Iodine	67 µg
		Iron	11.0 mg
		Zinc	6.4 mg

In a previous study, oral feeding of a standard diet supplemented with a water soluble enzymatic rice bran extract restored endothelial function and vascular contractility in obese rats through the reduction of vascular inflammation and oxidative stress. The authors suggest that the bran extract could be considered a candidate for functional food in the treatment of vascular complications associated with obesity [126].

Kang and co-worker [127] reported that an HFD supplemented with a rice bran and phytic acid reduced hyperlipidemia and oxidative stress when compared

with rats fed an HFD alone, mainly by increasing fecal lipid excretion and regulation of antioxidant and lipogenic enzyme activities. Rice bran and phytic acid possess antihyperlipidemic action and antioxidant status-improving ability, and may be beneficial as dietary supplements in the management of an HFD-induced hyperlipidemia.

Boonloh and others [128] reported that the rice bran protein from the KDML 105 rice variety can improve glucose and fat metabolism in high-calorie diet-induced metabolic syndrome in rats. The rice bran protein lead to amelioration of insulin resistance through modulation of adipokine secretions, upregulation of the PPAR-γ gene and downregulation of lipogenesis gene (SREBP-1) in liver tissue, and proinflammatory cytokine genes (IL-6, TNF-α and MCP-1) in adipose tissue.

Wang and others [22] reported that the administration of the aqueous enzymatic extract from rice bran reduced serum lipid levels compared with rats fed an HFD group. The administration of the aqueous enzymatic extract from rice bran significantly lowered hepatic lipid profiles, inhibited 3-hydroxyl-3-methylglutaryl CoA reductase activity, and efficiently promoted the fecal excretion of total lipids and total cholesterol. Moreover, the rat fed with an HFD supplemented with the aqueous enzymatic extract from rice bran enhanced antioxidant status in the serum, liver and brain by increasing the antioxidant enzyme activity (superoxide dismutase, catalase, and glutathione peroxidase) and decreasing the content of MDA and protein carbonyl.

Candiracci and others [21] reported that a rice bran enzymatic extract-supplemented diet decreased the overproduction of tumor necrosis factor-a, IL-6, IL-1β, and iNOS, as well as the overproduction of IL-6 and iNOS in visceral abdominal adipose tissue and visceral epididymal adipose tissue, respectively. A rice bran enzymatic extract-supplemented diet reduced the adipocyte-size distribution pattern in both abdominal and epididymal adipose tissue. The authors suggest that a rice bran enzymatic extract could be a suitable treatment to ameliorate the obesity-associated proinflammatory response.

In the human study, Qureshi and co-worker [23] reported that the effects of stabilized rice bran, its soluble, and fiber fractions on blood glucose levels and serum lipid parameters with diabetes mellitus. The fasting serum glucose levels were also reduced significantly with stabilized rice bran (9%), rice bran water solubles

(29%), and rice bran fiber concentrates (19%). Serum insulin levels were increased with rice bran water solubles in both types of diabetes. The reduction of glycosylated hemoglobin and a slight increase in insulin levels indicate that consumption of rice bran water solubles can control blood glucose levels in human diabetes. Serum total cholesterol, LDL-cholesterol, apolipoprotein B, and triglycerides levels were reduced with rice bran fiber concentrates in both type of diabetes.

Previous studies have shown that the treatment with RBE from the KDML 105 rice variety (at least 2,205 mg /kg) significantly reduced insulin resistance, as well as abdominal and hepatic fat deposition in rats fed an HFD for 4 weeks [24-25]. Although those studies suggested RBE could reduce blood glucose level and lipid profile parameters, but the mechanisms that regulate fat accumulation, insulin signaling, glucose sensing, cellular senescence, and oxidative stress in the pancreas remains unknown. Therefore, the aim of this study was to investigate the protective effect of RBE on pancreatic abnormalities in rats fed an HFD as a model of obesity induced by diet.

CHAPTER 3
RESEARCH METHODOLOGY

3.1 Materials

3.1.1 Instruments

1. Centrifuge machine	(Beckman coulter, USA)
2. Centrifuge machine (Sorvall® RC6 -PLUS)	(Thermo Electron Corporation, USA)
3. Refrigerated centrifuge machine	(Hettich Zentrifugen, Germany)
4. Microcentrifuge machine	(Denville Scientific, USA)
5. Vortex	(Scientific Indrusties, USA)
6. Autopipettes	(HTL Lab Solution, Poland)
7. Microcentrifuge tube	(Costar, USA)
8. Hot air oven (ULM 600)	(Memmert, Germany)
9. Hotplate and Stirrer	(Sterillin, France)
10. Lyophilizer	(Telstar, Spain)
11. Spectrophotometer	(Shimadzu, Japan)
12. Electrical balance	(Boeco, Germany)
13. Accu-Check pens and reader	(Roche, Thailand)
14. PowerWave XS Microplate reader	(BioTek, USA)
15. Light microscope (Eclipse Ci-L microscope)	(Nikon, Japan)
16. Digital camera (DS-Fi2 microscope camera)	(Nikon, Japan)
17. Nikon's NIS-Elements revolutionizes imaging software	(Nikon, Japan)
18. Axiovision AC microscopy software	(Carl Zeiss, Germany)
19. Micro centrifuge machine	(Bertec Enterprise, Taiwan)

20. MyCycler™ thermal cycler (Bio-Rad, USA)
21. StepOne™ Real-Time PCR System (Applied Biosystems, USA)
22. MicroAmp™ Optical 96-Well Reaction Plate (Applied Biosystems, USA)
23. MicroAmp™ Optical Adhesive Film (Applied Biosystems, USA)
24. Digital Dry Bath Incubator (Boekel Scientific, USA)
25. Mini-Rocker Shaker (Biosan, USA)

3.1.2 Chemicals

1. Glucose oxidase kit (Linear, Spain)
2. Rat insulin ELISA (Mercodia, Sweden)
3. Triglyceride testing kit (Linear, Spain)
4. Distilled water (Milford, USA)
5. Ethanol, Analytical grade (Merck, Germany)
6. D-glucose ($C_6H_{12}O_6$) (Amersham Biosciences, USA)
7. Sodium carbonate (Na_2CO_3) (Alpha, India)
8. Chloroform (Lab-Scan Analytical Science, Thailand)
9. Methanol (QRëCTM, New Zealand)
10. Sodium pentobarbital (nembutal) (Jagsonpal, India)
11. Glycerol standards (Sigma-Aldrich, USA)
12. Free glycerol reagent (Sigma-Aldrich, USA)
13. Phosphate buffered saline (PBS) tablets (Amresco, USA)
14. Tween 20 (Prolabo, UK)
15. RNAlater (Qiagen, Germany)
16. TRIzol reagent (Invitrogen, USA)
17. 2-propanol (Sigma, Germany)
18. Diethylpyrocarbonate (DEPC)-treated water (Ambion, USA)

19. High Capacity cDNA Reverse Transcription Kits (Applied Biosystems, USA)

20. TaqMan® Gene Expression Master Mix (Applied Biosystems, USA)

21. TaqMan® Gene Expression Assay (Applied Biosystems, USA)
    - SREBP-1c (Rn01495769_m1)
    - IRS-2 (Rn01482270_s1)
    - GLUT-2 (Rn00563565_m1)
    - GK (Rn00561265_m1)
    - NF-κB p50 (Rn01399572_m1)
    - NF-κB p65 (Rn01502266_m1)

22. Quick Start Bradford Protein Assay kit 2 (Bio-Rad, USA)

23. Hyaluronidase (Sigma-Aldrich, USA)

24. Hydrogen peroxide (Sigma-Aldrich, USA)

25. Bovine serum albumin (Sigma-Aldrich, USA)

26. Phosphate buffer saline tablets (Amresco, USA)

27. SABG polyclonal antibody (Abnova, Taiwan)

28. Horseradish peroxidase-conjugated anti-rabbit IgG (BioLegendinc., USA)

29. 3,3’-diaminobenzidine tetrahydrochloride (DAB) (Diagnostic BioSystems, USA)

30. Trichloroacetic acid (TCA) (Sigma-Aldrich, USA)

31. Thiobarbituric acid (TBA) (Sigma-Aldrich, USA)

32. 1,1,3,3-tetraethoxypropane (TEP) (Sigma-Aldrich, USA)

3.2 Methodology

3.2.1 Preparation of RBE

Rice bran of KDML 105 was purchased from the Rice Fund Surin Organic Agriculture Corporative, Ltd. in Surin province, Thailand. Rice farm is approved by the Organic Certification Thailand. Rice grains were harvested and milled to remove rice hull from brown rice. Then the brown rice was polished to obtain bran layers. Rice bran was stabilized by heating it to 130-140 °C for 3 minutes prior to cooling, thereby deactivating the lipase.

The details about rice bran extraction were described by Qureshi et al. [23] with slight modification (Appendix A). Stabilized rice bran about 2,000 g was dispersed in 8,000 mL warm-distilled water (DW). The solution is kept at 60-70 °C while stirring on magnetic hot-plate stirrer for 60 minutes. After cooling to ambient temperature, the suspension is centrifuged at 8,000 rpm, for 10 minutes at 25 °C. The supernatant was then mixed with digestive enzymes solution (100 mg α-amylase/65 mL DW and 50 μL amyloglucosidase solution). The mixture was shaken and incubated for 1 hour at 37 °C.

The pancreatic α-amylases, which is α-1,4 endo-glucosidases, hydrolyze starch to soluble glucose oligomers with linear and branched structures. Glucose is only a very minor product of the α-amylase digestion of starch [129]. Amyloglucosidase is an enzyme, which catalyze the hydrolyzing reaction of starch to glucose by breaking the α-1,4- and α-1,6-glycosidic linkages of polysaccharides [130]. Alpha-amylase was used in the liquefaction of starch-producing soluble dextrins and amyloglucosidase was used for further hydrolysis of the dextrins to glucose in the saccharification step [129-130]. Therefore, the stabilized rice bran fractionates into rice bran water solubles and fiber concentrates when treated with carbohydrate-cleaving enzymes (α-amylase). The rice bran water solubles contain simple carbohydrates as dextrins, and rice bran fiber concentrates contain high levels of dietary fibers (β-glucan, pectin, and gums). Both fractions contain microcomponents found in stabilized rice bran [23].

After the incubation period, the mixture was then centrifuged at 8,000 rpm for 10 minutes at 25 °C. The supernatant is transferred to a tray and freeze-dried

into dried solid by use a lyophilizer (Systems Inc., Kingston, NY, USA). The final dried extract was stored at −20 °C until required for analysis. Aliquots of the RBE were prepared for animal treatment.

3.2.2 Animal study

3.2.2.1 Animals

The Animal Committee of the Faculty of Medicine, Thammasat University had approved the animal study (AE 002/2013, Appendix B). Thirty male outbred Sprague-Dawley rats were used in this study. Their initial weight about 180-220 g and aged 6-8 weeks old were purchased from National Laboratory Animal Centre, Mahidol University at Salaya, NakhonPathom, Thailand. All animals were cared and housed individually in stainless steel cages. The environment is 24 ± 1°C and 60% humidity on a fixed 12:12-hour light/sleep-dark/awake cycle (lights on at 6 A.M.).

3.2.2.2 Experimental diets

Two types of diet were used in the present study as follow:

(1) Standard chow was purchase from the Charoen Pokphand Foods (CPF), Samut Prakan, Thailand and consisted of 13%, 55% and 31% of total energy derived from fat, carbohydrate and protein, respectively (energy density of 3.04 kcal/g).

(2) HFD was modified from the obesity-induced diet in which 65.4% of total energy derived from fat [131]. The HFD was prepared in the Nutrition Unit, Thammasat University Hospital, Pathum Thani, Thailand. As shown in Table 3.1, the ingredients of the HFD included pork belly, pork liver, margarine, sugar, wheat flour, standard chow, and egg (hen). In addition, there are 10 g of vitamins and minerals syrup (Merck, Thailand) per L of the ingredients. The Nutri Survey Program (Nutrition Division, Department of Health, Ministry of Public Health, Nonthaburi, Thailand) was used to calculate the amount of each item of the ingredients. The HFD consisted of 65.3%, 23.4% and 11.1% of total energy derived from fat, carbohydrate, and protein, respectively (energy density of 5.12 kcal/g).

Table 3.1 Ingredients of HFD were estimated by Nutri Survey Program from the Nutrition Divisions, Department of Health, Ministry of Public Health

Ingredients	Amount (g)	Carbohydrate (g)	Protein (g)	Fat (g)	Energy (kcal)
Sugar	58	57.7	-	-	223.5
Standard chow	100	41.8	24	4.5	304
Wheat flour	150	114.5	15.5	1.5	546.5
Pork liver	100	2.4	19.9	4	126
Egg white, hen	33	-	3.3	0.4	16.8
Pork belly	100	2.8	13.9	33.5	368.1
Margarine	200	0	0.8	172.6	1,558.8
Egg yolk, hen	200	4	28.6	60.2	672.1
Total	941	223.2	106	276.7	3,816
% Kcal	-	23.39%	11.11%	65.26%	-

Note; 941 g of composition mixture gave a result of 745 g biscuit.

3.2.3 Experimental design

Rats were fed *ad libitum* with standard chow and water for seven days of acclimation prior to the start of experiments. They were divided into five groups of eight rats each as follows:

Group 1: rats received standard chow diet as a control (C) group

Group 2: rats received HFD alone (as an HF group)

Group 3: rats received HFD and co-fed with RBE at the dose of 2,205 mg/kg rat weight (HFR1)

Group 4: rats received HFD and co-fed with RBE at the dose of 4,410 mg/kg rat weight (HFR2)

Group 5: rats received HFD and co-fed with metformin (HFM). The half dose of 19.1 mg metformin/kg rat weight was started at the fourth day. Then, the full dose was begun at the sixteenth day until the end of the study.

Rats in all groups were treated daily by oral feeding for four weeks. Both RBE and metformin were suspended in DW. Rats in C and HF groups were received only DW in the same volume. Body weight and food intake were recorded daily.

This dose was prepared so that a constant volume of 0.1 mL/100 g of body weight and there are administered to each rat. A dose of 2,205 and 4,410 mg RBE per kg body weight were based on the previous studies [24-25].

In this study, the dose of metformin was based on dose the treatment of hyperinsulinemic obese adolescences [97]. The dosage is calculated for rats using a program provided by Food and Drug Administration, Silver Spring, MD, USA.

3.2.4 Preparation and collection of blood and tissue samples

At the end of treatment, the animals were sacrificed by intraperitoneal injection of high dose (150 mg/kg) of sodium pentobarbital after approximately 16-hour fasting overnight period.

Under careful sterile conditions, the rats were cut open longitudinally from the top of the thorax to the pelvic region, exposing the internal organs. The pancreas was rapidly removed and gently cleaned in cold phosphate-buffered saline or normal saline. Pancreas was quickly transferred to a sterile laminar flow hood. The operations were carried out as rapidly as possible while maintaining care and precision.

After the operation, the pancreas was weighted. The body of the pancreas is used for analysis, which divided into four portions. The first portion was suspended in fresh RNAlater and the tissue was stored at −20 °C until used in the real-time PCR analysis. The second portion was fixed in 10% formalin for histological and immunohistochemical analysis. The third and fourth portion of pancreas cut into pieces of 50 mg tissue for measurement of pancreatic MDA and TG contents, respectively.

Other tissue or organ samples of interest, for example the abdominal fat, and epididymal fat pads were promptly harvested, rinsed with cold phosphate-buffered saline or normal saline, weighed and then store in 10% formalin.

After opening the thorax, blood was drawn from the apex of cardiac ventricle (cardiac puncture). Blood samples were collected into a sterile falcon tube and centrifuged at 2,000 rpm for 20 minutes at 4 °C, and the serum were transferred to a new microcentrifuge tubes and stored at −20 °C prior to use for determination of lipid profile, and insulin concentrations.

The absolute organ weight of each rat was normalized by the final body weight and reported as a relative value of organ weight per 100 g final body weight. The animal model and experimental design are shown in Appendix C and D, respectively. Relative organ weight (% of body weight or g/100 g body weight) is calculated as:

$$\text{Relative organ weight} = \frac{\text{Absolute organ weight (g)} \times 100}{\text{Final body weight (g)}}$$

3.2.5 Blood biochemical measurement

3.2.5.1 Determination of glucose homeostasis parameters

Classically, insulin resistance is strongly associated with metabolic syndrome and plays principal role in the pathogenesis of T2D. Insulin resistance is defined as an inability of insulin actions to maintain its physiological effects in which higher than normal insulin levels or normal insulin levels fail to accomplish a normal metabolic responses. Insulin has many physiological activities in which regulation of glucose, lipid and protein metabolism [4, 37-38].

Clinical consequences of insulin resistance were demonstrated by hyperglycemia, dyslipidemia, and hypertension. The hyperglycemia that appears with insulin resistance can have deleterious effects on tissue and organs such as pancreas. It is clearly established that the control of blood glucose and insulin sensitivity remains the major means by which the development of hyperglycemia/hyperinsulinemia-associated complications can be minimized [4, 37-38].

(1) Determination of glucose concentrations and glucose tolerance

The levels of glucose in blood were tested using the glucometer Accu-Check monitors. Strip reaction principle is: 1) glucose first reacts with the glucose dehydrogenase enzyme. Glucose is oxidized to gluconic acid and the enzyme is temporarily reduced by two electrons transferred from glucose to the enzyme. 2) The reduced enzyme next reacts with ferricyanide (M_{ox}), transferring a single electron to each of two mediator ions. The enzyme is returned to its original state, and the two M_{ox} are reduced to ferrocyanide (M_{red}). Ferricyanide and ferrocyanide are capable of rapidly transferring electrons with an electrode. The electrons may thus be transferred between glucose and the electrode via enzyme and mediator. The reactions are as follows:

$$\text{Glucose} \xrightarrow{\text{Peroxidase}} \text{Gluconic acid}$$

$$2 \text{ ferrocyanide } (M_{red}) + 2H^{+} \xleftarrow{\text{Peroxidase}} 2 \text{ ferricyanide } (M_{ox})$$

The blood sample is applied to the target area, covering both the working electrode and the reference electrode. This area is coated with enzymes that react in the presence of glucose to make a small electric current. The size of the current generated is proportional to the amount of glucose present in the blood drop.

Rats were fasted overnight (16 hours), weighed and clipped the tip tail for glycemic determinations. Blood samples were measured immediately prior to a glucose solution administration (at 0 hour) for fasting glucose concentrations and at 0.5, 1.0, 1.5, 2.0, and 2.5 hours after receiving of oral glucose loading (2 g/kg body weight) for the assay of oral glucose tolerance test. A series of half-hourly blood glucose of each rat were analyzed and glucose concentrations are plotted against the time of blood withdrawals. Area under the curve was calculated using trapezoidal rule. This method was use for determination of glucose concentrations and glucose tolerance as previously described with minor modification [132].

(2) Determination of plasma insulin level

The animals were fasted for 16 hours and blood samples were collected from cardiac puncture. Tubes were kept on ice until centrifugation at 3,000 rpm for 5 minutes. Serum was stored at −20 ºC before analyzed. Serum insulin levels were analyzed by using the commercial ELISA kits. Mercodia Insulin ELISA is a solid phase two-site enzyme immunoassay. Serum insulin content is determined as described previously [133].

It is based on the direct sandwich technique in which two monoclonal antibodies are directed against separate antigenic determinants on the insulin molecule. During incubation insulin in the sample reacted with peroxidase-conjugated anti-insulin antibodies and anti-insulin antibodies bound to microtitration well. A simple washing step removed unbound enzyme labelled antibody. The bound conjugate is detected by reaction with 3, 3', 5, 5'-tetramethylbenzidine (TMB). The reaction is stopped by adding acid to give a colorimetric endpoint that was read spectrophotometrically.

The concentrations of insulin serum was stored at −20 ºC before analyzed obtained by computerized data reduction of the absorbance for the calibrators, except for calibrator 0, versus the concentration using cubic spline regression by Prism GraphPad software.

3.2.5.2 Determination of blood lipid profile

Dyslipidemia was observed in rats with obesity. The major components of dyslipidemia associated with the metabolic syndrome is characterized by increased levels of TG, low levels of HDL-C, and small, dense low-density lipoprotein particles with normal or slightly increased LDL-C. The abnormality of lipid and lipoprotein metabolism frequently presented in insulin-resistant state in both patients with T2D and non-diabetes. This evidence is convincing that insulin resistance is the principal underlying abnormality for contribution to the dyslipidemia [34-36]. Moreover, Insulin-resistant adipose tissues lead to an elevated efflux of FFA from adipocytes to circulation and extra-adipose tissues such as liver, muscle, kidneys, as well as pancreatic tissue [68].

(1) Determination of total-C level

The level of cholesterol in serum is determined using the enzymatic colorimetric method [134]. Cholesterol is determined enzymatically using cholesterol esterase, cholesterol oxidase and peroxidase. The reactions are as follows:

$$\text{Cholesterol ester} + H_2O \xrightarrow{\text{Cholesterol esterase}} \text{Cholesterol} + \text{Fatty acids}$$

$$\text{Cholesterol} + O_2 \xrightarrow{\text{Cholesterol oxidase}} \text{Cholesten-3-one} + H_2O_2$$

$$2H_2O_2 + \text{Phenol} + \text{4-Aminoantipyrine} \xrightarrow{\text{Peroxidase}} \text{Quinieimine dye} + 4H_2O$$

Cholesterol esters are cleaved by the action of cholesterol esterase to yield cholesterol and fatty acids. Cholesterol is converted by oxygen and cholesterol oxidase to cholesterol-3-one and hydrogen peroxide (H_2O_2). H_2O_2 created forms a red dyestuff by reacting with 4-aminoantipyrine and phenol under catalytic reaction of peroxidase. The color intensity is directly proportional to concentration of cholesterol and can be determined photometrically.

A 10 µL of serum samples or cholesterol calibrator (200 mg/dL or 5.17 mmol/L) was added to a 1000 µL of cholesterol reagent (R1 reagent), mix and subsequently incubate for 10 minutes at room temperature. Cholesterol reagent consists of pipes buffer pH 6.9 (90 mmol/L), phenol (26 mmol/L), cholesterol oxidase (200 U/L), cholesterol esterase (300 U/L), peroxidase (1,250 U/L) and 4-aminoantipyrine (0.4 mmol/L). Within 60 minutes read absorbance (A) of cholesterol calibrator and serum samples against reagent blank. The concentration of cholesterol is quantitating by spectrophotometer at the wavelength of 546 nm. Cholesterol concentration is calculated according to the following equation:

$$\text{Cholesterol concentration} = \frac{\Delta A \text{ sample} \times \text{Calibrator concentration}}{\Delta A \text{ calibrator}}$$

The concentration of total-C was expressed as mg/dL.

(2) Determination of HDL-C level

The level of HDL-C in serum is determined using the enzymatic colorimetric method [134]. The chylomicrons, VLDL, and LDL-C are precipitated by phosphotungstic acid and magnesium chloride in precipitating reagent or HDL reagent. After centrifugation the supernatant contains the HDL-fraction, their cholesterol content is determined enzymatically.

A 200 µL of serum samples were added to a 500 µL of working precipitating reagent (dilute 4 parts of precipitating reagent with 1 part of DW), mix and subsequently incubate for 10 minutes at room temperature. Then, the mixture was centrifuged at 4,000 g for 10 minutes at room temperature. After centrifugation, the mixture was separated the HDL-containing supernatant from the precipitated lipoprotein.

A 100 µL of HDL supernatant was mixed with 1,000 µL of cholesterol reagent. The mixture was incubated for 10 minutes at room temperature. Then, the mixture was detected at 546 nm in the assay using the spectrophotometer. The concentration of HDL-C is expressed as mg/dL. The concentration of HDL-cholesterol is express as mg/dL similar to the determination of total-cholesterol.

(3) Determination of TG level

The level of TG in serum is determined using the enzymatic colorimetric method [134]. The triglycerides are hydrolyzed by lipoprotein lipase to generate glycerol and fatty acid. Glycerol is phosphorylated by glycerol kinase to produce the glycerol-3-phosphate (G-3-P) and adenosine diphosphate (ADP). The G-3-P is converted by G-3-P peroxidase to dihydroxyacetone phosphate (DAP) and H_2O_2. The H_2O_2 is then reacting with 4-aminophenazone and 4-chlorophenol under the catalytic reaction of oxidase to give a red quinoneimine dye (Trinder endpoint reaction). This red dye stuff can be measure spectrophotometrically at 546 nm. The reactions are as follows:

$$\text{Triglyceride} + 3H_2O \xrightarrow{\text{Lipoprotein lipase}} \text{Glycerol} + \text{Fatty acids}$$

$$\text{Glycerol} + \text{ATP} \xrightarrow[Mg^{2+}]{\text{Glycerol kinase}} \text{G-3-P} + \text{ADP}$$

$$\text{G-3-P} + O_2 \xrightarrow{\text{G-3-P oxidase}} \text{DAP} + H_2O_2$$

$$H_2O_2 + \text{4-aminophenazone} + \rho\text{-chlorophenole} \xrightarrow{\text{Peroxidase}} \text{4-}(\rho\text{-benzoguinone-monoimino})\text{-phenazone} + 2H_2O + HCL$$

A 10 µL of serum samples or triglyceride calibrator (200 mg/dL or 2.28 mmol/L) was added to a 1000 µL of triglyceride reagent (R1 reagent), mixed and subsequently incubated for 10 minutes at room temperature. Triglyceride reagent consisted of pipes buffer (50 mmol/L), ρ-chlorophenole (2 mmol/L), lipoprotein lipase (150,000 U/L), glycerol kinase (800 U/L), G-3-P oxidase (4,000 U/L), peroxidase (440 U/L), 4-aminoantipyrine (0.7 mmol/L), ATP (0.30 mmol/L, magnesium chloride (40 mmol/L), Na-cholat (0.20 mmol/L) and potassium-hexacyanoferrat (II) (1 µmol/L). Then read absorbance of serum samples and triglyceride calibrator against reagent blank within 60 minutes after start. The concentration of triglyceride is quantitating by spectrophotometer at the wavelength of 546 nm. Cholesterol concentration is calculated according to the following equation:

$$\text{Triglyceride concentration} = \frac{\Delta A \text{ sample} \times \text{Calibrator concentration}}{\Delta A \text{ calibrator}}$$

(4) Determination of LDL-C level

The concentration of LDL-C is expressed as mg/dL. The serum low-density lipoprotein-cholesterol (LDL-C) level was determined using the Friedewald equation [135], represented as follows:

$$\text{LDL-C} = (\text{Total-C}) - (\text{HDL-C}) - (\text{Triglyceride}/5)$$

(5) Determination of FFA level

Serum FFA contents is determined as described previously [136]. FFA contents in the serum were determined using enzymatic colorimetric method (Wako, Osaka, Japan). FFA in serum, when treated with acyl-CoA synthetase (ACS) in the presence of ATP and CoA, form the thiol esters of CoA known as acyl-CoA along with the byproducts AMP and pyro-phosphate (PPi). In the second portion of the procedure, the acyl-CoA is oxidized by added acyl-CoA oxidase (ACOD) to produce hydrogen peroxide which in the presence of added peroxidase (POD) allows for the oxidative condensation of 3-methyl-N-ethyl-N-(*β*-hydroxyethyl)-aniline (MEHA) with 4-aminoantipyrine to form a purple colored end product with an absorption maximum at 550 nm. Hence the amount of FFA in the sample can be determined form the optical density measured at 550 nm. The reactions are as follows:

$$\text{RCOOH + ATP + CoA} \xrightarrow{\text{ACS}} \text{Acyl-CoA + AMP + PPi}$$

$$\text{Acyl-CoA + O2} \xrightarrow{\text{ACOD}} \text{2,3-trans-Enoyl-CoA + } H_2O_2$$

$$2H_2O_2 + \text{4-aminoantipyrine+ MEHA} \xrightarrow{\text{POD}} \text{Quinoneimine-color + } 4H_2O$$

A 25 µL of serum samples or FFA calibrator (1 mEq/L oleic acid) was added to a 500 µL of R1 reagent (consists of ACS, CoA, ATP, 4-aminoantipyrine, ascorbate oxidase, and pH 7.0 phosphate buffer), mix and subsequently incubate for 10 minutes at 37 °C temperature. A 1,000 µL of R2 reagent (consists of ACOD, POD, and MEHA) was added to a mixed solution, mix well and incubate for 10 minutes at 37 °C temperature. Within 30 minutes read absorbance (A) of FFA calibrator and serum samples against reagent blank. The concentration of FFA is quantitating by spectrophotometer at the wavelength of 550 nm. FFA concentration is calculated according to the following equation:

$$\text{FFA concentration} = \frac{\Delta A \text{ sample} \times \text{Calibrator concentration}}{\Delta A \text{ calibrator}}$$

3.2.6 Determination of pancreatic TG level

The ectopic accumulation of lipid stores in pancreatic tissue is associated with a number of diseases such as insulin resistance, metabolic syndrome and T2D. Fatty infiltration in the pancreas has been termed pancreatic steatosis [5]. Excess intracellular fatty acids, associated with accumulation of TG in β-cells, can induce a variety of cellular stresses, leading to β-cell dysfunction such as impaired insulin secretion.

The pancreatic TG contents are determined as described previously [136]. A 50 mg of pancreas was homogenized and extracted with 1 mL of isopropanol. After centrifugation, TG contents in the supernatant were determined using enzymatic colorimetric method similar to the determination of serum TG [134].

A 10 µL of supernatant or TG calibrator (200 mg/dL or 2.28 mmol/L) was added to a 1,000 µL of TG reagent (R1 reagent), mixed and subsequently incubated for 10 minutes at room temperature. Then read absorbance of samples and triglyceride calibrator against reagent blank within 60 minutes after start. The concentration of triglyceride is quantitating by spectrophotometer at the wavelength of 546 nm. The concentration of pancreatic TG is expressed as mg/g tissue. The pancreatic TG concentration is calculated according to the following equation:

$$\text{Triglyceride concentration} = \frac{\Delta A \text{ sample} \times \text{Calibrator concentration}}{\Delta A \text{ calibrator}}$$

3.2.7 Determination of serum and pancreatic MDA levels

MDA is a major end product formed during the peroxidation of lipids and is regarded as marker of lipid peroxidation in tissues [79]. In the pancreas of patients with obesity, which leads to increased oxidation and generation of ROS, has been documented [80]. Yan et al. [81] reported that an HFD-induced obese rats increases lipid peroxidation and ROS, and decreases pancreatic microcirculation. These changes would result in an inflammatory state which was induces cellular senescence. Thus, the measuring tissues MDA was required to determine whether obese rats have increased oxidative stress and are more prone to cellular senescence.

The pancreas tissue was homogenized in 0.7 mL of 0.05 M phosphate buffer. Then, the mixture was centrifuged at 12,000 rpm for 15 minutes at 4 °C. A portion of cleared supernatant was used for the determination of MDA.

The concentration of MDA is measured by the double heating method and performed as previously described [137] with minor modification (Appendix E). MDA reacts with thiobarbituric acid producing thiobarbituric acid reactive substance (TBARS), a pink chromogen, which can be measured using enzymatic colorimetric method. A 1 mL of trichloroacetic acid (TCA) solution (10%, wt/vol) was added to 250 µL of serum or supernatant of the tissue preparation in each centrifuge tube, and tubes were placed in a boiling water bath for 15 minutes. The tubes were centrifuged at 1,000 g for 10 minutes at room temperature, and 800 µL of each sample supernatant transferred to a test tube containing 400 µL of TBA solution (0.67%, wt/vol). Each tube was placed in a boiling water bath for 15 minutes. After cooling to room temperature, the absorbance was measured at 532 nm. MDA concentrations is determined using 1,1,3,3-tetraethoxypropane (Sigma-Aldrich, Carlsbad, CA, USA) as standard and expressed as nmol/mg protein for pancreas tissues and as nmol/dL for serum.

For pancreas tissues, total protein levels were normalized with the MDA levels and determined by Bradford protein assay kit (Bio-Rad, Hercules, CA, USA) according to the manufacturer's instructions. A 20 µL of sample solution or bovine serum albumin (BSA) standard with a known concentration (125, 250, 500, 750, and 1,000 µg/mL) was mixed with a 1 mL of dye reagent (dye reagent composed of Coomassie Brilliant Blue-G-250 dye and other components). This mixture was incubated at room temperature for at least 5 minutes and detected at 595 nm in the assay using a spectrophotometer. The protein concentrations of unknown sample are determined by using the standard curve of BSA standard.

3.2.8 Determination of pancreatic mRNA expression

The differential displays of pancreatic mRNA for NF-κB, SREBP-1c, IRS-2, GLUT-2 and GK mRNA were measured by quantitative real-time polymerase chain reaction (real-time PCR) analysis. A flowchart for the determination of mRNA expression is shown in Appendix G.

SREBP-1c is now well established as a key transcription factor in the regulation of lipogenesis in the pancreas. The activation of SREBP-1c is essential for impaired insulin secretion and islet mass associated with the accumulation of TG [7, 8].

IRS-2 has particularly important roles in the control of cell survival, metabolic fuel homeostasis, and cell function. The down-regulation of IRS-2 gene in the β-cells led to impaired GSIS [9-10]. In addition, the impaired glucose sensing of the pancreatic β-cell resulted in the decrease of insulin secretion. This impairment is believed to be initiated after the down-regulation of GLUT-2 and GK gene, which are important glucose-sensing genes [12].

NF-κB is implicated in a multiple physiological and pathobiological pathways in the pancreas including inflammatory response, immune response, redox homeostasis, as well as cellular senescence. The suppression of NF-κB signaling by silencing of NF-κB subunits led to the evasion of senescence. In addition, the inhibition of NF-κB could reduce cellular senescence, oxidative stress and oxidative damage *in vitro* and *in vivo* [19-20]. All NF-κB family show as a homodimer or heterodimer in cells such as p50/p50 dimer, p50/p52 dimer and p50/p65 dimer; however, p50/p65 dimer is the most common NF-κB dimer and the most studied in the others mammalian cells [93-94].

3.2.8.1 Total RNA isolation

Pancreatic RNA was isolated using standard protocols as described previously [138]. Pancreas tissue was homogenized by sterile mortar on liquid nitrogen. A 1 mL of TRIzol® reagent (TRIzol® reagent consisted of phenol, guanidinium thiocyanate and other components) was added to homogenized tissue and incubated at room temperature for 5 minutes. The homogenates were mixed with a 200 µL of chloroform, shaken vigorously for 15 seconds and incubated for 2-3

minutes at room temperature. Then, the mixture was centrifuged at 12,000 × g for 15 minutes at 4 °C. This centrifuged mixture was separate into three phase. The RNA was harvested from the aqueous phase and placed to a 500 µL of 2-propanol (isopropanol). The mixture was incubated for 10 minutes at room temperature, followed by centrifugation at 12,000 × g for 10 minutes at 4 °C. Then, the supernatant was removed. The RNA pellet is washed with a 1 mL of 75% ethanol and then centrifuged at 7,500 × g for 5 minutes at 4 °C. The RNA pellet was dried for 10-15 minutes at room temperature. Dried RNA was dissolved with DEPC-treated water or RNase-free water.

The RNA concentration and quality measure by using the NanoDrop 2000 spectrophotometer. The purity of RNA was checked by ratio of sample absorbance at 260 and 280 nm (260/280 ratio), which should be approximately 1.9-2.1 for pure RNA.

3.2.8.2 Complementary deoxyribonucleic acid (cDNA) synthesis

Reverse transcription was employed to convert mRNAs into cDNAs by using the High Capacity cDNA Reverse Transcription Kits. A 10 µL of total RNA (20 ng/µL) was converted to cDNA with MultiScribe™ Reverse Transcriptase in a 10 µL volume of reverse transcription reaction mixture containing a 3.2 µL RNase-free water, 2.0 µL RT buffer, 2.0 µL RT random primers, 0.8 µL deoxyribonucleotide triphosphates (dNTPs) mix, 1.0 µL RNase inhibitor and 1.0 µL MultiScribe™ Reverse Transcriptase. The MyCycler™ thermal cycler conditions were programmed as follows: an initial set up cycle at 25 °C for 10 minutes and 37 °C for 120 minutes, followed by cycles at 85 °C for 5 minutes, and 4 °C for infinity. Each cDNA solution was kept at −80 °C until is used in the real-time PCR analysis.

3.2.8.3 Real-time PCR analysis

Real-time PCR was used to amplify a segment of a known sequence from cDNA with gene specific primers. cDNA is amplified by using the TaqMan® Gene Expression Master Mix [TaqMan Gene Expression Master Mix contains: AmpliTaq Gold® DNA Polymerase, Ultra Pure, Uracil-DNA glycosylase

(UDG), dNTPs with deoxyuridine triphosphate (dUTP), ROX™ Passive Reference and Optimized buffer components] and TaqMan® Gene Expression Assay.

Each reaction contained 4 µL cDNA solution (40 ng/µL), 10 µL TaqMan® Gene Expression Master Mix, 1.5 µL TaqMan® Gene Expression Assay and 4.5 µL RNase-free water in a final volume of 20 µL. This mixture was transferred into each well of a 96-well plate reaction. β-actin was used as internal control.

96-well plate was loaded into StepOne™ Real-Time PCR System (Applied Biosystems). Cycling conditions were as follows: an initial set up cycle at 50 °C for 2 minutes and 95 °C for 10 minutes, followed by 40 cycles at 95 °C for 15 seconds, and 60 °C for 1 minute. The cycling program used is presented in Table 3.2.

Table 3.2 The real-time PCR conditions

Step	UDG incubation	AmpliTaq Gold, UP enzyme activation	PCR	
	Hold	Hold	Cycle (40 cycles)	
			Denature	Anneal/extend
Temperature (°C)	50	95	95	60
Time	2 minutes	10 minutes	15 seconds	1 minute

Relative mRNA levels were measured using the system above via TaqMan analysis that employed gene-specific primers and probes [FAM dye-labeled minor groove binder (MGB) probe or TaqMan MGB probe]. TaqMan MGB probes composed of reporter dye (FAM dye) and nonfluorescent quencher (NFQ)-linked MGB at 5´and 3´ end, respectively. The quencher dye has a suppressible activity to fluorescence in the reporter. During PCR, the reporter dye was separated from the quencher dye by 5´ exonuclease activity of the DNA polymerase. The releasing of the reporter dye results in elevated fluorescence. This elevation was detected for determination of real-time PCR products (Appendix F).

The real-time PCR results were quantified base on the number of cycles required for amplification-produced fluorescence to reach a specific threshold of detection. The threshold cycle or C_T value for each individual PCR product was calculated by the instrument's software and C_T values obtained for the target gene were normalized by subtracting the C_T values obtained with the reference gene (C_T of target gene – C_T of reference gene, ΔC_T). The resulting ΔC_T values were then used to calculate relative expression levels of each sample. The relative quantitation (RQ) value using the comparative $2^{-\Delta\Delta CT}$ method and according to the equation:

$$RQ = 2^{-(\Delta CT \text{ of sample} - \Delta CT \text{ of reference sample})}$$
$$= 2^{-\Delta\Delta CT}$$

Details of the $2^{-\Delta\Delta CT}$ method have been previously described [139]. To allow for comparisons the fold expression levels of RQ value between control group and other groups, quantities of all targets in test samples were normalized to the constitutive reference gene β-actin (endogenous control).

3.2.9 Histological analysis

Details of the hematoxylin and eosin (H and E) staining have been previously described [140]. The epididymal adipose and body of pancreas tissues were fixed in 10% formalin in phosphate buffer and embedded in paraffin. The serial sections were cut into 4 μm thick and stained with H and E. The process of staining was shown in Figure 3.1. The samples were then examined for morphology of adipocytes, and pancreatic islet and acinar cells under a light microscope (Eclipse Ci-L microscope, Nikon, Tokyo, Japan) equipped with a digital camera (DS-Fi2 microscope camera, Nikon). The number of islets was counted per one square centimeter under a light microscope. Mean adipocyte and islets areas were calculated from 100 and 10 cells observed/cm^2 of section, respectively. Areas of the adipocytes and islets were measured by Axiovision AC microscopy software (Carl Zeiss, Bovenden, Germany).

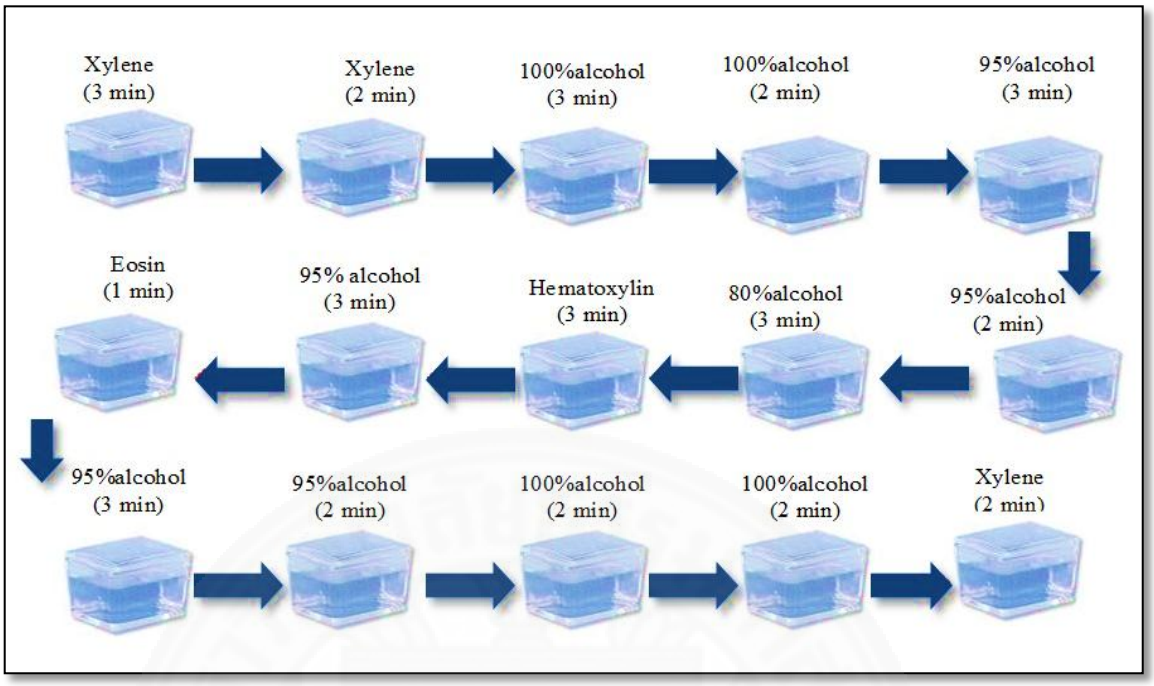

Figure 3.1 Process of staining with hematoxylin and eosin (modified from Feldman and Wolfe) [140]

3.2.10 Immunohistochemical analysis

SABG is known as a marker of senescent cells. In diabetic rats, HFD consumption led to progressive loss of β-cell mass associated with a prolonged increase activity of SABG [14-15]. Although senescent cells undergo phenotypic changes in morphology, including hypertrophy and flattening/enlargement of cells, the most common and reliable method for detection and differentiation from a quiescence state (a temporary arrest of the cell cycle) is the expression of SABG [89].

Details of the immunoperoxidase staining have been previously described [141]. Pancreatic tissues were fixed in buffered 10% formalin, processed to wax blocks and sectioned onto slides (4 µm thickness). Bake slides for 30 minutes at 60 °C prior to starting immunohistochemically detect SABG in pancreatic tissue sections (as shown in Figure 3.2). Then, slides were deparaffinized using the xylene, rehydrated through serial dilutions of ethyl alcohol (100%, 95%, 90%, 80% and 70% ethyl alcohol, respectively) and washed in DW for 5 minutes.

After rehydrated, the slides were outlined each section with a PAP pen and placed in dark moist chamber. The extracellular matrix was removed by

0.01% hyaluronidase in phosphate-buffered saline (PBS) for 10 minutes at 37 °C. Then, the sections were washed with DW and quenched endogenous peroxidase by incubating the tissue sections with 3% hydrogen peroxide in methyl alcohol for 30 minutes at 37 °C. After quenching, the sections were rinsed thrice with DW, then once in 1× PBST (1× PBS supplemented with 0.1% Tween-20) and blocked non-specific binding sites by incubating the tissue sections with 5% bovine serum albumin (BSA) in 1× PBST for 30 minutes at 37 °C. An SABG polyclonal antibody (1:100) as a primary antibody was added to the sections, incubated for 60 minutes at 37 ºC. Primary antibody was omitted and replaced it with 1× PBST during the procedures as negative control. The sections were washed 5 times in 1× PBST for 5 minutes each. Horseradish peroxidase-conjugated anti-rabbit IgG (1:1,000) were used as a secondary antibody. The sections were incubated for 60 minutes at 37 °C and washed 5 times in 1× PBST for 5 minutes each. 3', 3'-diaminobenzidine (DAB) solution as a chromogen was added and incubated for 3 minutes. When in the presence of peroxidase enzyme, DAB produces a brown precipitate that is insoluble in alcohol and xylene. The sections were stopped the color reaction with DW rapidly. Then, the sections were counterstained with Mayer's hematoxylin for 5 minutes. Rinse the section with tap water for 5 minutes and place in 1× PBS for 3 minutes. Finally, slides were dehydrated by increasing in the concentration of ethyl alcohol (95 and 100 % ethyl alcohol, respectively) and xylene. Slides were coverslipped with an Entellan® as a mounting media.

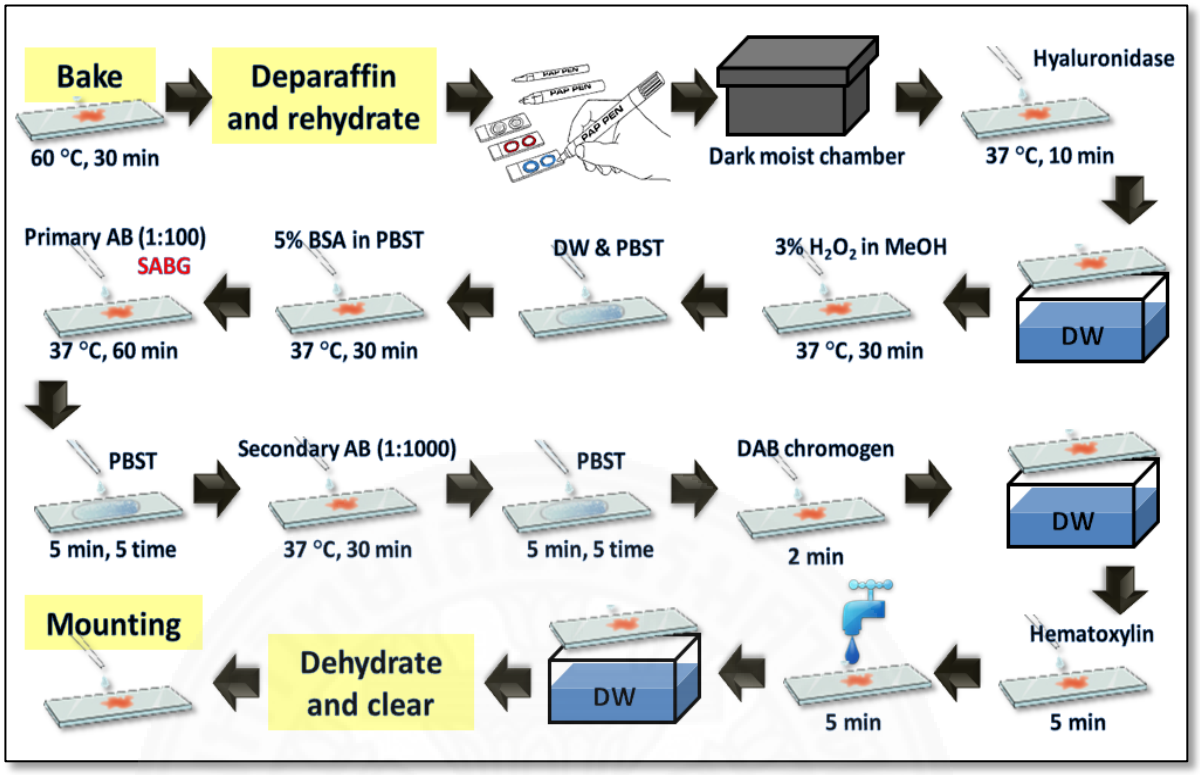

Figure 3.2 Process of staining with SABG

The DAB reaction was permanent and shown as stable brown pigment. The slides were photographed using a bright-field microscope coupled to a microscope camera. For semi-quantitative measurements of SABG expression, the densities of the islets were analyzed by the mean of ten different islets of cross section, using the NIS-Elements Documentation version 4.20 software.

3.2.11 Statistic analysis

Data were expressed as mean ± standard error of mean (S.E.M.). All data were analyzed using Statistics Package for the Social Sciences (SPSS) for Windows Version 16.0. A one-way analysis of variance (ANOVA) with post hoc least significant difference (LSD) test was used to determine significant differences between each experimental group. The level of significance was set at *p*-value less than 0.05.

CHAPTER 4
RESULTS AND DISCUSSION

4.1 Effects of RBE on daily dietary intakes and body weights

Human studies have shown that increased HFD intake is associated with body weight gain which can lead to obesity and other related metabolic diseases. Animal rodent models are therefore useful tools for studying obesity and obesity-related health problems [2, 142]. As shown in Table 4.1, the rats in C group consumed significantly ($p < 0.001$) more food than HF group per day. However, the energy intake was significantly ($p < 0.001$) higher in HF, HFR1, HFR2 and HFM groups than in C group. Food and energy intakes were not significantly different among HFD-fed rats. As shown in Table 4.2, the initial body weight of rats before treatment was not significantly differed among the experimental groups. After 4 weeks, the final body weight and body weight gain of rats were significantly ($p < 0.001$) increased in the HF group compared with the C group. Consistent with previous studies, obesity, and increased body weight gain were observed in rats fed an HFD alone when compared with rats fed a standard chow [24, 25]. Body weight increment of rats may result from excessive abnormal fat accumulation.

However, these elevations were significantly decreased after rats were treated with the RBE and metformin ($p < 0.001$ and $p < 0.05$, respectively). Thus, our results imply that RBE and metformin treatment may lead to the amelioration of the HFD-induced obesity. The mechanism of anti-obesity effect may, therefore, be mediated via the inhibition of fat accumulation in other organs, especially in adipose tissue. These results further support the anti-obesity property of rice bran enzymatic extract and metformin previously reported in animal models of metabolic syndrome [24, 127].

Table 4.1 Daily dietary intakes

Groups	Dietary intake	
	Food (g/day)	Energy (kcal/day)
C	23.21 ± 0.05	70.56 ± 0.16
HF	19.07 ± 0.33***	97.66 ± 1.69***
HFR1	18.59 ± 0.50***	95.21 ± 2.81***
HFR2	18.23 ± 0.54***	94.84 ± 2.06***
HFM	19.73 ± 0.20***	101.06 ± 1.02***

Values are expressed as mean ± SEM (n = 6).

***$p < 0.001$ vs C

Table 4.2 Body weights

Groups	Body weight (g)		
	Initial	Final	Gain
C	244.30 ± 2.08	366.05 ± 0.93	123.55 ± 1.13
HF	243.69 ± 1.80	413.24 ± 2.28***	168.52 ± 1.86***
HFR1	244.06 ± 1.20	367.20 ± 6.85†††	121.45 ± 3.98 †††
HFR2	241.34 ± 1.80	358.78 ± 7.35†††	117.58 ± 7.72 †††
HFM	242.99 ± 1.96	393.27 ± 4.21***,†	149.09 ± 3.78***,†

Values are expressed as mean ± SEM (n = 6).

***$p < 0.001$ vs C

†$p < 0.05$, †††$p < 0.001$ vs HF

4.2 Effects of RBE on intra-abdominal fat accumulation

Abdominal obesity, especially with an excess of intra-abdominal or visceral adipose tissue is associated with pancreatic abnormalities [1]. Obesity is characterized by excess adipose tissue mass resulting from hypertrophy and/or hyperplasia of adipocytes [31]. In addition, insulin-resistant adipocytes lead to an increased efflux of FFA from adipocytes to circulation and extra-adipose tissues such as liver, muscle, kidney, heart, blood vessel, and pancreatic β-cell as well as reflect to adipose tissue. This active adipocytes-macrophages crosstalk leading to dysregulated secretion of a variety of adipokines such as low adiponectin levels and massive amounts of intracellular lipid and its toxic metabolites accumulation (lipotoxicity) result in metabolic derangement, insulin resistance, inflammation, oxidative stress, and multiple organ dysfunction on numerous ectopic tissues, which include the pancreas [29-33].

Relative fat weights of rats are shown in Table 4.3. The relative weights of omental and epididymal fat tissues were significantly ($p < 0.001$) increased in the HF group as compared with the C group. Consistent with previous studies, an increased in omental and epididymal fat tissues were observed in rats fed an HFD alone when compared with rats fed a standard chow [24-25]. An excess of intra-abdominal or visceral adipose tissue may lead to fat infiltration of multiple organs including the heart, kidneys, liver, as well as pancreas [30, 33].

RBE supplementation caused a significant ($p < 0.001$) decrease in both omental and epididymal fat weight when compared to rats fed an HFD alone. At the same time, the HFM group also exhibited significantly lower relative weights of omental fat ($p < 0.001$) and epididymal fat ($p < 0.05$) tissues than HF group. Examination of H and E-stained sections of the epididymal fat is shown in Figure 4.1. The epididymal fat was examined for morphology and area of adipocytes (Table 4.3). The epididymal adipocyte size in the HFD-fed group was markedly ($p < 0.001$) larger than in the C group. However, the adipocyte size was significantly ($p < 0.001$) smaller in the HFR1, HFR2 and HFM groups than in the HF group. The result indicates that an oral administration of RBE and metformin markedly suppressed the body weight gain, intra-abdominal fat deposition and adipocyte size of the HFD-induced obesity in

rats independently of food intake. The current results are in agreement with previous reports indicating that the RBE and metformin treatment caused a significant decrease in abdominal fat weight and adipocyte size in HFD-fed rats [24-25]. Previous studies have also reported the anti-obesity effects of rice bran enzymatic extract and rice bran in animals with metabolic syndrome [21].

Table 4.3 Abdominal fat accumulation

Groups	Fat weights (g/100 g body weight)		Adipocyte size (μm^2)
	Omental fat	Epididymal fat	
C	1.29 ± 0.06	1.45 ± 0.03	3,231.29 ± 88.49
HF	2.18 ± 0.04***	2.04 ± 0.05***	5,008.60 ± 6.30***
HFR1	1.39 ± 0.09†††	1.60 ± 0.05†††	3,488.83 ± 60.25**,†††
HFR2	1.49 ± 0.15†††	1.69 ± 0.10*,†††	3,590.39 ± 47.20***,†††
HFM	1.52 ± 0.08†††	1.84 ± 0.05***,†	4,041.78 ± 30.51***,†††

Values are expressed as mean ± SEM (n = 6)

$^{*}p < 0.05$, $^{**}p < 0.01$, $^{***}p < 0.001$ vs C

$^{\dagger}p < 0.05$, $^{\dagger\dagger\dagger}p < 0.001$ vs HF

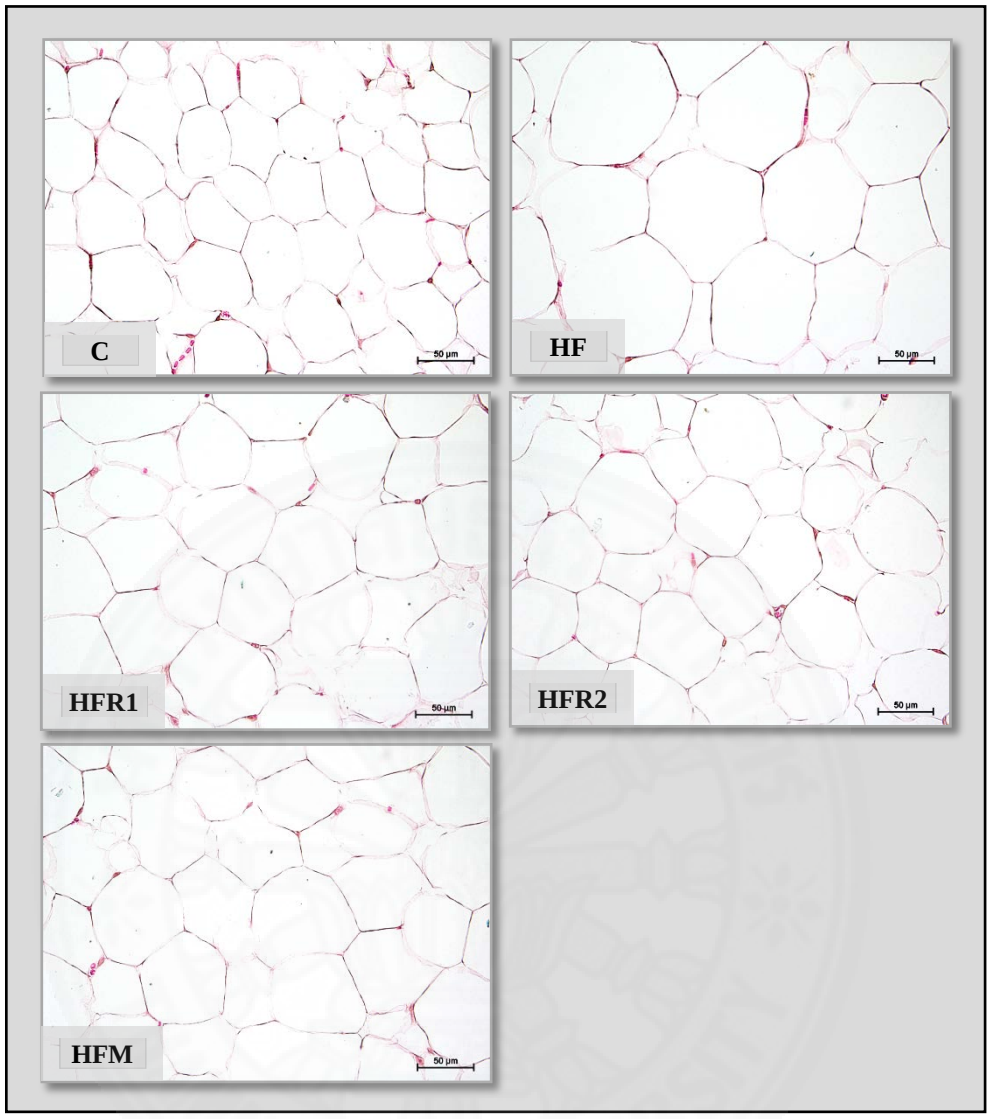

Figure 4.1 Histology (H and E staining) of epididymal adipocytes (400× magnification; scale bar = 50 μm)

4.3 Effects of RBE on glucose homeostasis parameters

Impaired glucose metabolism, including hyperglycemia, impaired glucose tolerance and insulin resistance, are the common pathological features of obesity and T2D, and are associated with pancreatic abnormalities [1, 4]. The hyperglycemia that appears with insulin resistance can have deleterious effects on tissue and organs such as pancreas. The control of blood glucose and insulin sensitivity remains the major

means by which the development of hyperglycemia- or hyperinsulinemia-associated complications can be minimized [4, 37-38].

Table 4.4 shows the effect of RBE on glucose homeostasis parameters. The HF group exhibited significantly higher levels of FBG ($p < 0.001$), serum insulin ($p < 0.05$) and AUC-G ($p < 0.001$) than C group. Moreover, the OGTT of HF group was significantly ($p < 0.001$) increased blood glucose in fasting state and at 0.5, 1.0, 1.5, 2.0, and 2.5 hours after glucose feeding as compared with the C group (Figure 4.2). These alterations may result in structure and function of pancreatic cell such as loss of β-cell mass [63], β-cell dysfunction [49], oxidative stress [12, 51], as well as cellular senescence [15].

Interestingly, treatment with RBE in HFR1 and HFR2 groups significantly ($p < 0.05$) decreased both FBG ($p < 0.001$) and serum insulin ($p < 0.01$) levels as compared with the HF group. AUC-G showed a tendency to be reduced in the HFR2 group compared with the HF group, but the difference was not significant. However, HFR1 group exhibited significantly ($p < 0.01$) lower AUC-G than HF group (Table 4.4). In addition, the OGTT of HFR1 group showed significant lower blood glucose ($p < 0.01$) in fasting state and at 1.0, 1.5, 2.0, and 2.5 hours after glucose feeding as compared with the HF group (Figure 4.2). While the OGTT of HFR2 group showed significant lower blood glucose ($p < 0.01$) in fasting state and at 2.0 and 2.5 hours. This illustrates that RBE was able to prevent impaired fasting glucose and impaired glucose tolerance induced by the HFD feeding of the rats. To support this notion, rice bran protein and phytic acid, the important bioactive compounds in rice bran, have also been shown to exert significant hypoglycemic effect in high-calorie-fed animals [128, 143].

Metformin, a widely used anti-diabetic drug for the treatment of T2D, attenuates hyperglycemia by inhibiting hepatic gluconeogenesis, enhancing muscle glucose uptake, improving insulin sensitivity, suppressing lipogenesis, and inhibiting absorption in gastrointestinal [144]. In the presence of metformin, an administration of metformin showed a significant ($p < 0.001$) decrease in AUC-G when compared with the HF group. Insulin in serum also showed a tendency to decrease in the HFM group, but the differences were not statistically significant (Table 4.4). As shown in Figure 4.2, the OGTT of HFM group presented a significant ($p < 0.05$) low blood

glucose at 2.0 and 2.5 hours after glucose feeding as compared with the HF group. Also in this study, improvement of serum FBG and insulin levels by metformin was not significant reduction, but with normalization of glucose utilization (AUC-G of OGTT). The present findings suggest that decreased of AUC-G level by metformin treatment may result from improved insulin sensitivity in HFD-induced obese rats. However, how metformin functions in pancreatic β-cells is still uncertain [145].

Table 4.4 Glucose homeostasis parameters

Groups	FBG (mg/dL)	AUC-G (mg/dL.min.)	Insulin (mU/L)
C	105.00 ± 1.53	2,530.29 ± 110.88	35.46 ± 2.86
HF	116.17 ± 1.05***	4,025.00 ± 244.85***	45.06 ± 1.93*
HFR1	105.67 ± 1.45†††	2,922.74 ± 339.02††	32.21 ± 1.32††
HFR2	107.33 ± 2.30†††	3,369.03 ± 226.76*	33.10 ± 3.50††
HFM	118.67 ± 0.76***	2,674.55 ± 139.20†††	38.18 ± 4.49

Values are expressed as mean ± SEM (n = 6).

$^{*}p < 0.05$, $^{***}p < 0.001$ vs C

$^{\dagger}p < 0.05$, $^{\dagger\dagger}p < 0.01$, $^{\dagger\dagger\dagger}p < 0.001$ vs HF

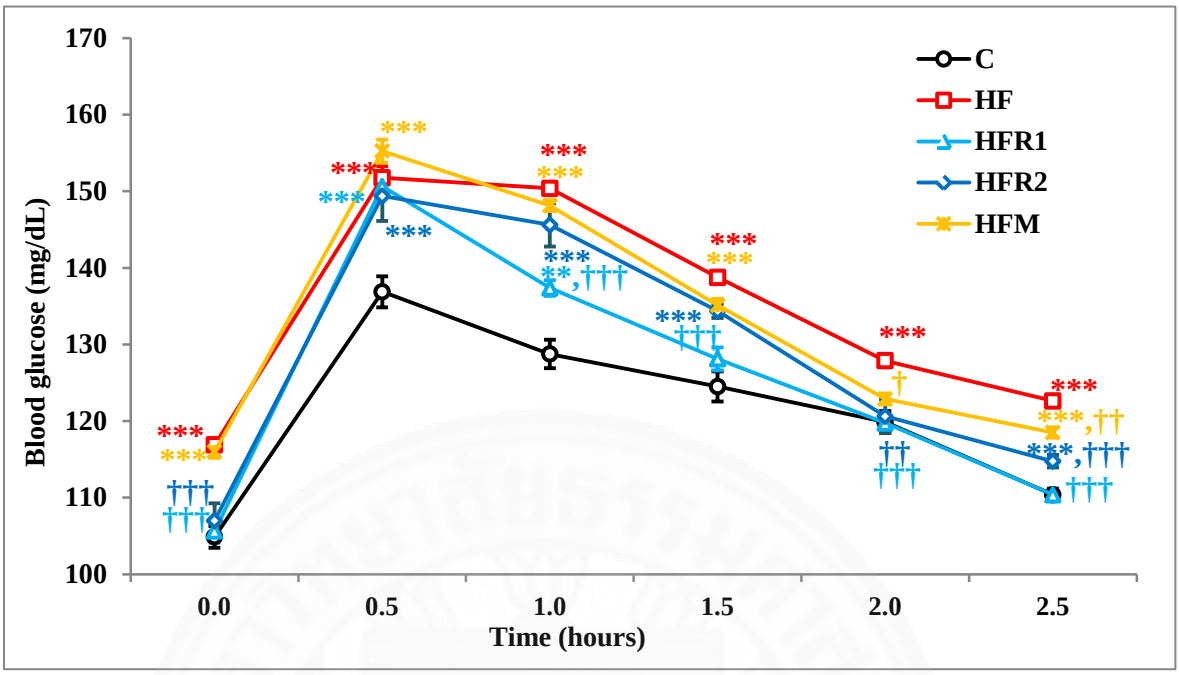

Figure 4.2 Blood glucose levels during an oral glucose tolerance test (OGTT)
Values are expressed as mean ± S.E.M., (n= 6).
$^{**}p < 0.01$, $^{***}p < 0.001$ vs C
$^{\dagger}p < 0.05$, $^{\dagger\dagger}p < 0.01$, $^{\dagger\dagger\dagger}p < 0.001$ vs HF

4.4 Effects of RBE on serum lipid profile

The dyslipidemia related to insulin resistance and obesity is characterized by increased TG and LDL-C levels, and decreased HDL-C level [35]. It is generally accepted that dyslipidemia, including the increased circulating FFA levels, are involved in the β-cells dysfunction and death [35, 146-147]. FFA acts as potent signaling molecules in several cellular processes, including insulin secretion [145, 148]. Experimental evidence indicates that prolonged exposure to high FFA concentrations has lipotoxicity effects on β-cells, including reduced GSIS, suppressed proinsulin biosynthesis, and β-cell loss by apoptosis [111, 149]. Thus, prolonged exposure to high FFA can reduce generations of β-cells, as in T2D.

As shown in Table 4.5, HFD-fed rats showed significantly increased total-C ($p < 0.05$), TG ($p < 0.05$), LDL-C ($p < 0.001$) and FFA ($p < 0.05$) levels while

significantly decreased HDL-C ($p < 0.05$) levels in serum when compared with the C group. However, RBE-treated rats had significantly lower levels of serum total-C, TG (except HFR1 group), LDL-C and FFA compared to rats fed an HFD alone. HDL-C showed a tendency to be increased in the HFR1 and HFR2 groups compared with the HF group, but the difference was not significant. The hypolipidemic effect of RBE could probably be due to its components such as protein and phytic acid, which were shown to have anti-hyperlipidemic properties [22, 127-128].

Metformin not only was used to improve hyperglycemia, but also suppressing lipogenesis, and inhibiting absorption in gastrointestinal [144]. In the present study, the serum total-C and LDL-C levels of metformin-treated rats were significantly lower than those of the HFD-fed rats ($p < 0.001$ and $p < 0.05$, respectively). While TG, HDL-C and FFA levels of HFM group was not significantly different from HF group. Unlike present results, these differences may be due to the dose of metformin, and experimental designs [150-152].

Table 4.5 Serum lipid profile

Groups	Serum lipid profile (mg/dL)				
	Total-C	TG	LDL-C	HDL-C	FFA
C	85.00 ± 1.50	32.60 ± 2.82	25.48 ± 2.56	53.79 ± 0.83	15.11 ± 0.79
HF	94.87 ± 2.93*	41.52 ± 2.65*	37.77 ± 3.01***	46.97 ± 1.56*	17.14 ± 0.55*
HFR1	85.11 ± 2.92†	34.98 ± 1.76	30.94 ± 0.95†	50.87 ± 3.68	14.38 ± 0.45††
HFR2	83.62 ± 3.80††	32.75 ± 2.29†	26.98 ± 2.23††	49.18 ± 2.56	14.10 ± 0.77††
HFM	78.43 ± 1.85†††	38.51 ± 2.23	29.96 ± 1.89†	44.75 ± 1.57**	16.64 ± 0.34

Values are expressed as mean ± SEM (n = 6).

$^{*}p < 0.05$, $^{**}p < 0.01$, $^{***}p < 0.001$ vs C

$^{\dagger}p < 0.05$, $^{\dagger\dagger}p < 0.01$, $^{\dagger\dagger\dagger}p < 0.001$ vs HF

4.5 Effects of RBE on pancreas weight, islet area, and islet number

Pancreatic islets are important micro-organs which consist of several endocrine cell types that function together to maintain glucose homeostasis. The islets have a well-defined structure with a central core of β-cells representing 60-80% of the cells of the islet and a layer of other endocrine cells surrounding the core [39]. Insulin is secreted from the β-cells of the pancreatic islets in response to an elevation of blood glucose concentration [42]. In individual with obesity, an expansion in β-cell mass occurs to provide sufficient insulin and to prevent hyperglycemia [153]. In contrast, chronic hyperglycemia leads to progressive loss of β-cell mass with a prolonged increase in the rate of β-cell apoptosis without a compensatory increase in β-cell growth [147, 154]. Thus, the balance between cell proliferation and apoptosis is an important factor in the maintenance of β-cell mass.

In the present study, relative pancreatic weights and number of islets were not significantly different in all groups of experiment (Table 4.6). These results are also in agreement with previous studies [24-25]. When compared to the C group, the area of islet was significantly ($p < 0.01$) larger in the HF group (Table 4.6). These increases may be attributed to the increased cell proliferation in the pancreatic islets of HFD-fed rats. The HFR1, HFR2 and HFM groups exhibited significantly smaller islet area than the HFD alone group ($p < 0.01$, $p < 0.05$ and $p < 0.01$, respectively). Examination of H and E-stained sections of the pancreatic islets in the C group revealed no obvious changes (Figure 4.3). Irregular and larger shapes of islets were observed after the rats were fed with HFD for 4 weeks. The islets of HFR1, HFR2 and HFM groups that received two doses of RBE exhibited smaller shape than those in the HF group. Therefore, the present data suggest that the RBE- and metformin-treated rats may inhibit HFD-induced pancreatic abnormalities by reducing the induction of excessive cell proliferation in islets.

Table 4.6 Pancreas weight, islet area, and islet number

Groups	Pancreas weights (g/100 g body weight)	Islet area (×1,000 μm^2)	Islet number (per 1 cm^2)
C	0.50 ± 0.04	8.35 ± 0.14	27.33 ± 3.71
HF	0.48 ± 0.03	17.98 ± 1.54**	18.67 ± 4.67
HFR1	0.51 ± 0.02	10.17 ± 0.63††	28.67 ± 8.51
HFR2	0.50 ± 0.02	11.85 ± 2.90†	25.33 ± 6.36
HFM	0.51 ± 0.04	10.71 ± 0.99††	26.67 ± 4.37

Values are expressed as mean ± SEM (n = 6 for pancreas weights and n = 3 for area and number of Islet).

$^{**}p < 0.01$ vs C

$^{†}p < 0.05$, $^{††}p < 0.01$ vs HF

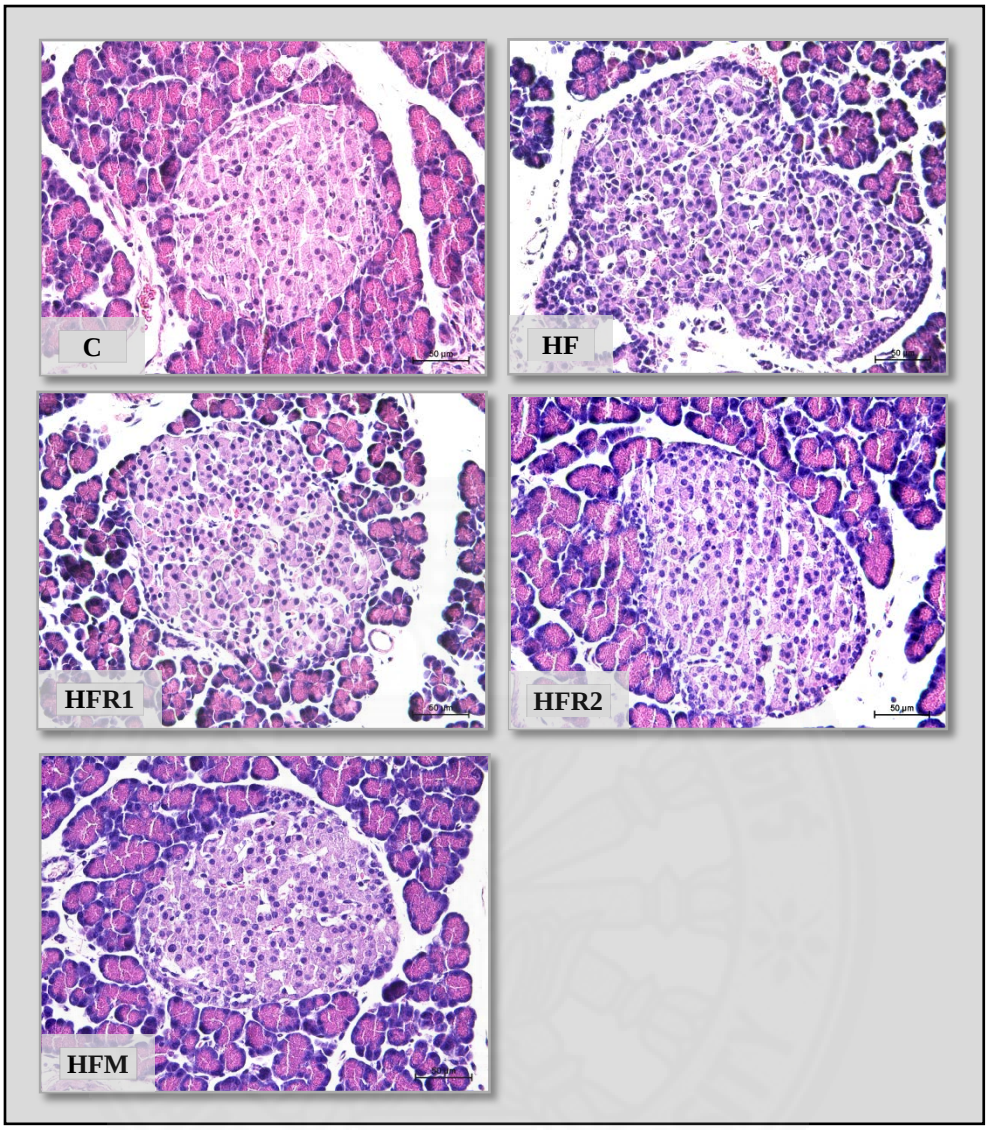

Figure 4.3 Histology (H and E staining) of pancreatic Islets (400× magnification; scale bar = 50 μm)

4.6 Effects of RBE on pancreatic steatosis

We also evaluated the effect of RBE on HFD-induced ectopic fat deposition in the pancreas. Excessive lipid accumulation in the pancreatic tissue is one of the important pathogenesis of pancreatic disorder, which can promote insulin resistance, oxidative stress, and apoptosis in tissues [155]. SREBP-1c has been proposed to be a major lipogenic transcription factor in various tissues including the pancreas [7]. The activation of SREBP-1c in response to various metabolic stimuli,

including hyperinsulinemia, hyperglycemia, and high FFA levels, results in the up-regulation of lipogenic genes, such as fatty acid synthase (FAS) gene [8, 156]. The up-regulation of this transcription factor in the pancreas was found in association with the accumulation of TG [7, 76].

As presented in Figure 4.4, HF group exhibited significantly increased both pancreatic TG ($p < 0.001$) and SREBP-1c mRNA ($p < 0.01$) levels as compared with C group. However, the pancreatic TG and SREBP-1c mRNA levels were significantly decreased in RBE-treated rats when compared with the rats fed an HFD alone. SREBP-1c mRNA level in pancreas showed a tendency to decrease in the HFM group, but the differences were not statistically significant. However, an administration of metformin showed a significant ($p < 0.001$) decrease in pancreatic TG level when compared with the HF group. Examination of H and E-stained sections of the pancreatic acinar cells in the C group revealed no obvious changes (Figure 4.5). After 4 weeks, vacuoles were obvious in acinar cells of obese rats. Similar results were found in animal models of metabolic syndrome [157-158]. However, acinar cells of the RBE- and metformin-treated rats revealed decreased vacuoles compared to the HF group (Figure 4.5). Our results indicate that the RBE treatment may prevent ectopic fat deposition in the pancreas, at least in part, via a decrease in SREBP-1c expression. Furthermore, our preliminary study demonstrated that the administration of RBE significantly decreased TG levels and SREBP-1c expression in the liver and heart of HFD-fed rats. The inhibitory effect of RBE on SREBP-1c may be mediated, at least in part, by the reduction of serum insulin, glucose, and FFA levels. To support these results, Boonloh et al. [128] showed that hepatic SREBP-1c and FAS mRNA expression were down-regulated by the consumption of rice bran protein hydrolysates in rats fed a high-energy diet.

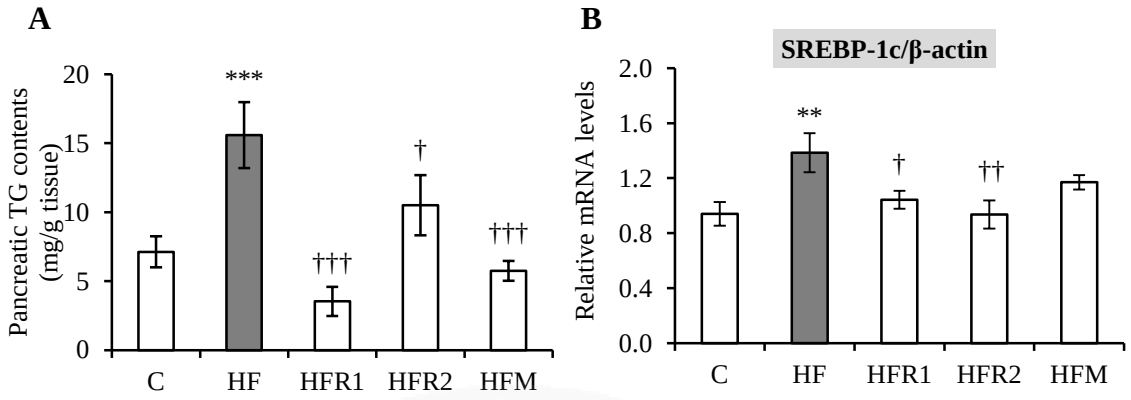

Figure 4.4 Pancreatic TG contents (A) and SREBP-1c mRNA expression (B)

Values are expressed as mean ± SEM (n = 6)

$^{**}p < 0.01$, $^{***}p < 0.001$ vs C

$^{\dagger}p < 0.05$, $^{\dagger\dagger}p < 0.01$, $^{\dagger\dagger\dagger}p < 0.001$ vs HF

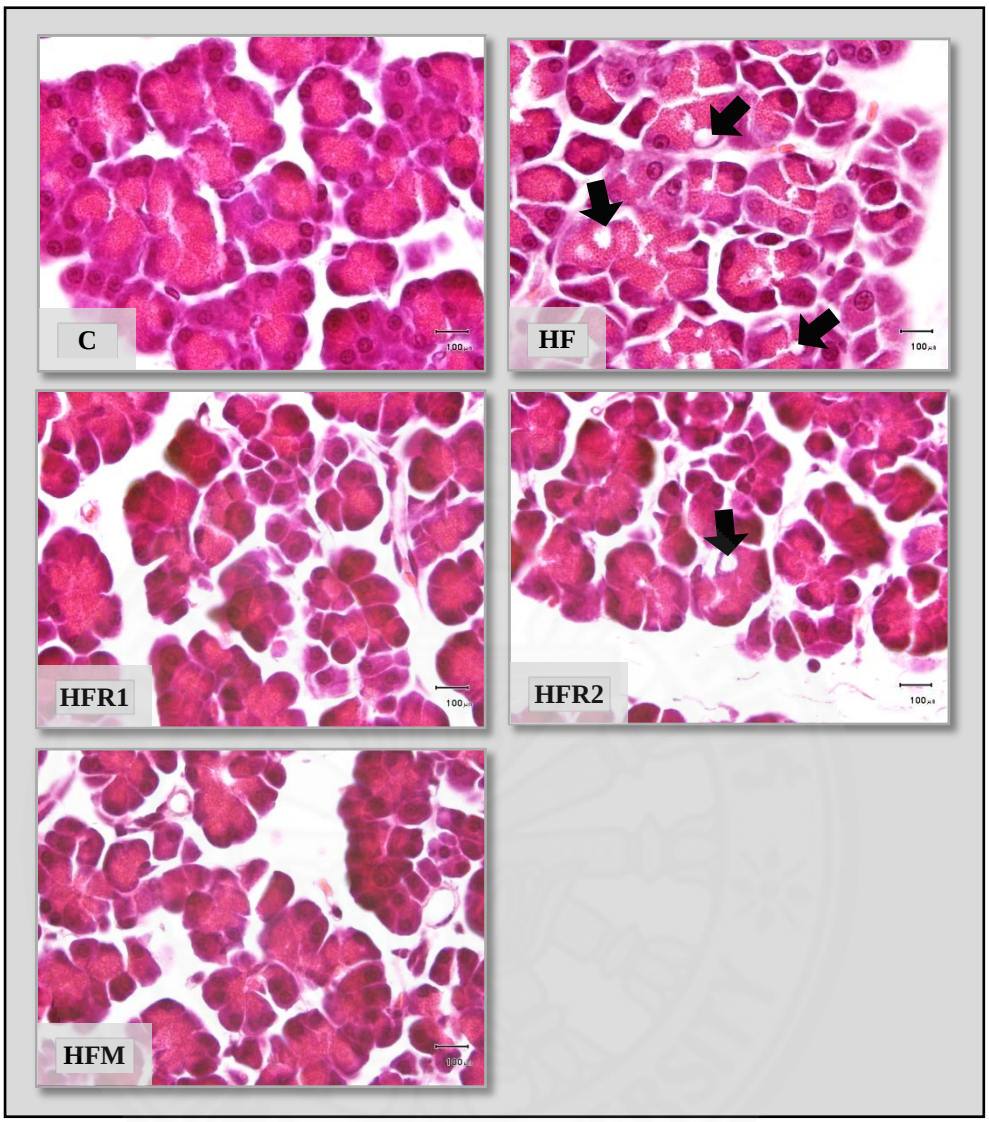

Figure 4.5 Histology (H and E staining) of pancreatic acinar cells (1,000× magnification; scale bar = 100 µm)**.** Arrows represent clear vacuoles in pancreatic acinar cells.

4.7 Effect of RBE on pancreatic insulin signaling and glucose-sensing pathways

IRS-2 plays an important role in regulating pancreatic mass, insulin synthesis, and glucose sensing. Under HFD condition, the down-regulation of IRS-2 was observed in the pancreas in association with the impairment of pancreatic mass and function [159]. In addition to the abnormal insulin signaling, the down-regulations of GLUT-2 and GK genes were observed in the pancreas induced by HFD, thus reducing glucose sensing [12]. The down-regulation of IRS-2, GLUT-2 and GK genes may, therefore, lead to hyperglycemia and glucose intolerance [9, 12].

As presented in Figure 4.6, the mRNA levels of IRS-2, GLUT-2 and GK were significantly decreased in the HFD alone feed group when compared with the C group ($p < 0.01$, $p < 0.05$ and $p < 0.001$, respectively). Thus, these results suggest that HFD might interfere with insulin signaling and glucose-sensing pathways in the pancreas. In contrast to the HF group, GLUT-2 and IRS-2 mRNA levels were significantly increased in the HFR1 and HFR2 groups. GK mRNA levels were also significantly ($p < 0.05$) increased in the HFR1 group. RBE2-treated rats also showed a tendency towards increased GK expression, but the difference was not significant. Our findings suggest that RBE treatments might prevent the impairment of insulin signaling and glucose-sensing pathways in the pancreas. To support these findings, the enhancement of GK activity in mice fed with an HFD supplemented with rice bran and phytic acid caused an increase in the utilization of blood glucose for energy production in the liver, thereby reducing blood glucose level [143]. Moreover, the rice bran protein consumption in high-energy diet-induced insulin-resistant rats ameliorated the insulin sensitivity, resulting in the reduction of FBG and AUC-G of OGTT [128].

In the present study, the mRNA levels of IRS-2 and GK in pancreas also showed a tendency to increase in the HFM group, but the differences were not statistically significant. However, metformin-treated rats had significantly ($p < 0.001$) higher GLUT-2 mRNA level compared to HFD-fed rats. In generally, metformin is used anti-diabetic drug for the treatment of T2D, attenuates hyperglycemia by inhibiting hepatic gluconeogenesis, enhancing muscle glucose uptake, and improving

insulin sensitivity [144]. However, how metformin functions in pancreatic β-cells about the insulin signaling and glucose-sensing pathways is still unknown [145].

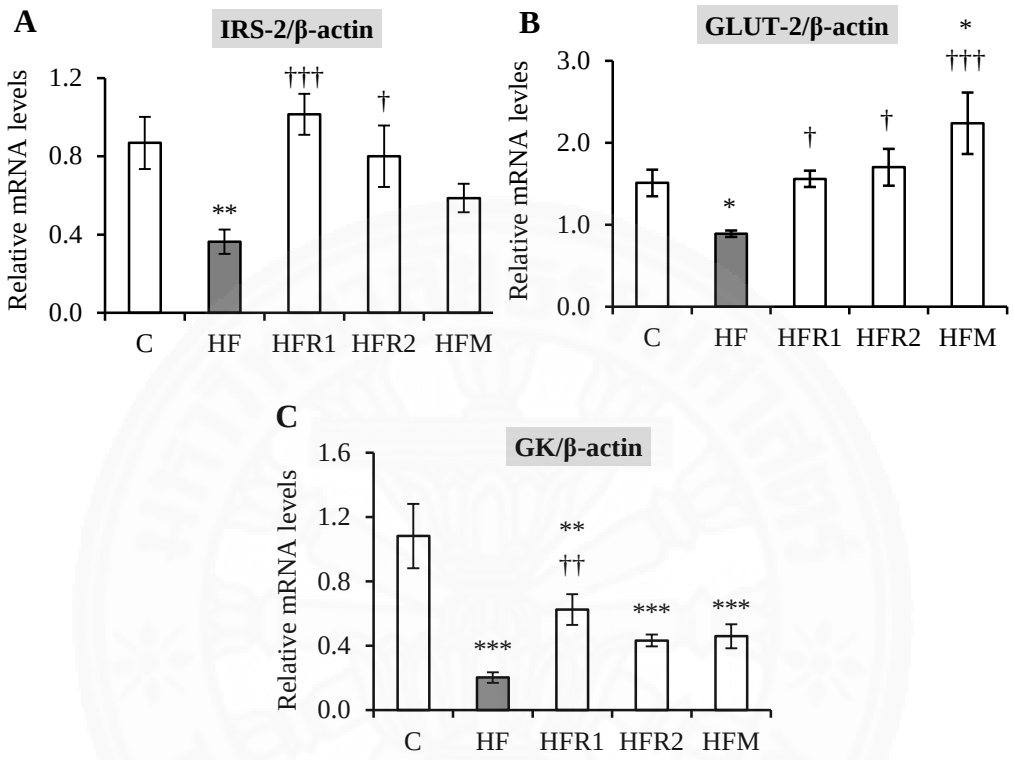

Figure 4.6 Pancreatic mRNA expression levels of IRS-2 (A), GLUT-2 (B) and GK (C)

Values are expressed as mean ± SEM (n = 6)

$^{*}p < 0.05$, $^{**}p < 0.01$, $^{***}p < 0.001$ vs C

$^{\dagger}p < 0.05$, $^{\dagger\dagger}p < 0.01$, $^{\dagger\dagger\dagger}p < 0.001$ vs HF

4.8 Effect of RBE on oxidative stress and pancreatic islet cell senescence

Pancreatic β-cell senescence has become increasingly important in the development of diabetes mellitus [13]. In HFD-induced diabetic rat, β-cell proliferation was increased to compensate for the enhanced insulin demand caused by insulin resistance, which led to the generation of ROS. There are many reports about the excess generation of ROS in response to high glucose results in oxidative stress that may trigger β-cells damage [160-162]. An accumulation of ROS might then lead to increased β-cell senescence [15-16]. As noted above, the accumulating evidence indicates that the activation of NF-κB plays the main role in the progression of the cellular senescence and oxidative stress [20]. In the present study, the increased MDA levels were found in both serum ($p < 0.01$) and pancreas ($p < 0.01$) of rats fed an HFD alone (Figure 4.7). Moreover, the HF group exhibited significantly ($p < 0.05$) higher gene expression of NF-κB p50 than the C group and also tended to increase pancreatic NF-κB p65 mRNA levels when compared with the C group (Figure 4.8).

NF-κB p65 (RelA) contains C-terminal transcriptional activation domains (TADs), which enable them to activate target gene expression. In contrast, NF-κB p50 do not contain C-terminal TADs, therefore NF-κB p50 homodimer repress transcription unless it is bound to a protein containing a TAD, such as RelA (a related transcriptional co-activator). Moreover, NF-κB p65 shows a weak DNA-binding site which could contribute directly to DNA binding in the NF-κB complex [163-164]. Thus, NF-κB heterodimeric p50/p65 is the most common form of study. The translocation of p50/p65 transcription factors into the nucleus, where they activate a range of target genes involved in inflammatory responses, apoptosis, as well as senescence [163-165].

The increased expression of NF-κB genes may be attributed to the increased expression of senescent marker in the pancreatic islets of HFD-fed rats. Cellular senescence in islets was observed after the rats were fed an HFD (Figure 4.9). Consistently, the mean density of SABG expression in islet cells was significantly higher in the HF group than the C group. Interestingly, the RBE-treated groups suppressed the increase of serum MDA, pancreatic MDA, NF-κB p50 mRNA and SABG expression levels (Figure 4.7-4.9). The mRNA levels of NF-κB p65 also

tended to reduce in the RBE-treated rats (Figure 4.8). Our study demonstrated that all RBE treatments effectively reduced pancreatic islet senescence, and its associated parameters including oxidative damage and NF-κB up-regulation. Therefore, the present data indicate that the RBE treatment may inhibit HFD-induced pancreatic senescence by reducing oxidative stress, increased islet cell proliferation, and expression of NF-κB gene. In line with our findings, previous studies have revealed that the consumption of rice bran and phytic acid markedly decreased the MDA levels in the plasma and erythrocytes of HFD-fed mice [127]. Moreover, the treatment with Khao Dawk Mali 105 rice bran peptides also significantly reduced the levels of plasma MDA and vascular superoxide in the hypertensive animal [128].

Metformin has been widely used for treating T2D and exerts its glucose-lowering effect primarily by suppressing hepatic glucose production with increased peripheral insulin sensitivity [144]. Recent research showed novel activities in different tissues and cell types, but its role remains controversial in pancreatic β-cells. In this regard, this study proposed that metformin could reverse the HFD-induced β-cell senescence. In the present study, the oxidative markers in pancreas were not significantly improved in the HFM group. However, metformin treatment effectively reduced serum MDA level (Figure 4.7A) and pancreatic islet senescence (Figure 4.9) in HFD-induced obese rats. These data demonstrated that metformin drastically increased pancreatic cell viability, which is regulated by low serum MDA concentrations. In line with these findings, the generation of ROS in response to high glucose has been associated with the induction of apoptosis, and inhibition of lipid peroxidation by metformin confers cell survival [166-167].

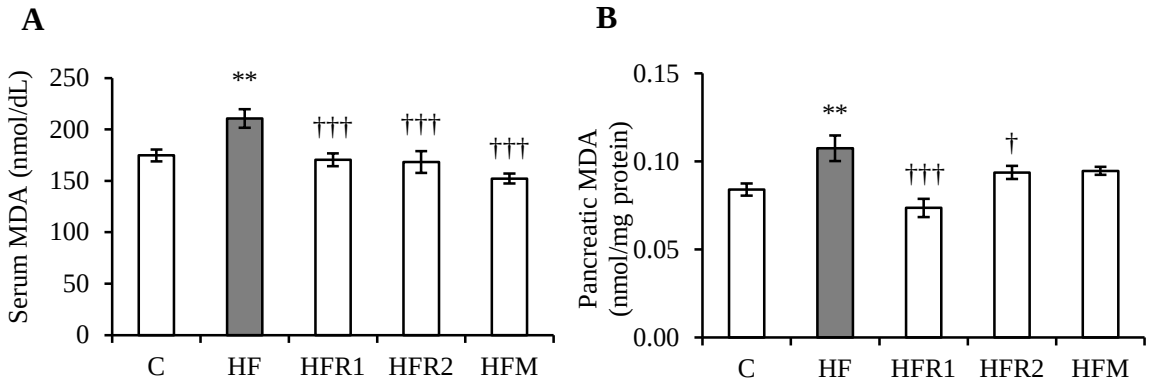

Figure 4.7 MDA contents in serum (A) and pancreatic tissues (B)

Values are expressed as mean ± SEM (n = 6)

$^{*}p < 0.05$, $^{**}p < 0.01$, $^{***}p < 0.001$ vs C

$^{\dagger}p < 0.05$, $^{\dagger\dagger}p < 0.01$, $^{\dagger\dagger\dagger}p < 0.001$ vs HF

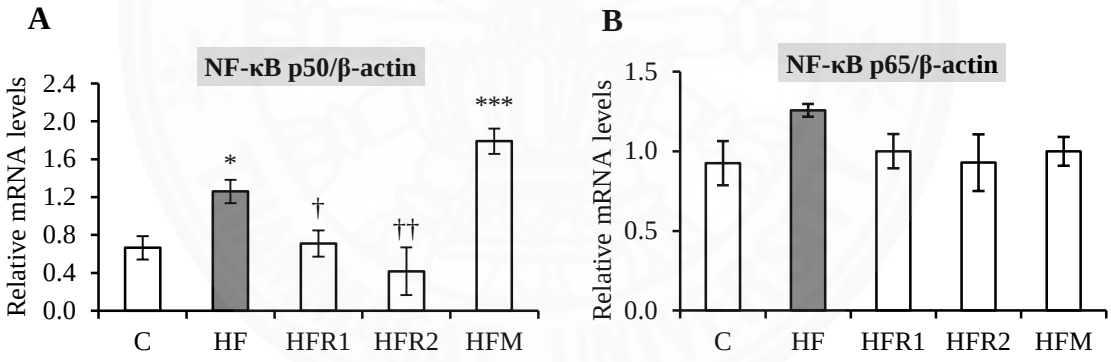

Figure 4.8 Pancreatic mRNA expression levels of NF-κB p50 (A) and p65 (B)

Values are expressed as mean ± SEM (n = 6)

$^{*}p < 0.05$, $^{***}p < 0.001$ vs C

$^{\dagger}p < 0.05$, $^{\dagger\dagger}p < 0.01$ vs HF

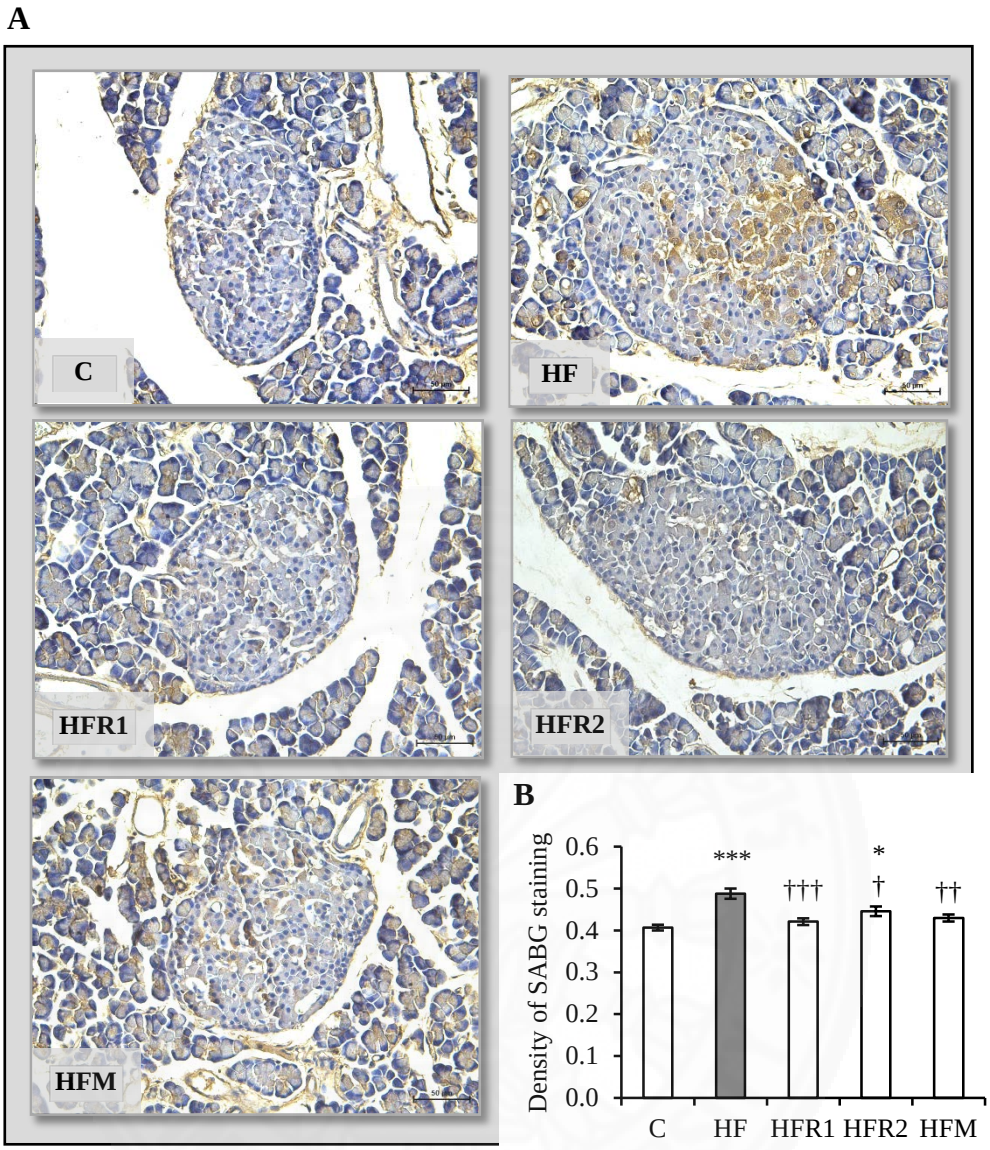

Figure 4.9 Immunohistochemistry (SABG staining) of pancreatic islet cells (A) and mean density of SABG staining in islet cells (B)

$^{*}p < 0.05$, $^{***}p < 0.001$ vs C

$^{\dagger}p < 0.05$, $^{\dagger\dagger}p < 0.01$, $^{\dagger\dagger\dagger}p < 0.001$ vs HF

CHAPTER 5
CONCLUSIONS AND RECOMMENDATIONS

In conclusion, the present study demonstrates that treatment of the obesity induced by diet in rats with RBE moderates or reverses the changes in metabolic parameters, abdominal fat accumulation, as well as fat deposition in pancreas. The RBE consumption could attenuate the abnormalities in the pancreas by reducing fat deposition as well as improving insulin signaling and glucose sensing. The mechanisms of these protective effects may be mediated via the inhibition of lipogenic gene (SREBP-1c) expression and activation of insulin signaling and glucose-sensing gene (IRS-2, GLUT-2, and GK) expression. In addition, the RBE consumption also exhibited protective effects against HFD-induced senescence in rat pancreatic islet cells by decreasing oxidative stress marker (MDA and NF-κB expression levels) and islet cell proliferation. Thus, these protections by RBE could be attributed to improve glucose homeostasis in the setting of diet-induced obesity, which the protective effects and possible molecular mechanisms of RBE are summarized in Figure 5.1. Hence, RBE could be considered as an alternative nutritional complement in combination with the preventive and therapeutic strategies against abnormalities of the pancreas associated obesity. However, further studies will be needed to determine the bioactive compounds associated with their beneficial activities in RBE.

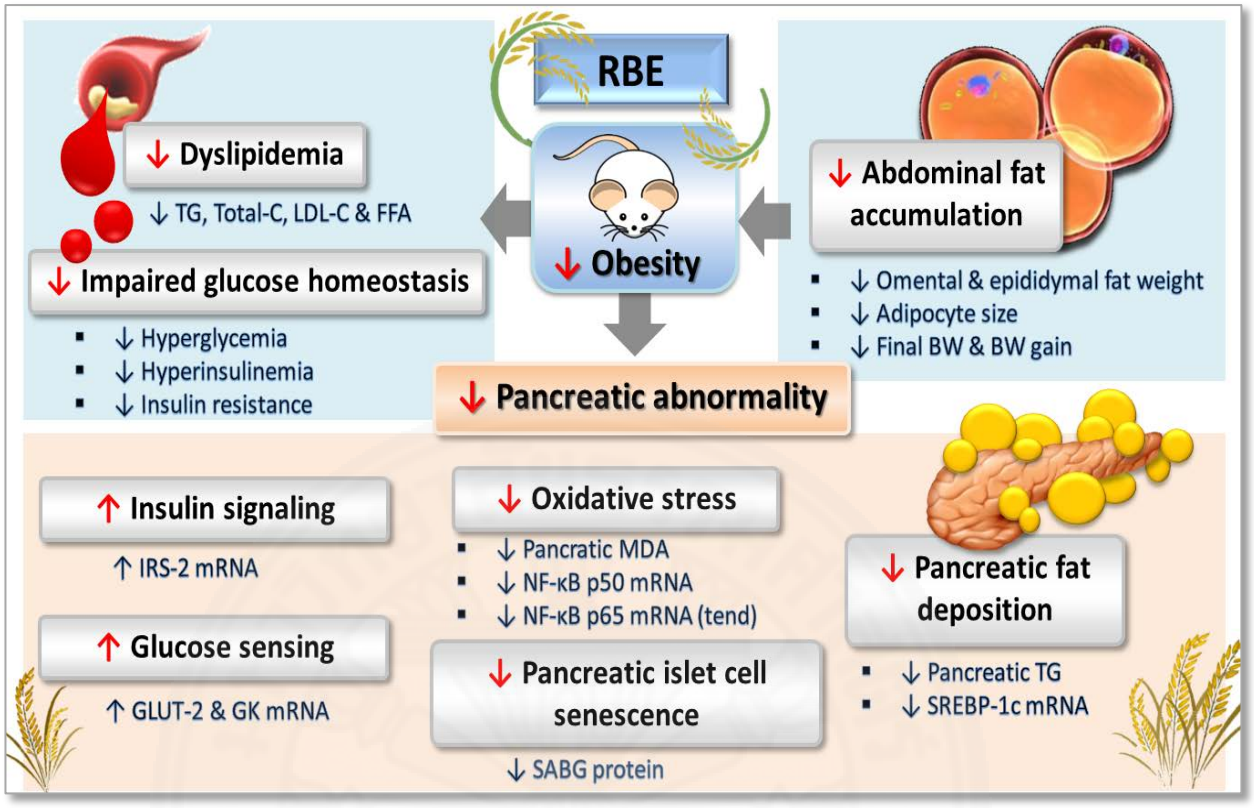

Figure 5.1 Conclusion of the proposed mechanisms responsible for the effects of RBE on HFD-induced pancreatic abnormalities

↑, increased; ↓, decreased

REFERENCES

1. Singla P, Bardoloi A, Parkash AA. Metabolic effects of obesity: A review. World J Diabetes 2010; 1(3): 76-88.

2. Buettner R, Schölmerich J, Bollheimer LC. High-fat diets: modeling the metabolic disorders of human obesity in rodents. Obesity 2007; 15(4): 798-808.

3. Aronoff SL, Berkowitz K, Shreiner B, Want L. Glucose metabolism and regulation: beyond insulin and glucagon. Diabetes Spectrum 2004; 17(3): 184-190.

4. Panchal SK, Poudyal H, Iyer A, Nazer R, Alam A, Diwan V, et al. High-carbohydrate high-fat diet–induced metabolic syndrome and cardiovascular remodeling in rats. J Cardiovasc Pharmacol 2011; 57(1): 51-64.

5. Pezzilli R, Calculli L. Pancreatic steatosis: Is it related to either obesity or diabetes mellitus? World J Diabetes 2014; 5(4): 415-419.

6. Zhang X, Cui Y, Fang L, Li F. Chronic high-fat diets induce oxide injuries and fibrogenesis of pancreatic cells in rats. Pancreas 2008; 37(3): e31-38.

7. Shao S, Yang Y, Yuan G, Zhang M, Yu X. Signaling molecules involved in lipid-induced pancreatic beta-cell dysfunction. DNA Cell Biol 2013; 32(2): 41-49.

8. Takahashi A, Motomura K, Kato T, Yoshikawa T, Nakagawa Y, Yahagi N, et al. Transgenic mice overexpressing nuclear SREBP-1c in pancreatic beta-cells. Diabetes 2005; 54(2): 492-499.

9. Assmann A, Ueki K, Winnay JN, Kadowaki T, Kulkarni RN. Glucose effects on beta-cell growth and survival require activation of insulin receptors and insulin receptor substrate 2. Mol Cell Biol 2009; 29(11): 3219-3228.

10. Hashimoto S, Kubota N, Sato H, Sasaki M, Takamoto I, Kubota T, et al. Insulin receptor substrate-2 (Irs2) in endothelial cells plays a crucial role in insulin secretion. Diabetes 2015; 64(3): 876-886.

11. Ahrén B. Beta- and alpha-cell dysfunction in subjects developing impaired glucose tolerance: outcome of a 12-year prospective study in postmenopausal caucasian women. Diabetes 2009; 58(3): 726-731.

12. Cerf ME. High fat diet modulation of glucose sensing in the beta-cell. Med Sci Monit 2007; 13(1): RA12-17.

13. Testa R, Ceriello A, Pathogenetic loop between diabetes and cell senescence. Diabetes Care 2007; 30(11): 2974-2975.

14. Tavana O, Zhu C. Too many breaks (brakes): pancreatic β-cell senescence leads to diabetes. Cell Cycle 2011; 10(15): 2471-2484.

15. Sone H, Kagawa Y. Pancreatic beta cell senescence contributes to the pathogenesis of type 2 diabetes in high-fat diet-induced diabetic mice. Diabetologia 2005; 48(1): 58-67.

16. Liu DH, Chen YM, Liu Y, Hao BS, Zhou B, Wu L, et al. Rb1 protects endothelial cells from hydrogen peroxide-induced cell senescence by modulating redox status. Biol Pharm Bull 2011; 34 (7):1072-1077.

17. Li N, Brun T, Cnop M, Cunha DA, Eizirik DL, Maechler P. Transient oxidative stress damages mitochondrial machinery inducing persistent beta-cell dysfunction. J BiolChem 2009; 284(35): 23602-23612.

18. Oprescu AI, Bikopoulos G, Naassan A, Allister EM, Tang C, Park E, et al. Free fatty acid-induced reduction in glucose-stimulated insulin secretion: evidence for a role of oxidative stress in vitro and in vivo. Diabetes 2007; 56(12): 2927-2937.

19. Rovillain E, Mansfield L, Caetano C, Alvarez-Fernandez M, Caballero OL, Medema RH, et al. Activation of nuclear factor-kappa B signalling promotes cellular senescence. Oncogene 2011; 30(20): 2356-2366.

20. Tilstra JS, Robinson AR, Wang J, Gregg SQ, Clauson CL, Reay DP, et al. NF-kappa B inhibition delays DNA damage-induced senescence and aging in mice. J Clin Invest 2012; 122 (7): 2601-2612.

21. Candiracci M, Justo ML, Castaño A, Rodriguez-Rodriguez R, Herrera MD. Rice bran enzymatic extract-supplemented diets modulate adipose tissue inflammation markers in Zucker rats. Nutrition 2014; 30(4): 466-472.

22. Wang YX, Li Y, Sun AM, Wang FJ, Yu GP. Hypolipidemic and antioxidative effects of aqueous enzymatic extract from rice bran in rats fed a high-fat and-cholesterol diet. Nutrients 2014; 6(9): 3696-3710.

23. Qureshi AA, Sami SA, Khan FA. Effects of stabilized rice bran, its soluble and fiber fractions on blood glucose levels and serum lipid parameters in humans with diabetes mellitus Types I and II. J NutrBiochem 2002; 13(3): 175-187.

24. Chakhonpunya C, Sireeratawong S, Komindr S, Lerdvuthisopon N. Effect of rice-bran water extract on energy metabolism in rats fed a high-fat diet. Thammasat Medical Journal 2011; 11(2): 221-230.

25. Kaendee N, Sireeratawong S, Burawat B, Utama-Ang N, Lerdvuthisopon N.. The effect of rice bran extract on insulin resistance in high fat diet-induced obese rats. Thammasat Medical Journal 2009; 9(2): 140-147.

26. WHO S. Obesity: preventing and managing the global epidemic. Geneva: World Health Organization; 1998.

27. Wang P, Mariman E, Renes J, Keijer J. The secretory function of adipocytes in the physiology of white adipose tissue. J Cell Physiol 2008; 216: 3-13.

28. Sell H, Deshaies Y, Richard D. The brown adipocyte: update on its metabolic role. Int J Biochem Cell Biol 2004; 36: 2098-2104.

29. Attie AD, Scherer PE . Adipocyte metabolism and obesity. Journal of Lipid Research 2008; 50(Suppl.): S395-S399.

30. Cusi K. The role of adipose tissue and lipotoxicity in the pathogenesis of type 2 diabetes. Current Diabetes Reports 2010; 10(4): 306-315.

31. Lionetti L, Mollica MP, Lombardi A, Cavaliere G, Gifuni G, Barletta A. From chronic overnutrition to insulin resistance: the role of fat storing capacity and inflammation. Nutrition, Metabolism & Cardiovascular Disease 2009; 19(2): 146-152.

32. Lottenberg AM, da Silva Afonso M, Lavrador MS, Machado RM, Nakandakare E R. The role of dietary fatty acids in pathology of metabolic syndrome. Journal of Nutritional Biochemistry 2012; 23(9): 1027-1040.

33. Snel M, Jonker JT, Schoones J, Lamb H, de Roos A, Pijl H, et al. Ectopic fat and insulin resistance: pathophysiology and effect of diet and lifestyle interventions. International Journal of Endocrinology. 2012: 1-18.

34. Bays HE, Toth PP, Kris-Etherton PM, Abate N, Aronne LJ, Brown WV, et al. Obesity, adiposity, and dyslipidemia: a consensus statement from the National Lipid Association. J Clin Lipidol 2013; 7(4): 304-383.

35. Klop B, Elte JWF, Cabezas MC, Dyslipidemia in Obesity: Mechanisms and Potential Targets. Nutrients 2013; 5(4): 1218-1240.

36. Parekh S, Anania FA. Abnormal lipid and glucose metabolism in obesity: implications for nonalcoholic fatty liver disease. Gastroenterology 2007; 132(6): 2191-2207.

37. Fery F. Role of hepatic glucose production and glucose uptake in the pathogenesis of fasting hyperglycemia in type 2 diabetes: normalization of glucose kinetics by short-term fasting. J Clin Endocrinol Metab 1994; 78: 536-542.

38. Radziuk J, Pye S. Production and metabolic clearance of glucose under basal conditions in type II (non-insulin-dependent) diabetes mellitus. Diabetologia 2001; 44: 983-991.

39. Edlund H. Pancreatic organogenesis-developmental mechanisms and implications for therapy. Nature Reviews Genetics 2002; 3: 524-532.

40. Nielsen JH, Galsgaard ED, Møldrup A, Friedrichsen BN, Billestrup N, Hansen JA, et al. Regulation of beta-cell mass by hormones and growth factors Diabetes 2001; 50 Suppl 1:S25-29.

41. Bratanova-Tochkova TK, Cheng H, Daniel S, Gunawardana S, Liu YJ, Mulvaney-Musa J, et al. Triggering and augmentation mechanisms, granule pools, and biphasic insulin secretion. Diabetes 2002; 51 Suppl. 1:S83-90.

42. Fernandes J, Sudubray JM, van den Berghe editors Inborn Metabolic Diseases: Diagnosis and treatment. (3rd ed): Springer, Heidelberg Germany; 2000. 117-126.

43. Soria B, Quesada I, Ropero AB, Pertusa JA, Martin F, Nadal A. Novel players in pancreatic islet signaling: from membrane receptors to nuclear channels. Diabetes 2004; 53 Suppl 1:S86-91.

44. Rutter GA, Pullen TJ, Hodson DJ, Martinez-Sanchez A. Pancreatic β-cell identity, glucose sensing and the control of insulin secretion. Biochemical Journal 2015; 466(2): 203-218.

45. Alberti KGMM, Zimmet P, Defronzo RA, Keen H editors. International Textbook of Diabetes Mellitus (2nd ed) John Wiley & Sons, New York; 1997. 315-336.

46. Rees DA , Alcolado JC . Animal models of diabetes mellitus. Diabet Med 2005; 22: 359-370.

47. Jörns A , Tiedge M , Ziv E , Shafrir E , Lenzen S. Gradual loss of pancreatic beta-cell insulin, glucokinase and GLUT2 glucose transporter immunoreactivities

during the time course of nutritionally induced type-2 diabetes in Psammomys obesus (sand rat) . Virchows Arch 2002; 440: 63-69.

48. Khan A , Chandramouli V , Ostenson CG , Low H , Landau BR , Efendic S. Glucose cycling in islets from healthy and diabetic rats . Diabetes 1990; 39: 456-459.

49. Gremlich S, Roduit R, Thorens B. Dexamethasone induces posttranslational degradation of GLUT2 and inhibition of insulin secretion in isolated pancreatic beta cells. Comparison with the effects of fatty acids. J Biol Chem 1997; 272(6): 3216-3222.

50. Kim Y, Iwashita S, Tamura T, Tokuyama K, Suzuki M. Effect of high-fat diet on the gene expression of pancreatic GLUT2 and glucokinase in rats. Biochem Biophys Res Commun 1995; 208: 1092-1098.

51. Schuit FC, Huypens P, Heimberg H, Pipeleers DG. Glucose Sensing in Pancreatic β-Cells: A Model for the Study of Other Glucose-Regulated Cells in Gut, Pancreas, and Hypothalamus. Diabetes 2001; 50(1): 1-11.

52. Kim HI, Cha JY, Kim SY, Kim JW, Roh KJ, Seong JK, et al. Peroxisomal proliferator-activated receptor- gamma upregulates glucokinase gene expression in beta-cells. Diabetes 2002; 51(3): 676-685.

53. Grimsby J, Sarabu R, Corbett WL, Haynes NE, Bizzarro FT, Coffey JW, et al. Allosteric activators of glucokinase: potential role in diabetes therapy. Science 2003; 301(5631): 370-383.

54. Kamata K, Mitsuya M, Nishimura T, Eiki J, Nagata Y. Structural basis for allosteric regulation of the monomeric allosteric enzyme human glucokinase. Structure 2004; 12(3): 429-438.

55. Efanov AM, Barrett DG, Brenner MB, Briggs SL, Delaunois A, Durbin JD, et al. A novel glucokinase activator modulates pancreatic islet and hepatocyte function. Endocrinology 2005; 146(9): 3696-3701.

56. Coope GJ, Atkinson AM, Allott C, McKerrecher D, Johnstone C, Pike KG, et al. Predictive blood glucose lowering efficacy by glucokinase activators in high fat fed female Zucker rats. Br J Pharmacol 2006; 149(3): 328-335.

57. Matschinsky FM 1990 Glucokinase as glucose sensor and metabolic signal generator in pancreatic beta-cells and hepatocytes. Diabetes 1990; 39(6): 647-652.

58. Coghlan M, Leighton B. Glucokinase activators in diabetes management. Expert Opin Investig Drugs 2008; 17(2): 145-67.

59. Fatrai S, Elghazi L, Balcazar N, Cras-Méneur C, Krits I, Kiyokawa H, et al. Akt induces beta-cell proliferation by regulating cyclin D1, cyclin D2, and p21 levels and cyclin-dependent kinase-4 activity. Diabetes 2006; 55(2): 318-325.

60. Wrede CE, Dickson LM, Lingohr MK, Briaud I, Rhodes CJ. Protein kinase B/Akt prevents fatty acid-induced apoptosis in pancreatic beta-cells (INS-1). J Biol Chem 2002; 277(51): 49676-49684.

61. Skolnik EY, Batzer A, Li N, Lee CH, Lowenstein E, Mohammadi M, et al. The function of GRB2 in linking the insulin receptor to Ras signaling pathways. Science 1993; 260(5116): 1953-1965.

62. Kefas BA, Heimberg H, Vaulont S, Meisse D, Hue L, Pipeleers D, et al. AICA-riboside induces apoptosis of pancreatic beta cells through stimulation of AMPactivated protein kinase. Diabetologia 2003; 46(2): 250-264.

63. Muoio DM, Newgard CB. Molecular and metabolic mechanisms of insulin resistance and β-cell failure in type 2 diabetes. Nature Reviews Molecular Cell Biology 2008; 9: 193-205.

64. Golson ML, Misfeldt AA, Kopsombut UG, Petersen CP, Gannon M. High Fat Diet Regulation of β-Cell Proliferation and β-Cell Mass. Open Endocrinol J 2010; 4: 66-77.

65. Withers DJ, Burks DJ, Towery HH, Altamuro SL, Flint CL, White MF. Irs-2 coordinates Igf-1 receptor-mediated beta-cell development and peripheral insulin signalling. Nat Genet 1999; 23: 32-40.

66. Kubota N, Tobe K, Terauchi Y, Eto K, Yamauchi T, Suzuki R, et al. Disruption of insulin receptor substrate 2 causes type 2 diabetes because of liver insulin resistance and lack of compensatory beta-cell hyperplasia. Diabetes 2000; 49(11): 1880-1889.

67. Hennige AM, Burks DJ, Ozcan U, Kulkarni RN, Ye J, Park S, et al. Upregulation of insulin receptor substrate-2 in pancreatic beta cells prevents diabetes. J Clin Invest 2003; 112(10): 1521-1532.

68. Lee Y, Hirose H, Ohneda M, Johnson JH, McGarry JD, Unger RH. β-Cell lipotoxicity in the pathogenesis of non-insulin dependent diabetes mellitus of obese

rats: impairment in adipocyte-β-cell relationships. Proc Natl Acad Sci 1994; 91: 10878-10882.

69. Hori M, Takahashi M, Hiraoka N, Yamaji T, Mutoh M, Ishigamori R, et al. Association of pancreatic Fatty infiltration with pancreatic ductal adenocarcinoma. Clin Transl Gastroenterol 2014; 5: e53.

70. Matsuzaka T, Shimano H, Yahagi N, Amemiya-Kudo M, Okazaki H, Tamura Y, et al. Insulin-independent induction of sterol regulatory element-binding protein-1c expression in the livers of streptozotocintreated mice. Diabetes 2004; 53: 560-569.

71. Lin J, Yang R, Tarr PT, Wu PH, Handschin C, Li S, et al. Hyperlipidemic effects of dietary saturated fats mediated through PGC-1beta coactivation of SREBP. Cell 2005; 120: 261-273.

72. Wang H, Maechler P, Antinozzi PA, Herrero L, Hagenfeldt-Johansson KA, Bjorklund A, et al. The transcription factor SREBP-1c is instrumental in the development of beta-cell dysfunction. J Biol Chem 2003; 278: 16622-16629.

73. Yamashita T, Eto K, Okazaki Y, Yamashita S, Yamauchi T, Sekine N, et al. Role of uncoupling protein-2 up-regulation and triglyceride accumulation in impaired glucose-stimulated insulin secretion in a beta-cell lipotoxicity model overexpressing sterol regulatory elementbinding protein-1c. Endocrinology 2004; 145: 3566-3577.

74. Kakuma T, Lee Y, Higa M, Wang Z, Pan W, Shimomura I, et al. Leptin, troglitazone, and the expression of sterol regulatory element binding proteins in liver and pancreatic islets. Proc Natl Acad Sci USA 2000; 97: 8536-8541.

75. Kato T, Shimano H, Yamamoto T, Yokoo T, Endo Y, Ishikawa M, et al. Granuphilin is activated by SREBP-1c and involved in impaired insulin secretion in diabetic mice. Cell Metab 2006; 4: 143-154.

76. Shimano H, Amemiya-Kudo M, Takahashi A, Kato T, Ishikawa M, Yamada N. Sterol regulatory element-binding protein-1c and pancreatic beta-cell dysfunction. Diabetes Obes Metab 2007; 9 Suppl 2: 133-139.

77. Furukawa S, Fujita T, Shimabukuro M, Iwaki M, Yamada Y, Nakajima Y, et al. Increased oxidative stress in obesity and its impact on metabolic syndrome. J Clin Invest 2004; 114(12): 1752-1761.

78. Fullenkamp AM, Bell LN, Robbins RD, Lee L, Saxena R, Alloosh M, et al. Effect of different obesogenic diets on pancreatic histology in Ossabaw miniature swine. Pancreas 2011; 40(3): 438-443.

79. Parslow RA, Sachdev P, Salonikas C, Lux O, Jorm AF, Naidoo D. Associations between plasma antioxidants and hypertension in a community-based sample of 415 Australians aged 60-64. Journal of Human Hypertension 2005; 19: 219-226.

80. Langin D. Diabetes, insulin secretion, and the pancreatic beta cell mitochondrion. N Engl J Med 2001 13; 345: 1772-1784.

81. Yan MX, Li YQ, Meng M, Ren HB, Kou Y. Long-term highfat diet induces pancreatic injuries via pancreatic microcirculatory disturbances and oxidative stress in rats with hyperlipidemia. Biochem Biophys Res Commun 2006; 347: 192-199.

82. Sussman MA, Anversa P. Myocardial aging and senescence: where have the stem cells gone? Annu Rev Physiol 2004; 66: 29-48.

83. Harman D. Aging: a theory based on free radical and radiation chemistry. J Gerontol 1956 ; 11(3): 298-300.

84. Dimri GP, Lee X, Basile G, Acosta M, Scott G, Roskelley C, et al. A biomarker that identifiessenescent human cells in culture and in aging skin in vivo. Proc Natl Acad Sci USA 1995; 92: 9363-9367.

85. Ressler S, Bartkova J, Niederegger H, Bartek J, Scharffetter-Kochanek K, Jansen-Dürr P, et al. p16INK4A is a robust in vivo biomarker of cellular aging in human skin. Aging Cell 2006; 5: 379-389.

86. Liu Y, Sanoff HK, Cho H, Burd CE, Torrice C, Ibrahim JG, et al. Expression of p16(INK4a) in peripheral blood T-cells is a biomarker of human aging. Aging Cell 2009; 8: 439-448.

87. Beausejour CM, Krtolica A, Galimi F, Narita M, Lowe SW, Yaswen P, et al. Reversal of human cellular senescence: roles of the p53 and p16 pathways. EMBO J 2003; 22: 4212-4222.

88. Kuilman T, Peeper DS. Senescence-messaging secretome: SMS-ing cellular stress. Nat Rev Cancer 2009; 9: 81-94.

89. Rodier F, Campisi J. Four faces of cellular senescence. J Cell Biol 2011; 192: 547-556.

90. Freund A, Patil CK, Campisi J. p38MAPK is a novel DNA damage response-independent regulator of the senescence associated secretory phenotype. EMBO J 2011; 30: 1536-1548.

91. Kuilman T, Michaloglou C, Mooi WJ, Peeper DS. The essence of senescence. Genes Dev 2010; 24: 2463-2479.

92. Freund A, Orjalo AV, Desprez PY, Campisi J. Inflammatory networks during cellular senescence: causes and consequences. Trends Mol Med 2010; 16: 238-246.

93. Hoffmann A, Baltimore D. Circuitry of nuclear factor κB signaling. Immunol Rev 2006; 210: 171-186.

94. Wan F, Lenardo MJ. Specification of DNA Binding Activity of NF-κB Proteins. Cold Spring Harb Perspect Biol 2009; 1(4): a000067.

95. Moore R, Grant AM, Howard AN, Mills IH. Treatment of obesity with triiodothyronine and a very-low-calorie liquid formula diet. Lancet 1980; 1: 223-226.

96. Goldstein DJ, Rampey AH Jr, Enas GG, Potvin JH, Fludzinski LA, Levine LR. Fluoxetine: a randomized clinical trial in the treatment of obesity. Int J Obes Relat Metab Disord 1994; 18: 129-135.

97. Kay JP, Alemzadeh R, Langley G, D'Angelo L, Smith P, Holshouser S. Beneficial effects of metformin in normoglycemic morbidly obese adolescents. Metabolism 2001; 50(12): 1457-1461.

98. Zhou G, Myers R, Li Y, Chen Y, Shen X, Fenyk-Melody J, et al. Role of AMP-activated protein kinase in mechanism of metformin action. J Clin Invest 2001; 108: 1167-1174.

99. Viollet B, Guigas B, Sanz Garcia N, Leclerc J, Foretz M, Andreelli F. Cellular and molecular mechanisms of metformin: an overview. Clin Sci (Lond) 2012; 122(6): 253-270.

100. El-Mir MY, Nogueira V, Fontaine E, Averet N, Rigoulet M, Leverve X. Dimethylbiguanide inhibits cell respiration via an indirect effect targeted on the respiratory chain complex I. J Biol Chem 2000; 275: 223-228.

101. Brunmair B, Staniek K, Gras F, Scharf N, Althaym A, Clara R, et al. Thiazolidinediones, like metformin, inhibit respiratory complex I: a common mechanism contributing to their antidiabetic actions? Diabetes 2004; 53: 1052-1059.

102. Hinke SA, Martens GA, Cai Y, Finsi J, Heimberg H, Pipeleers D, et al. Methyl succinate antagonises biguanide-induced AMPK-activation and death of pancreatic beta-cells through restoration of mitochondrial electron transfer. Br J Pharmacol 2007; 150: 1031-1043.

103. Marchesini G, Marzocchi R, Agostini F, Bugianesi E. Nonalcoholic fatty liver disease and the metabolic syndrome. Curr Opin Lipidol 2005; 16: 421-427.

104. Shu Y, Sheardown SA, Brown C, Owen RP, Zhang S, Castro RA, et al. Effect of genetic variation in the organic cation transporter 1 (OCT1) on metformin action. J. Clin. Invest 2007; 117: 1422-1431.

105. Leclerc I, Rutter GA. AMP-activated protein kinase: a new beta-cell glucose sensor?: regulation by amino acids and calcium ions. Diabetes 2004; 53: S67-S74.

106. Richards SK, Parton LE, Leclerc I, Rutter GA, Smith RM. Over-expression of AMP-activated protein kinase impairs pancreatic {beta}-cell function in vivo. J Endocrinol 2005; 187: 225-235.

107. Wang CZ, Wang Y, Di A et al. 5-amino-imidazole carboxamide riboside acutely potentiates glucose-stimulated insulin secretion from mouse pancreatic islets by KATP channel-dependent and -independent pathways. Biochem Biophys Res Commun 2005; 330: 1073-1079.

108. Salt IP, Johnson G, Ashcroft SJ, Hardie DG. AMP-activated protein kinase is activated by low glucose in cell lines derived from pancreatic beta cells, and may regulate insulin release. Biochem J 1998; 335: 533-539.

109. Zhang S, Kim KH. Glucose activation of acetyl-CoA carboxylase in association with insulin secretion in a pancreatic beta-cell line. J Endocrinol 1995; 147: 33-41.

110. McKiney JM, Irwin N, Flatt PR, Bailey CJ, McClenaghan NH. Acute and long-term effects of metformin on the function and insulin secretory responsiveness of clonal β-cells. Biol Chem 2010; 391(12): 1451-1459.

111. Patanè G, Piro S, Rabuazzo AM, Anello M, Vigneri R, Purrello F. Metformin restores insulin secretion altered by chronic exposure to free fatty acids or high glucose: a direct metformin effect on pancreatic beta-cells. Diabetes 2000; 49(5): 735-740.

112. Piro S, Rabuazzo AM, Renis M, Purrello F. Effects of Metformin on oxidative stress, adenine nucleotides balance and glucose-induced insulin release impaired by chronic FFA exposure in rat pancreatic islets. J Endocrinol Invest 2012; 35(5): 504-510.

113. Lablanche S, Cottet-Rousselle C, Lamarche F, Benhamou P-Y, Halimi S, Leverve X, et al. Protection of pancreatic INS-1 beta-cells from glucose- and fructose-induced cell death by inhibiting mitochondrial permeability transition with cyclosporin A or metformin. Cell Death Dis 2011; 2(3): e134.

114. Kefas BA, Cai Y, Kerckhofs K, Ling Z, Martens G, Heimberg H, et al. Metformin-induced stimulation of AMP-activated protein kinase in beta-cells impairs their glucose responsiveness and can lead to apoptosis. Biochem Pharmacol 2004; 68(3): 409-416.

115. Leclerc I, Woltersdorf WW, da Silva Xavier G, Rowe RL, Cross SE, Korbutt GS, et al. Metformin, but not leptin, regulates AMP-activated protein kinase in pancreatic islets: impact on glucose-stimulated insulin secretion. Am J Physiol Endocrinol Metab 2004; 286(6): E1023-E1031.

116. Wang Q, Cai Y, Van de Casteele M, Pipeleers D, Ling Z. Interaction of glibenclamide and metformin at the level oftranslation in pancreatic beta cells. J Endocrinol, 2011. 208(2): 161-169.

117. Hinke SA, Martens GA, Cai Y, Finsi J, Heimberg H, Pipeleers D, et al. Methyl succinate antagonises biguanide-induced AMPK-activation and death of pancreatic beta-cells through restoration of mitochondrial electron transfer. Br J Pharmacol 2007. 150(8): 1031-1043.

118. Sum CF, Webster JM, Johnson AB, Catalano C, Cooper BG, Taylor R. The effect of intravenous metformin on glucose metabolism during hyperglycaemia in type 2 diabetes. Diabet Med 1992; 9(1): 61-65.

119. Wilcock C, Bailey CJ. Accumulation of metformin by tissues of the normal and diabetic mouse. Xenobiotica 1994; 24(1): 49-57.

120. Bailey CL. Biguanides and NIDDM. Diubetes Care 1992; 15: 755-772.

121. Krogh CME, ed. Compendium of Pharmaceuticals and Specialties. 28th ed. Ottawa, Ontario, Canada: Canadian Pharmaceutical Association; 1993: 506.

122. Foo KY, Hameed BH. Utilization of rice husk ash as novel adsorbent: a judicious recycling of the colloidal agricultural waste. Adv. Colloid Interface Sci. 2009; 152: 39-47.

123. Sharif MK, Butt MS, Anjum FM, Khan SH. Rice bran: a novel functional ingredient. Crit Rev Food Sci Nutr 2014; 54(6): 807-16.

124. Houston D.F. (Ed). Rice: chemistry and technology. American Association of Cereal Chemists, incorporated St Paul, Minnesota, 1972.

125. Department of Grain Science and Technology. CFTRI. Rice Bran. RESC Scientific Series No 7, Central Food Technological Research Institute, Mysore, 59 (Revised), 1995.

126. Justo ML, Candiracci M, Dantas AP, de Sotomayor MA, Parrado J, Vila E, et al. Rice bran enzymatic extract restores endothelial function and vascular contractility in obese rats by reducing vascular inflammation and oxidative stress. J Nutr Biochem 2013; 24(8):1453-61.

127. Kang MY, Kim SM, Rico CW, Lee SC. Hypolipidemic and antioxidative effects of rice bran and phytic acid in high fat-fed mice. Food Sci Biotechnol 2012; 21(1): 123-128.

128. Boonloh K, Kukongviriyapan V, Kongyingyoes B, Kukongviriyapan U, Thawornchinsombut S, Pannangpetch P. Rice bran protein hydrolysates improve insulin resistance and decrease pro-inflammatory cytokine gene expression in rats fed a high carbohydrate-high fat diet. Nutrients 2015; 7(8): 6313-6329.

129. Peng H, Zheng Y, Chen M, Wang Y, Xiao Y, Gao Y. A starch-binding domain identified in α-amylase (AmyP) represents a new family of carbohydrate-binding modules that contribute to enzymatic hydrolysis of soluble starch. FEBS Lett 2014; 588(7): 1161-1167.

130. Gupta K, Jana AK, Kumar S, Maiti M. Immobilization of α-amylase and amyloglucosidase onto ion-exchange resin beads and hydrolysis of natural starch at high concentration. Bioprocess Biosyst Eng 2013; 36(11): 1715-1724.

131. Claret M, Corominola H, Canals I, Nadal BN, Chavanieu A, Pfeiffer B, et al. S23521 decrease food intake and body weight gain in diet-induced obese rats. Obesity Research 2004; 12(10): 1596-1603.

132. Wolever TM, Jenkins DJ, Jenkins AL, Josse RG. The glycemic index: methodology and clinical implications. American Society for Clinical Nutrition 1991; 54(5): 846-854.

133. Richard MM, Rita P, Alexander Z, Michael SK, Emily O, Konstantin V, et al. Filter Paper Blood Spot Enzyme Linked Immunoassay for Insulin and Application in the Evaluation of Determinants of Child Insulin Resistance. PLoS One 2012; 7(10): e46752.

134. Cohn JS, McNamara JR, Schaefer EJ. Lipoprotein cholesterol concentrations in the plasma of human subjects as measured in the fed and fasted states. Clin Chem 1988; 34(12): 2456-2459.

135. Friedewald WT, Levy RI, Fredrickson DS. Estimation of the concentration of low-density lipoprotein cholesterol in plasma without use of the preparative ultracentrifuge. Clinical Chemistry 1972; 18(6): 499-502.

136. Oakes ND, Thalén PG, Jacinto SM, Ljung B. Thiazolidinediones increase plasma-adipose tissue FFA exchange capacity and enhance insulin-mediated control of systemic FFA availability. Diabetes 2001; 50(5): 1158-1165.

137. Ardestani A, Yazdanparast R, Jamshidi Sh. Therapeutic effects of Teucriumpolium extract on oxidative stress in pancreas of streptozotocin-induced diabetic rats. J Med Food 2008; 11(3): 525-532.

138. Susanna C. Highly efficient method for isolation of total RNA from adipose tissue. BMC Res Notes 2013; 6: 472-476.

139. Livak KJ, Schmittgen TD. Analysis of relative gene expression data using real-time quantitative PCR and the 2(-Delta Delta C(T)) Method. Methods 2001; 25(4): 402-408.

140. Feldman AT, Wolfe D. Tissue processing and hematoxylin and eosin staining. Methods Mol Biol 2014; 1180: 31-43.

141. Jafari M, Monsef-Esfahani A, Solimani B. Diagnostic value of immunoperoxidase staining and immunofluorescence in the study of kidney biopsy specimens. Iran J Kidney Dis 2015; 9(4): 286-290.

142. van Heek M, Compton DS, France CF, Tedesco RP, Fawzi AB, Graziano MP, et al. Diet-induced obese mice develop peripheral, but not central, resistance to leptin. J Clin Invest 1997; 99: 385-390.

143. Kim SM, Rico CW, Lee SC, Kang MY. Modulatory effect of rice bran and phytic acid on glucose metabolism in high fat-fed C57BL/6N Mice. J ClinBiochemNutr 2010; 47(1): 12-17.

144. Joshi SR. Metformin: old wine in new bottle--evolving technology and therapy in diabetes. J Assoc Physicians India 2005; 53: 963-972.

145. Riccio A, Del Prato S, Vigili de Kreutzenberg S, Tiengo A. Glucose and lipid metabolism in non-insulin-dependent diabetes: effect of metformin. Diabete Metab 1991; 17: 180-184.

146. Karpe F, Dickmann JR, Frayn KN, Fatty acids, obesity, and insulin resistance: Time for a reevaluation. Diabetes 2011; 60(10): 2441-2449.

147. Cerf ME. Beta Cell Dysfunction and Insulin Resistance. Front Endocrinol (Lausanne). 2013; 4(37): 1-12.

148. McGarry JD, Dobbins RL. Fatty acid, lipotoxicity and insulin secretion. Diabetologia 1999; 42(2): 128-138.

149. Shimabukuro M, Higa M, Zhou YT, Wang MY, Newgard CB, Unger RH. Lipoapoptosis in beta-cells of obese prediabetic fa/fa rats: role of serine palmitoyltransferase overexpression. J Biol Chem 1998; 273: 32487-32490.

150. Sreenan S, Sturis J, Pugh W, Burant CF, Polonski KS. Prevention of hyperglycemia in the Zucker diabetic fatty rat by treatment with metformin or troglitazone. Am J Physiol 1996; 271: E742–E747.

151. Paolisso G, Gambardella A, Amato L, Tortoriello R, D'Amore A, Varricchio M, et al. Opposite effects of short- and long-term fatty acid infusion on insulin secretion in healthy subjects. Diabetologia 1995; 38:1295-1299.

152. Boden G, Chen X, Rosner J, Barton M. Effects of a 48h fat infusion on insulin secretion and glucose utilization. Diabetes 1995; 44: 1239-1242.

153. Linnemann AK, Baan M, Davis DB. Pancreatic β-cell proliferation in obesity. Adv Nutr 2014; 5(3): 278-288.

154. Matveyenko AV, Butler PC. Relationship between β-cell mass and diabetes onset. Diabetes Obes Metab 2008; 10(0 4): 23-31.

155. van Raalte DH, van der Zijl NJ, Diamant M. Pancreatic steatosis in humans: cause or marker of lipotoxicity? Curr Opin Clin Nutr Metab Care 2010; 13(4): 478-485.

156. Gosmain Y, Dif N, Berbe V, Loizon E, Rieusset J, Vidal H, et al. Regulation of SREBP-1 expression and transcriptional action on HKII and FAS genes during fasting and refeeding in rat tissues. J Lipid Res 2005; 46(4): 697-705.

157. Lee Y, Lingvay I, Szczepaniak LS, Ravazzola M, Orci L, Unger RH. Pancreatic steatosis: harbinger of type 2 diabetes in obese rodents. International Journal of Obesity 2010; 34: 396-400.

158. Matsuda A, Makino N, Tozawa T, Shirahata N, Honda T, Ikeda Y, et al. Pancreatic fat accumulation, fibrosis, and acinar cell injury in the zucker diabetic fatty rat fed a chronic high-fat diet. Pancreas 2014; 43(5): 735-743.

159. Park S, Hong SM, Lee JE, Sung SR. Exercise improves glucose homeostasis that has been impaired by a high-fat diet by potentiating pancreatic beta-cell function and mass through IRS2 in diabetic rats. J Appl Physiol 2007; 103(5): 1764-1771.

160. Karunakaran U, Park KG. A systematic review of oxidative stress and safety of antioxidants in diabetes: focus on islets and their defense. Diabetes Metab J 2013; 37(2): 106-112.

161. Maritim AC, Sanders RA, Watkins JB. Diabetes, oxidative stress, and antioxidants: a review. J Biochem Mol Toxicol 2003; 17(1): 24-38.

162. Tang C, Han P, Oprescu AI, Lee SC, Gyulkhandanyan AV, Chan GNY, Wheeler MB, Giacc A. Evidence for a Role of Superoxide Generation in Glucose-Induced β-Cell Dysfunction In Vivo. Diabetes 2007; 56(11): 2722-2731.

163. Zheng C, Yin Q, Wu H. Structural studies of NF-κB signaling. Cell Res 2011; 21(1): 183-195.

164. Ghosh G, Wang VY, Huang DB, Fusco A. NF-κB regulation: lessons from structures. Immunol Rev 2012; 246(1):36-58.

165. Lawrence T. The nuclear factor NF-kappaB pathway in inflammation. Cold Spring Harb Perspect Biol 2009; 1(6): a001651.

166. Mokhtari D, Myers JW, Welsh N. The MAPK kinase kinase-1 is essential for stress-induced pancreatic islet cell death. Endocrinology 2008; 149(6): 3046-3053.

167. Marchetti P, Del Guerra S, Marselli L, Lupi R, Masini M, Pollera M, et al. Pancreatic islets from type 2 diabetic patients have functional defects and increased apoptosis that are ameliorated by metformin. J Clin Endocrinol Metab 2004; 89(11): 5535-5541.

APPENDICES

APPENDIX A

A FLOWCHART FOR THE PREPARATION OF RICE BRAN

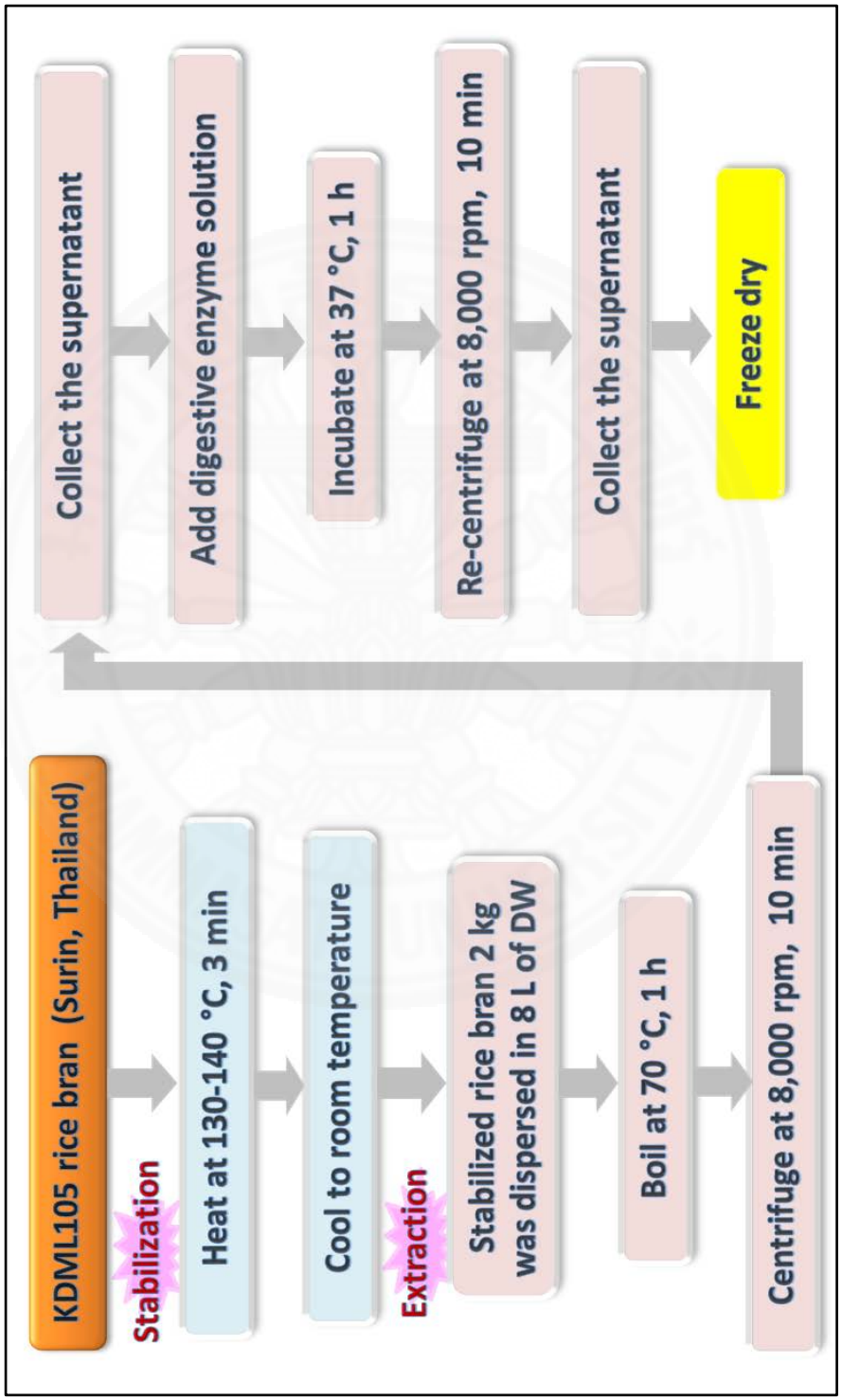

APPENDIX B

THE ANIMAL ETHIC APPROVAL

เลขที่ AE 002/2013

ใบรับรองให้ดำเนินการวิจัยในสัตว์ทดลอง

คณะกรรมการจรรยาบรรณการใช้สัตว์เพื่องานทางวิทยาศาสตร์

คณะแพทยศาสตร์ มหาวิทยาลัยธรรมศาสตร์

ชื่อข้อเสนอการวิจัย

(ภาษาไทย) ผลของสารสกัดรำข้าวต่อภาวะไขมันเป็นพิษต่อระบบหัวใจหลอดเลือดในหนูที่ได้รับอาหารไขมันสูง

(ภาษาอังกฤษ) The effect of rice-bran extract on cardiovascular lipotoxicity in rats fed a high-fat diet

ชื่อ-สกุล ผู้เสนอโครงการวิจัย	นายณรงค์ศักดิ์ มั่นคง
หน่วยงานสังกัด (คณะ/กอง)	นักศึกษาบัณฑิตศึกษา คณะแพทยศาสตร์
(มหาวิทยาลัย/กรม)	มหาวิทยาลัยธรรมศาสตร์
(กระทรวง)	

คณะกรรมการจรรยาบรรณการใช้สัตว์เพื่องานทางวิทยาศาสตร์ คณะแพทยศาสตร์ มหาวิทยาลัยธรรมศาสตร์ มีมติให้โครงการดังกล่าวสามารถดำเนินการวิจัยได้ โดยยึดหลักจรรยาบรรณการใช้สัตว์อย่างเคร่งครัด หากได้ตรวจสอบพบว่าผู้ดำเนินการวิจัยในโครงการนี้ได้ดำเนินการวิจัยผิดหลักจรรยาบรรณการใช้สัตว์ คณะกรรมการจรรยาบรรณการใช้สัตว์เพื่องานทางวิทยาศาสตร์ คณะแพทยศาสตร์ มหาวิทยาลัยธรรมศาสตร์มีสิทธิเพิกถอนใบรับรองนี้

ลงนาม.....	ลงนาม.....
(รองศาสตราจารย์ ดร. นายสัตวแพทย์สิวบูรณ์ สีรีรัฐวงศ์)	(รองศาสตราจารย์ นายแพทย์จักรชัย จึงธีรพานิช)
ประธานคณะกรรมการจริยธรรม	รองคณบดีฝ่ายวิจัย
การใช้สัตว์เพื่องานทางวิทยาศาสตร์	
วัน/เดือน/ปี ๒๕ มีนาคม ๒๕๕๖	วัน/เดือน/ปี ๒๕ มีนาคม ๒๕๕๖

APPENDIX C

THE ANIMAL MODEL

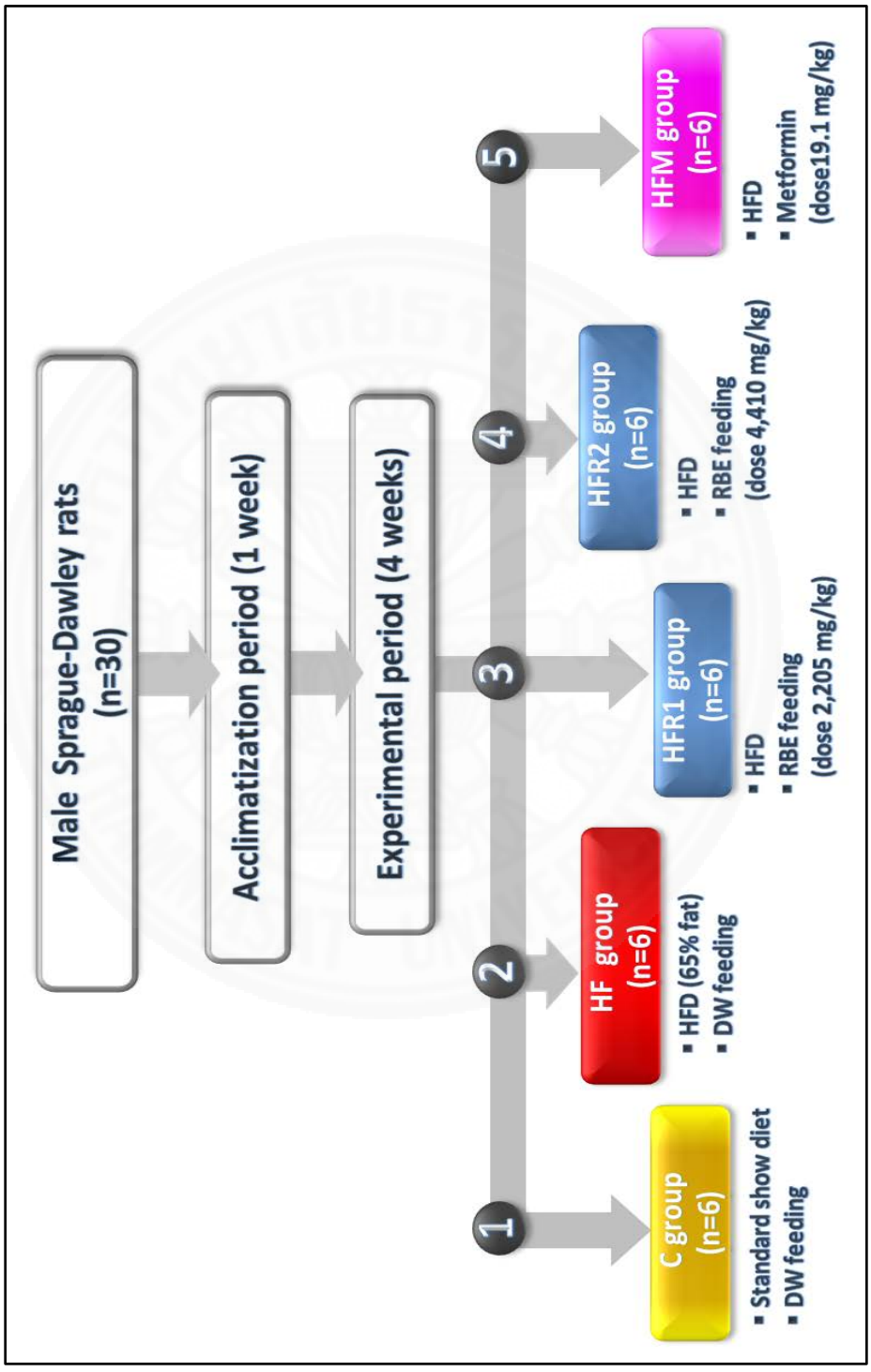

APPENDIX D

THE EXPERIMENTAL DESIGN

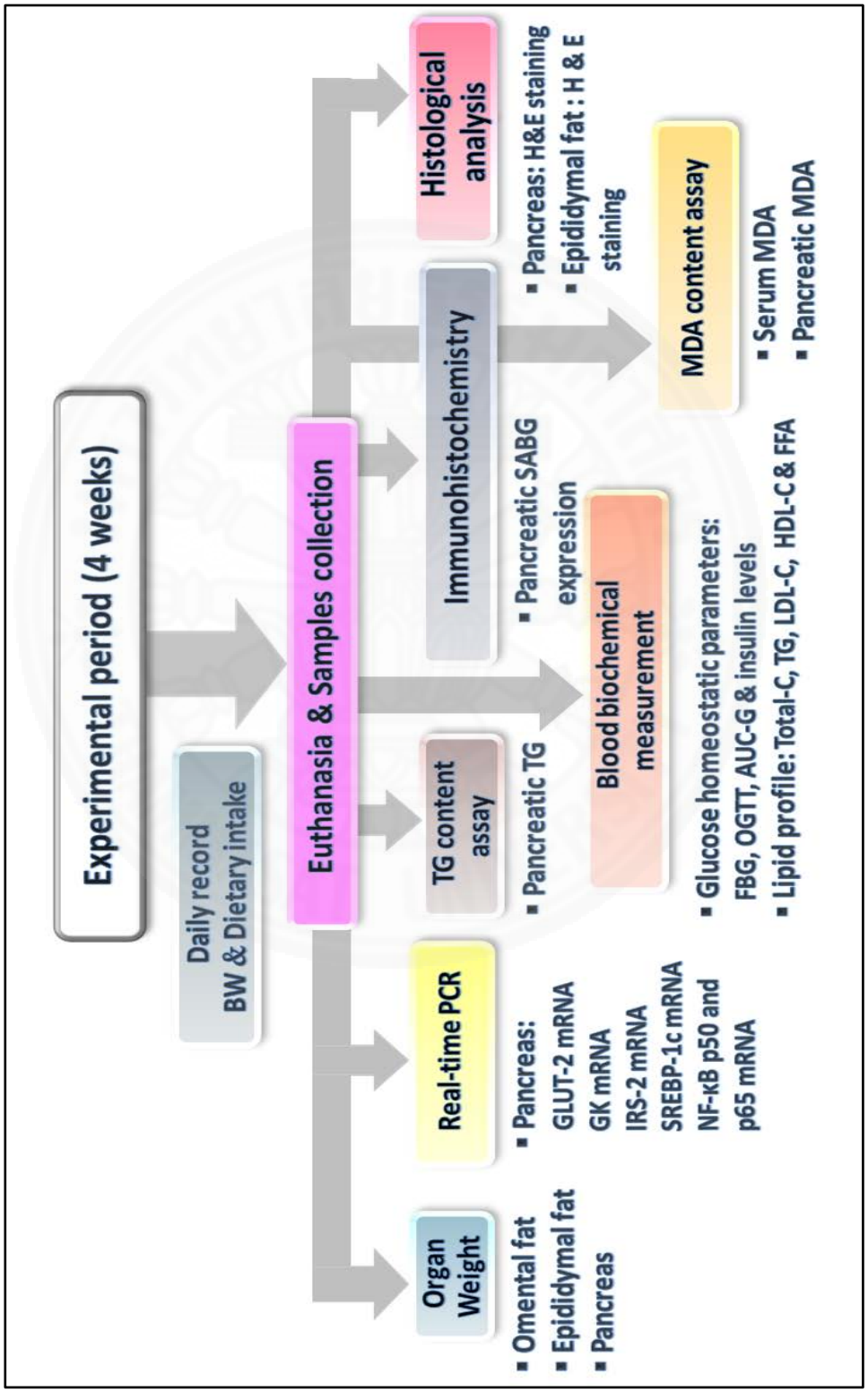

APPENDIX E

A FLOWCHART FOR THE DETERMINATION OF MDA

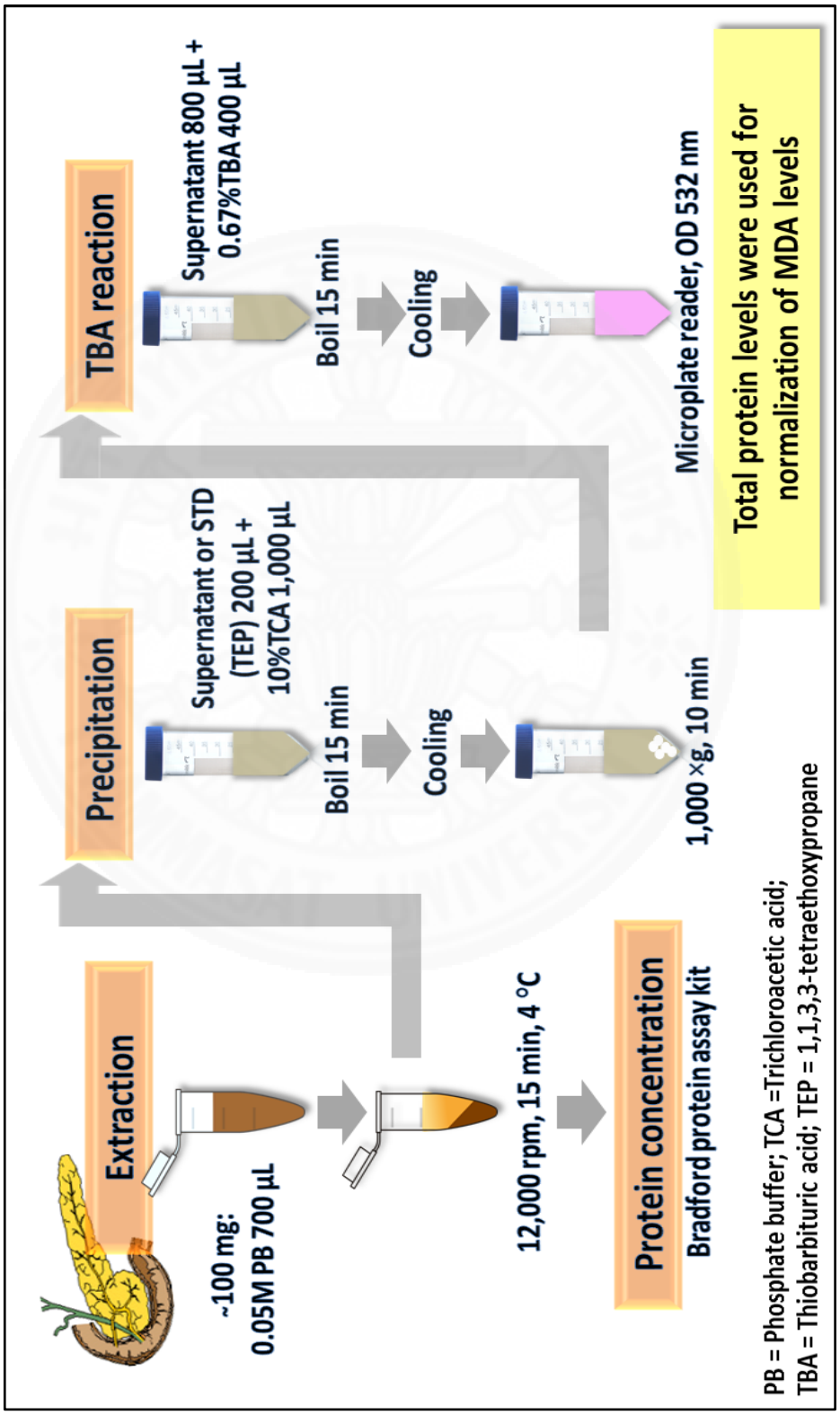

APPENDIX F

THE PRINCIPLE OF TAQMAN REAL-TIME PCR

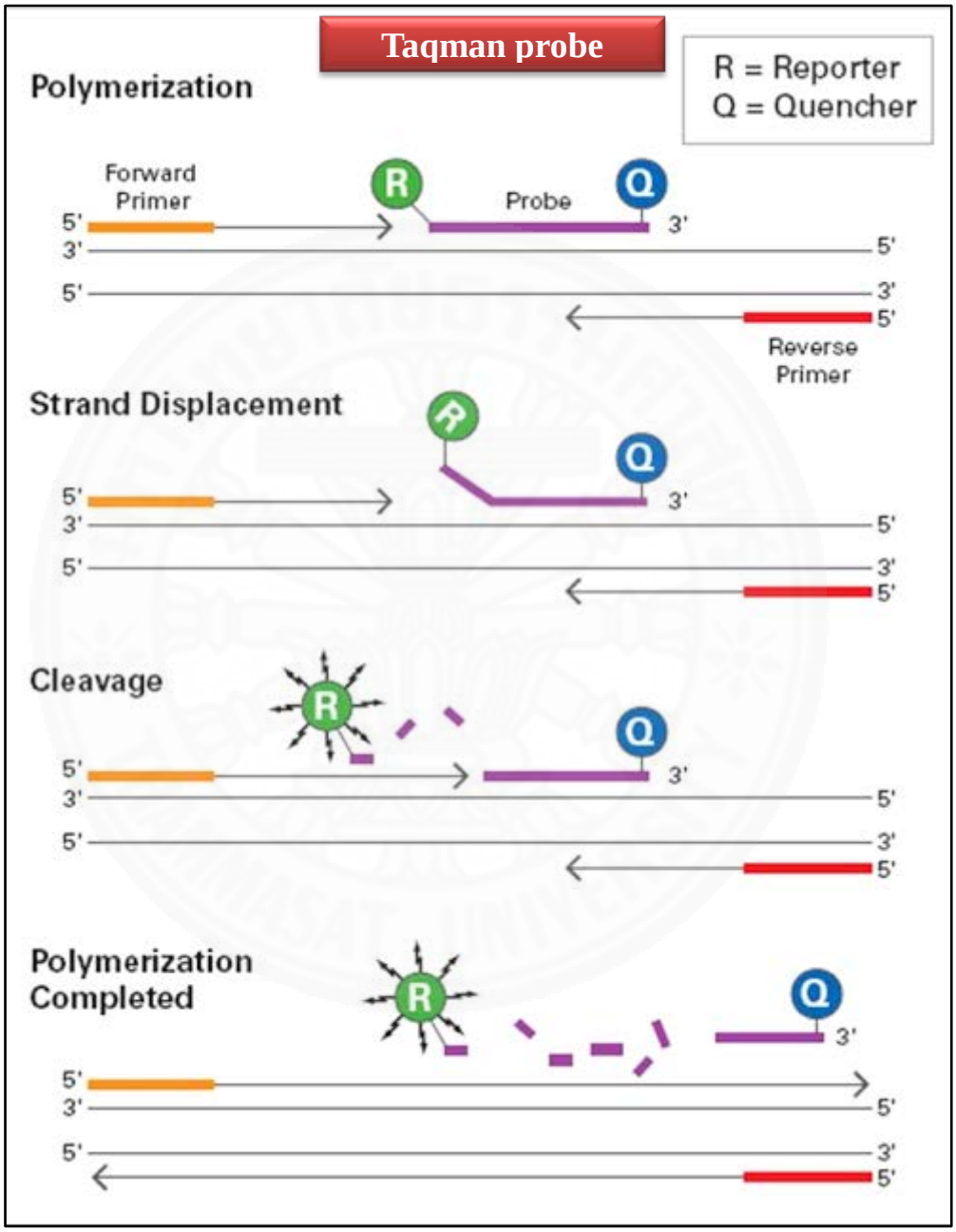

Retrieved form http://technologyinscience.blogspot.com/2013/05/taqman-assay-vs-sybr-green-assay.html

APPENDIX G

A FLOWCHART FOR THE DETERMINATION OF mRNA EXPRESSION

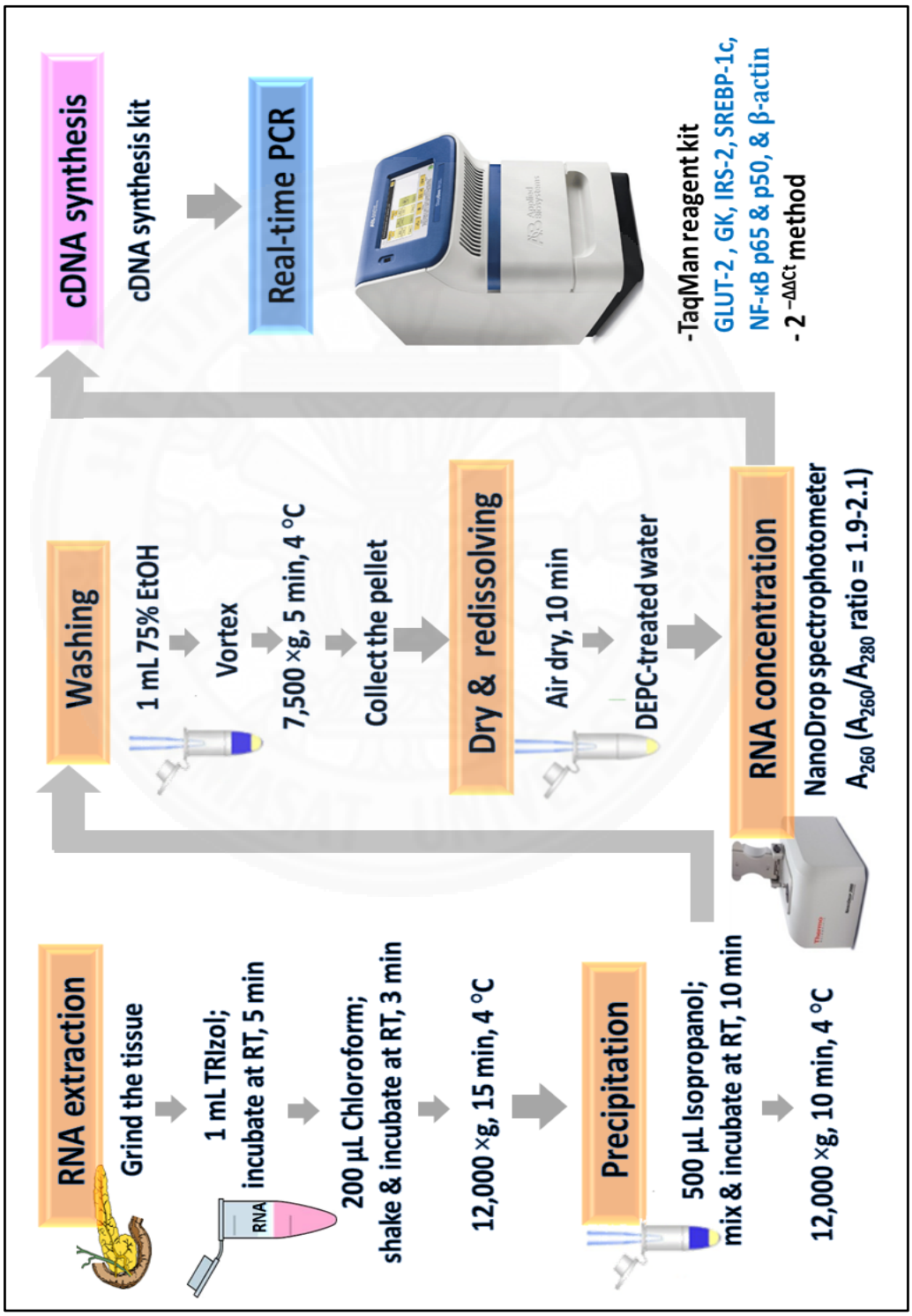

BIOGRAPHY

Name	Mister Wason Parklak
Date of Birth	May 11, 1986
Educational Attainment	Academic Year 2008: Bechelor of Science (Food Science), Burapha University, Thailand

Publication

Parklak W, Munkong N, Somnuk S, Somparn N, Naowaboot J, Yoysungnoen B, Lerdvuthisopon N. Rice bran water extract attenuates pancreatic abnormalities in high-fat diet-induced obese rats. Trop J Pharm Res 2017; 16(4): 819-825.

Oral presentation

Parklak W, Munkong N, Somnuk S, Lerdvuthisopon N. Rice bran water extract improves pancreatic insulin signaling and glucose-sensing pathways in high-fat diet-induced obese rats. “Patient-Centered Care” Academic Conference 2016, Faculty of Medicine, Thammasat University, Thailand (2nd place presentation).

Poster presentation

Parklak W, Munkong N, Somnuk S, Kaendee N, Lerdvuthisopon N. Preventive effects of rice bran water extract on pancreatic islet cell senescence in rats fed a high-fat diet. “Misconception in everyday practice” Academic Conference 2015, Faculty of Medicine, Thammasat University, Thailand (1st place presentation).